

**DEVELOPMENT OF MULTIFUNCTIONAL MEMBRANES FOR VISUAL
DETECTION AND ADSORPTIVE REMOVAL OF HEAVY METAL IONS
FROM AQUEOUS SOLUTIONS**

ZHANG LINZI

**NATIONAL UNIVERSITY OF SINGAPORE
2012**

**DEVELOPMENT OF MULTIFUNCTIONAL MEMBRANES FOR VISUAL
DETECTION AND ADSORPTIVE REMOVAL OF HEAVY METAL IONS
FROM AQUEOUS SOLUTIONS**

ZHANG LINZI
(B. Eng., Xi'an Jiaotong University)

**A THESIS SUBMITTED
FOR THE DEGREE OF DOCTOR OF PHILOSOPHY
DEPARTMENT OF CIVIL AND ENVIRONMENTAL
ENGINEERING**

**NATIONAL UNIVERSITY OF SINGAPORE
2012**

DECLARATION

I hereby declare that the thesis is my original work and it has been written by me in its entirety. I have duly acknowledged all the sources of information which have been used in the thesis.

This thesis has also not been submitted for any degree in any university previously.

Zhang Linzi

May 1st, 2012

ACKNOWLEDGEMENTS

First and foremost, I would like to express my heartfelt gratitude to my supervisor, Associate Professor Bai Renbi, for his sincere help and guidance, continuous support and encouragement throughout my Ph.D. study. His passion and intuition in scientific research have deeply inspired me and enriched my growth as a student, a researcher and a scientist that I want to be. I have broadened my knowledge as well as developed my research planning and scientific writing skills under his kind supervision. His enthusiasm, sincerity and meticulous attitude towards scientific research have greatly impressed me and will benefit to my life-long study.

Acknowledgement also goes to my colleagues for their help and assistant, especially to Dr. Li Nan, Dr. Liu Changkun, Dr. Han Wei, Dr. Wee Kin Ho, Dr. Zhao Yonghong, Dr. Han Hui, Dr. Zhu Xiaoying and Ms. Tu Wenting. I would also appreciate the assistance and cooperation from all lab and administrative officers in the Department of Civil and Environmental Engineering, National University of Singapore. In addition, I would also like to show my special thanks to Ms. Ge Xiaomeng and her mother Madam Su Yeming for their help and support during the days I live with them in Singapore.

Last but not the least, I would like to give my dearest thanks to my parents, Mr. Zhang Yanyuan and Madam Lin Aiping, my grandmother Madam Qu Juying, my late grandfather Mr. Lin Yunhu and all my relatives for their continuous and infinite love, support and encouragement.

Table of Contents

ACKNOWLEDGEMENTS	i
SUMMARY	v
LIST OF TABLES	vii
LIST OF FIGURES	viii
NOMENCLATURE	xiii
CHAPTER 1 INTRODUCTION	1
1.1 Overview	2
1.2 Research objectives and scopes of the work	4
CHAPTER 2 LITERATURE REVIEW	8
2.1 Heavy metal	9
2.2 Heavy metal pollution	10
2.2.1 Lead (Pb)	13
2.2.2 Cadmium (Cd)	13
2.2.3 Mercury (Hg)	14
2.3 Heavy metal removal technology	15
2.4 Heavy metal monitoring technology	22
2.4.1 Instrumental analysis	24
2.4.2 Chemical sensor	25
2.4.3 Optical chemical sensor with visual detection property	28
2.5 Significance of this study	32
CHAPTER 3 DEVELOPMENT OF A NOVEL MULTIFUNCTIONAL MEMBRANE FOR VISUAL DETECTION AND ADSORPTIVE REMOVAL OF LEAD(II) IONS IN AQUEOUS SOLUTIONS	34
3.1 Introduction	36
3.2 Materials and methods	37
3.2.1 Materials	37
3.2.2 Preparation of porous CS/CA blend membrane	37
3.2.3 Immobilization of DZ on CS/CA membrane	38
3.2.4 Experiments for chromatic response of the membranes in detection of lead ions in solutions	38
3.2.5 Lead adsorption experiments	39
3.2.6 Experiments on interference study	41

3.3 Results and discussion	41
3.3.1 Mechanisms of DZ immobilization and DZ interaction with lead ions	41
3.3.2 Effect of solution pH	42
3.3.3 Effect of contact time	43
3.3.4 Effect of lead concentration	43
3.3.5 Adsorption kinetics of lead ions on the membrane	45
3.3.6 Adsorption isotherms	46
3.3.7 Interference of other cations	49
3.3.8 Reusability of the prepared membrane	50
3.4 Conclusion	51
CHAPTER 4 SIMULTANEOUS DETECTION AND REMOVAL OF MERCURY IONS IN AQUEOUS SOLUTIONS BY TPPS FUNCTIONALIZED CS/CA MULTIFUNCTIONAL MEMBRANE	52
4.1 Introduction	54
4.2 Materials and Methods	57
4.2.1 Preparation of multifunctional membrane	57
4.2.2 Performance evaluation through batch adsorption experiments	58
4.2.3 Performance evaluation through batch filtration experiments	59
4.2.4 Other analyses	60
4.3 Results and Discussion	62
4.3.1 Membrane characteristics	62
4.3.2 Optical response of CS/CA-TPPS membrane to Hg(II) ions in water	65
4.3.3 Effect of TPPS immobilization amount on the performance of CS/CA-TPPS membrane	66
4.3.4 Effect of pH on the performance of CS/CA-TPPS membrane	70
4.3.5 Effect of ionic strength on the performance of CS/CA-TPPS membrane	72
4.3.6 Influence of initial Hg(II) concentration on the performance of CS/CA-TPPS membrane	73
4.3.7 Interference of other metal ions on the performance of CS/CA-TPPS membrane	74
4.3.8 Desorption	76
4.3.9 Application to real water samples	78
4.4 Conclusion	80
CHAPTER 5 THE EFFECT OF HUMIC ACID ON THE DETECTION AND REMOVAL OF HG(II) FROM AQUEOUS SOLUTIONS BY THE CS/CA-TPPS MEMBRANE	82
5.1 Introduction	85
5.2 Methods and Materials	88
5.2.1 Materials	88

5.2.2 Experiments	88
5. 3 Result and discussion	91
5.3.1Batch adsorption	91
5.3.2 Filtration performance.....	100
5.4 Conclusion	108
CHAPTER 6 A VERSATILE METHOD FOR THE IMMOBILIZATION OF OPTICAL INDICATORS ON THE BASE MEMBRANE: APPLICATION TO CADMIUM(II).....	110
6.1 Introduction.....	112
6.2 Materials and methods.....	114
6.2.1 Materials	114
6.2.2 Preparation of CS/CA blend base membrane	114
6.2.3 Grafting of polymer brushes on CS/CA base membrane for indicator immobilization.....	115
6.2.4 Coupling of cadmium indicator (TMPyP) onto CS/CA-SMP membrane.	116
6.2.5 Characterization of membranes	117
6.2.6 Experiments for examining chromatic response of the membranes in detecting cadmium ions in solutions.....	117
6.2.7 Cadmium adsorption performance experiments	118
6.2.8 Experiments on interference study.....	120
6.3. Results and discussion	120
6.3.1 Functionalization of membrane surface for cadmium ions	120
6.3.2 Morphology and permeability of prepared membranes	126
6.3.3 Response time of CS/CA-SMP-TMPyP membrane to cadmium detection	127
6.3.4 Effect of pH on cadmium detection by the prepared membrane	128
6.3.5 Response of CS/CA-SMP-TMPyP membrane in detecting cadmium ions with different concentrations.....	131
6.3.6 Adsorption performance	132
6.3.7 Interference of coexisting ions.....	136
6.4 Conclusion	137
CHAPTER 7 CONCLUSIONS AND RECOMMENDATIONS	138
7.1 Conclusions.....	139
7.2 Recommendations and future work.....	142
REFERENCE	145
LIST OF PUBLICATIONS.....	155

SUMMARY

As a result of increased industrial and urban activities, the occurrence of heavy metal contaminants has been dramatically augmented. Heavy metal contaminants are often introduced into the environment through the effluents discharged from various industries such as electroplating, mining, electric device manufacturing and metal finishing. They are toxic, non-biodegradable and highly carcinogenic, thus posing a serious threat to the lives of human beings even at low concentrations. This necessitates the development of technologies that can effectively detect the presence of heavy metal ions as well as remove them from the contaminated waters.

In recent years, optical sensors have been regarded as an effective method for water quality monitoring due to their advantages of simple and naked-eye detection that requires minimum labor and less sophisticated equipments. Whilst, in the field of heavy metal removal, adsorptive membranes have appeared as a novel membrane technology that attracted considerable research attention due to their high efficiency and low energy consumption even when the heavy metal containments are at relatively low concentrations. Over the decades, adsorptive membranes and optical sensors have been developed respectively in their individual disciplines. There is a desire to explore the possibility of incorporating the two technologies together for simultaneous on-site and in-situ detection and removal of heavy metal ions. This innovation may open the prospect of an integrated system for simultaneous water treatment and water quality surveillance. It may also have distinct advantages in actual applications, such as enhancing the treatment efficiency, simplifying the treatment system and reducing the environmental footprint.

In the present work, attempts were made to develop multifunctional membranes for visual detection and removal of heavy metal ions in aqueous solutions. Lead (Pb), mercury (Hg) and cadmium (Cd) were selected as the target ions due to their high occurrence in industrial wastewaters and high toxicity to the public and environmental health. Different types of optical indicators were immobilized onto chitosan/cellulose acetate (CS/CA) blend membrane through different methods based on their individual physiochemical properties. The effects of various factors, including the amount of immobilized indicators, solution pH, solution ionic strength, initial heavy metal concentrations, the presence of interference ions and co-existed organic contaminants were investigated through a series of experiments. The results in this study proved the concept of multifunctional membrane for simultaneous visual detection and removal of heavy metal ions was feasible and achievable. The prepared multifunctional membranes can detect and remove heavy metal ions in a wide variation of solution conditions, and the used membranes can be regenerated and reused without significant loss of their functionalities. Therefore, the proposed multifunctional membrane technology demonstrates a great potential in the remediation of heavy metal contamination, especially for the remote areas where there is a lack of or not convenient to use sophisticated instruments.

LIST OF TABLES

- Table 2.1 Drinking water regulations on heavy metal contaminants (USEPA, NPDWR).
- Table 2.2 Typical energy consumption and product recovery values for various membrane systems (Metcalf and Eddy 2004).
- Table 2.3 Advantages and disadvantages of membrane treatment technologies (Metcalf and Eddy 2004).
- Table 2.4 Heavy metals contamination caused by natural or man-made disasters.
- Table 3.1 Parameters of Langmuir and Freundlich isotherms for adsorption of Pb(II) ions on the membranes (CS/CA, CS/CA-DZ) at initial pH5, 22-23°C.
- Table 3.2 Color response of 1mg/L Pb(II) ions in presence of interfering cations in the solutions (initial pH5, 22-23°C).
- Table 4.1 Characteristic property of CS/CA and CS/CA-TPPS membranes
- Table 4.2 Immobilized TPPS amounts on various CS/CA-TPPS multifunction membranes.
- Table 4.3 Effect of initial Hg(II) concentrations on the adsorption amount of Hg(II) on the membrane (mg/g) and the residual Hg(II) concentration in the solution (initial pH6, 22-23°C, 100mL of solution volume, 0.02g membrane, contact time 300min).
- Table 4.4 The concentrations of major dissolved components in the various real water samples
- Table 5.1 Results of pseudo second-order kinetics model fitted to experiment data of Hg(II) adsorption on CS/CA-TPPS and CS/CA-TPPS-HA at different initial solution pH values.
- Table 6.1 Pure water fluxes (PWF) of CS/CA, CA/CA-SMP and CS/CA-SMP-TMPyP membranes (22-23°C).
- Table 6.2 The fitting parameters of the Langmuir and Freundlich isotherm models to the adsorption data of Cd(II) on the membranes of CS/CA, CS/CA-SMP-TMPyP (initial pH8, 22-23°C).
- Table 6.3 Uptake of Cd(II) by CS/CA-SMP-TMPyP membrane in the presence of other cations.

LIST OF FIGURES

- Fig. 2.1 Chemical structure of chitosan.
- Fig. 2.2 Comparison of morphology of the CS/CA membrane with higher CS/CA ratio (3-12) as compared to that with a lower CS/CA ratio (2-18) (Liu and Bai, 2006b).
- Fig. 2.3 Schematic representation of the composition and function of a chemical sensor (Lobnik 2006).
- Fig. 2.4 Classification of chemical sensor according to the operation principle of the receptor and transducer (Lobnik 2006).
- Fig. 2.5 Formation of ion-indicator complex.
- Fig. 3.1 Schematics showing the immobilization mechanism of DZ on CS/CA base membrane and the reaction with Pb(II) ions.
- Fig. 3.2 Chromatic change of CS/CA-DZ in 5mg/L lead solutions at different initial pH values (22-23°C).
- Fig. 3.3 The kinetic response of CS/CA-DZ membrane in the detection of 5mg/L lead solution at initial pH5, 22-23°C. (a) Color transition pattern (b) UV/Vis spectra.
- Fig. 3.4 (a) Color change and (b) UV/Vis spectra of CS/CA-DZ in response to Pb(II) ions with concentrations ranging from 0.1mg/L to 200mg/L at initial pH5, 22-23°C (A and A_0 are the absorption intensities of the CS/CA-DZ membranes at 490nm after and before reacting with Pb(II) ions).
- Fig. 3.5 Kinetic adsorption results of lead ions on CS/CA and CS/CA-DZ membranes ($C_0=10\text{mg/L}$, initial pH5; 22-23°C). Error bars are determined from three repeated tests, with errors<5%.
- Fig. 3.6 Experimental adsorption isotherm data and the fitted results of the Langmuir and Freundlich isotherm models to the experimented data. Error bars are determined from three repeated tests, with errors<5% (initial pH5; 22-23°C).
- Fig. 4.1 Schematic of the unit used for filtration study
- Fig. 4.2 SEM images showing the morphologies of CS/CA and CS/CA-TPPS membranes.
- Fig. 4.3 FTIR spectra of (a) TPPS powder; (b) CS/CA base membrane; (c) CS/CA-TPPS multifunctional membrane

- Fig. 4.4 Response of CS/CA-TPPS membrane to Hg(II) ions in a solution with the contact time: (a) optical color change and (b) variation of UV/Vis light absorbance spectrum versus wavelength (TPPS immobilized amount 1.0mg/g, 0.02g membrane, 100mL of solution, initial Hg(II) concentration 1mg/L, initial pH6, 22-23°C).
- Fig. 4.5 Performance of CS/CA-TPPS membranes with different amounts of TPPS immobilized in detection and adsorptive removal of Hg(II): (a) kinetic variation of color changes; (b) variation of UV/Vis light absorbance intensity (in terms of $A-A_0$) at 450nm; and (c) Hg(II) uptake amounts (initial Hg(II) concentration: 200 μ g/L, initial pH6, 22-23°C, 100mL of solution volume, 0.02g membrane; A and A_0 are UV/Vis light absorbance intensity of the membrane at 450nm before and after in contact with Hg(II) ions in the solution).
- Fig. 4.6 Proposed detection (color change) and adsorption enhancement mechanism of Hg(II) by CS/CA-TPPS multifunctional membrane.
- Fig. 4.7 Effect of initial solution pH on the performance of CS/CA-TPPS membrane (a) color change of the membrane after 20min contact time; (b) Hg(II) adsorption uptakes from solutions with initial pH ranging from 4 to 8 (22-23°C, initial Hg concentration 200 μ g/L, 100mL of solution volume, 0.02g membrane).
- Fig. 4.8 Effect of ionic strength on the performance of CS/CA-TPPS multifunctional membrane: (a) variation of UV/Vis light absorbance intensity ($A-A_0$) of the membrane at 450nm and (b) adsorption uptakes of Hg(II) by the membrane (200 μ g/L Hg(II) ions in the solutions with different ionic strength ranging from 0 to 0.2M NaNO₃ (initial pH6, 22-23°C, 100mL of solution volume, 0.02g membrane). Note: The photos in the insert of Fig. 4.8(a) were the membrane samples after 20min contact with the Hg(II) solutions.
- Fig. 4.9 Color change of CS/CA-TPPS multifunctional membrane in Hg(II) solutions with different initial Hg(II) ion concentrations (initial pH6, 22-23°C, 100mL of solution volume, 0.02g membrane).
- Fig. 4.10 Effect of interference metal ions on the performance of the CS/CA-TPPS membrane: (a) the developed color; (b) the UV/Vis light absorption difference (in terms of $A-A_0$) at 450nm after 5min of contact time with the Hg(II) solutions and (c) Hg(II) adsorption uptakes after 300min of contact time with the Hg(II) solutions (initial pH6, 22-23°C, Hg(II) concentration 10⁻⁶M, other cation concentrations 10⁻⁴M, 0.02g membrane).
- Fig. 4.11 Results from the adsorption and desorption experiments: (a)

mercury uptake amount and (b) changes in the light absorbance intensity and developed color in the adsorption and desorption cycles (initial pH6, 22-23°C, initial Hg concentration 10mg/L, 0.02g membrane).

- Fig. 4.12 (a) Color change of the membrane after filtration of and (b) Removal rate of Hg (II) from the various simulated Hg(II) contaminated natural water samples (initial mercury concentration 200µg/L; 22-23°C; membrane area 11.8cm²; applied pressure 1bar).
- Fig. 5.1 Results of individual (a) Hg(II) (800µg/L) and (b) HA (15mg/L) adsorption on CS/CA-TPPS membrane in solutions with initial pH from 6.5 to 8.5. (22-23°C, 0.02g membrane and 100mL solution for each adsorption, inserted photos were obtained after the contact time of 5min for Hg(II) solution and 300min for HA solution).
- Fig. 5.2 Results of sequential adsorption. (a) Hg(II) (800µg/L) adsorption on CS/CA-TPPS-HA membrane; and (b) HA (15mg/L) adsorption on CS/CA-TPPS-Hg membrane in solutions with initial pH from 6.5 to 8.5 (22-23°C, 0.02g membrane and 100mL solution for each adsorption, the inserted picture was obtained after 30min of contact time).
- Fig. 5.3 Changes of developed membrane colors in terms of UV/Vis light absorbance intensity difference ($A-A_0$) at 450nm (A_0 and A are the light absorbance intensities of the membrane surface at 450nm before and after Hg(II) adsorption).
- Fig. 5.4 Desorption results of Hg(II) ions from CS/CA-TPPS-Hg membrane during sequential adsorption of HA. (a) Hg(II) desorption amount; (b) changes in absorbance intensity ($A'-A_0'$) at 450nm and (c) the color change of CS/CA-TPPS-Hg membrane after sequential HA adsorption (22-23°C, initial HA concentration 15mg/L, 100mL, 0.02g membrane).
- Fig. 5.5 The proposed mechanisms of sequential adsorption of (a) Hg(II) and (b) HA on CS/CA-TPPS membrane.
- Fig. 5.6 Result of co-adsorption of 800g/L Hg(II) and 15mg/L HA in the same solution (a) Hg(II) adsorption; (b) HA adsorption; (c) membrane color after adsorption 300min (22-23°C, 100mL solution, initial pH6.5-8.5, 0.02g membrane).
- Fig. 5.7 The color response and Hg(II) uptake amount (q_e) of CS/CA-TPPS membrane in Hg(II) and HA mixed solution (22-23°C, initial Hg concentration 800µg/L, initial HA concentration from 2, 8, or 15mg/L, initial pH6.5, 100mL solution, 0.02g membrane).

- Fig. 5.8 Result of Hg(II) solution filtration by CS/CA-TPPS membrane (a) Removal rate of Hg(II) and (b) membrane color change after filtration of Hg(II) (22-23°C, initial Hg concentration 800µg/L, initial pH6.5, membrane area 11.8cm², applied pressure 1 bar, filtration duration 150min, permeate flux 12.3L/m²·h).
- Fig. 5.9 Result of HA solution filtration. (a) Removal rate of HA and (b) membrane colors after filtration of HA by CS/CA-TPPS membrane (22-23°C, initial HA concentration 15mg/L, initial pH6.5, membrane area 11.8cm², applied pressure 1 bar, filtration duration 150min, permeate flux dropped continuously from 11.5L/m²·h to 7.4 L/m²·h).
- Fig. 5.10 Filtration of Hg(II) solution by CS/CA-TPPS-HA membrane. (a) Removal rate of Hg(II) and (b) the membrane colors before and after sequential Hg solution filtration (22-23°C, Initial Hg(II) concentration 800µg/L, initial pH6.5, membrane area 11.8cm², applied pressure 1 bar, filtration duration 150min, permeate flux around 7.3L/m²·h).
- Fig. 5.11 Filtration of HA solution by CS/CA-TPPS-Hg membrane. (a) Removal rate of HA and (b) the developed color after HA filtration (22-23°C, Initial HA concentration 15mg/L, initial pH6.5, membrane area 11.8cm², applied pressure 1 bar, filtration duration 150min, permeate flux dropped continuously from around 12.1L/m²·h to 8.3L/m²·h).
- Fig. 5.12 Desorption of Hg(II) from CS/CA-TPPS-Hg membrane in the sequential filtration of 15mg/L HA solution.
- Fig. 5.13 Filtration of the solution containing 800µg/L Hg and 15mg/L HA. Removal rate of (a) Hg(II); (b) HA and (c) the membrane color before and after the filtration (22-23°C, initial pH6.5, membrane area 11.8cm², applied pressure 1bar, filtration duration 150min, permeate flux continuously dropped from 11.2L/m²·h to 6.7L/m²·h).
- Fig. 5.14 Filtration of solutions containing both HA and Hg(II) at different HA/Hg(II) ratios. Removal rate of (a) Hg(II), (b) HA and (c) the membrane color changes before and after the filtration runs (22-23°C, initial Hg(II) concentration 800µg/L, initial HA concentration 2mg/L, 8mg/L and 15mg/L, respectively, initial pH6.5, membrane area 11.8cm², applied pressure 1 bar, filtration duration 150min).
- Fig. 6.1 Mechanism of ATRP.
- Fig. 6.2 Schematic representation of the processes to obtain the multifunctional membrane. (a) Immobilization of the surface initiator and the polymerization of negatively charged monomer

(SMP) on CS/CA base membrane surface; (b) coupling of TMPyP molecules to obtain CS/CA-SMP-TMPyP; (c) interaction between cadmium ions and CS/CA-SMP-TMPyP membrane.

- Fig. 6.3 FTIR spectra of (a) TMPyP powder; (b) CS/CA base membrane; (c) surface initiated CS/CA membrane; (d) CS/CA-SMP membrane; (e) CS/CA-SMP-TMPyP membrane.
- Fig. 6.4 UV/Vis spectra of (a) initial TMPyP solution; and final TMPyP solution after adsorption equilibration with (b) CS/CA base membrane; and (c) CS/CA-SMP membrane
- Fig. 6.5 SEM image of (a) CS/CA base membrane; (b) surface initiated CS/CA membrane; (c) CS/CA-SMP membrane; (d) CS/CA-SMP-TMPyP membrane.
- Fig. 6.6 Color change of CS/CA-SMP-TMPyP membrane in responding to Cd(II) ions with (a) different contact time ($C_0=50\text{mg/L}$, initial pH8, 22-23°C); (b) different initial solution pH values ($C_0=50\text{mg/L}$, 22-23°C); (c) different initial concentrations (contact time: 20min, initial pH8, 22-23°C).
- Fig. 6.7 UV/Vis spectra in time response of CS/CA-SMP-TMPyP membrane for detecting Cd(II) ions ($C_0=50\text{mg/L}$, initial pH8, 22-23°C).
- Fig. 6.8 Difference in the absorbance intensity at 445nm for CS/CA-SMP-TMPyP membrane in response to cadmium solution with (a) different initial pH values; (b) different concentrations. The A_0 and A are the absorption signal responses of the CS/CA-SMP-TMPyP membranes at 445nm before and after equilibrating with Cd(II) ions
- Fig. 6.9 Kinetic adsorption results of cadmium ions on CS/CA and CS/CA-SMP-TMPyP membrane ($C_0=50\text{mg/L}$, initial pH8, 22-23°C). Error bars are determined from three repeated tests, with errors<5%.
- Fig. 6.10 Fitting of pseudo second-order kinetic adsorption model to experimental results of cadmium ion adsorption on CS/CA base membrane and on CS/CA-SMP-TMPyP membrane
- Fig. 6.11 Experimental adsorption isotherm data and the fitted results of the Langmuir and Freundlich isotherm models to the experimental data. Error bars are determined from three repeated tests, with errors<5% (initial pH8, 22-23°C).

NOMENCLATURE

AAS	Atomic Absorption Spectrometry
ACDA	2-amino-1 cyclopentene-1 dithiocarboxylic acid
AFS	Atomic Fluorescence Spectrometry
ATRP	Atom Transfer Radical Polymerization
ATSDR	Agency for Toxic Substances and Disease Registry
BE	Binding Energy
BPY	2'2-bipyridyl
CA	Cellulose Acetate
CS	Chitosan
CS/CA membrane	Chitosan/Cellulose Acetate blend membrane
CS/CA-DZ membrane	DZ immobilized on CS/CA membrane
CS/CA-SMP	SMP grafted CS/CA membrane
CS/CA-SMP-TMPyP	TMPyP immobilized on SMP grafted CS/CA membrane
CS/CA-TPPS membrane	TPPS functionalized CS/CA membrane
DPC	1.5-diphenylcarbazine
DZ	Dithizone
EDTA	Ethylenediamine Tetra-acetic Acid
FA	Formic Acid
FTIR/ATR	Attenuated Total Reflectance Fourier Transform Infrared Spectroscopy
FOCS	Fiber optic chemical sensor
HA	Humic Acid
ICP	Inductively Coupled Plasma
ICP-OES	Inductively Coupled Plasma-Optical Emission

	Spectrometer
MCL	Maximum Contaminant Level
MCLG	Maximum Contaminant Level Goal
MF	Microfiltration Membrane
MWCO	Molecular Weight Cut-Off
NF	Nanofiltration Membrane
NOM	Natural Organic Matter
NPDWR	National Primary Drinking Water Regulation
PWF	Pure Water Flux
RO	Reverse Osmosis Membrane
SEM	Scanning Electron Microscope
SiNW	Silicon nanowires
SMP	3-Sulfopropyl methacrylate potassium salt
TEA	Triethylamine
THF	Tetrahydrofuran
TMPyP	5,10,15,20-Tetrakis (1-methyl-4-pyridinio) porphyrin tetra (p-toluenesulfonate)
TPPS	5,10,15,20-tetraphenolporphine tetrasulfonic acid
TT	Treatment Technique
UF	Ultrafiltration Membrane
USEPA	U.S. Environmental Protection Agency
USFDA	U. S. Food and Drug Administration
XRF	X-Ray fluorescence

CHAPTER 1 INTRODUCTION

1.1 Overview

Heavy metals are natural components of the Earth's crust. Their unique properties, including malleability, ductility, resistance to corrosion, high electric and thermal conductivity, make them undoubtedly crucial to the development of human society. Some heavy metals such as copper, selenium and zinc are essential to human body as trace elements to maintain a proper metabolism. However, excessive intake of heavy metals may have detrimental effects to mental and central nervous systems, blood composition, lungs, kidneys, liver and other vital organs. Heavy metals cannot be degraded through the biological metabolism could not be easily excreted from the body. Once entering the human body, even in a small amount, they will accumulate in organs and tissues, and eventually develop chronic toxic effects, such as physical, muscular and neurological degeneration, Parkinson's disease, muscular dystrophy, multiple sclerosis and cancer (de Castro Dantas et al. 2001; Inglezakis et al. 2003; Sanyal et al. 2005).

Ever since the first industrial revolution, heavy metal contaminants have been dramatically increased due to the intensified industrial and urban activities. The major source of heavy metal contaminants is usually from the wastewaters of industries such as electroplating, mining, electric device manufacturing, and metal finishing. Improper effluent discharge, insufficient treatment or poor management of the industrial wastes has introduced an excessive amount of heavy metal contaminants into the natural water system (rivers, lakes and seas), thus posing a great threat to the lives of human beings and other living organisms. Therefore, in order to safeguard the environmental and public health, it is greatly desirable to develop technologies that can effectively warn the presence of heavy metal ions as well as remove them from

the contaminated water.

With the emphasis on water safety and security enhancement in recent years, many efforts have been devoted to develop on-site and in-situ monitoring of heavy metal ions. Among all the technologies, optical sensors have attracted considerable research attention in recent years. Unlike the conventional detection methods such as machine-based analysis devices, optical sensors depending on naked-eye recognition require minimum labor and less sophisticated equipment (Klimant and Otto 1992). The mechanism of the optical sensors is based on the use of optical indicators that can generate and transduce optical signal, i.e., color change, as a response to the presence of certain metal species. For the convenience of applications, the optical indicators are usually immobilized onto solid supporting materials (Balaji et al. 2006).

In the meantime, technologies for heavy metal removal have also been extensively developed. Adsorptive membrane is one of the most promising technologies that are newly developed in recent years. The adsorptive membrane is usually a type of porous membrane bearing functional groups on its external and internal surfaces. These functional groups, such as $-\text{COOH}$, $-\text{SO}_3\text{H}$ or $-\text{NH}_2$, can bond with heavy metal ions through the surface complexation or ion exchange mechanism. Thus, heavy metal ions that are usually at relatively small amounts can be removed from the passing liquid (e.g. water or wastewater) when they are in contact with the membrane surface, even though the dimensions of the metal ions to be removed are much smaller than the pore sizes of the membrane. In comparison with the conventional porous membranes that are designed for the removal of particles with relatively large sizes, the adsorptive membrane provides the additional advantages of efficiently removing

dissolved heavy metal ions, as that could only be achieved by the conventional nanofiltration or reverse osmosis membranes but with much lower energy consumption and higher permeate flux (Liu and Bai 2006a). Although various adsorptive membranes have been developed, chitosan-based adsorptive membrane has appeared to be a promising type. Chitosan (CS) is a biopolymer that widely exists in the shells of crustaceans such as shrimps, crabs, lobsters, and can be easily obtained from seafood processing wastes. The presence of a large percentage of free amine and hydroxyl groups on chitosan structure renders it special chemical property that is particularly suitable for the sorption of heavy metal ions (Guibal 2004).

Over the years, the adsorptive membrane and optical sensor have been developed individually in their respective disciplines. Therefore, a logical interest is raised to explore the possibility of combining the two technologies together. So far, however, there have not been any reported attempts to incorporate adsorptive removal and optical sensing together in a single membrane system to tackle the issue of heavy metal pollution. The present work, therefore, intends to bridge the gap by developing multifunctional membranes for simultaneous visual detection and adsorptive removal of heavy metal ions from aqueous solutions, which will have significant importance in heavy metal pollution control and remediation.

1.2 Research objectives and scopes of the work

The main objective of this work is to develop multifunctional membranes that incorporate the functions of adsorptive removal and visual detection for heavy metal ions with a filtration membrane. However, we may encounter many challenges or issues during the innovation, such as how to immobilize optical indicators on the base

membranes; how to achieve high performance in the new functions without compromising the original function of the base membranes, and what are the influence of water solution compositions on the performance of the developed multifunctional membranes. In order to tackle the issues mentioned above as well as explore the applications of the prepared membranes, this research work is carried out from several aspects and the thesis is organized in the order as described below.

(a) Feasibility of multifunctional membrane concept development

In this study, the first effort was made to immobilize an optical indicator for lead ions, dithizone (DZ), onto a CS/CA blend adsorptive membrane. The obtained membrane (CS/CA-DZ) was tested for its optical response as well as adsorption performance towards lead ions. Experimental results showed that the CS/CA-DZ membrane can achieve visual detection and adsorptive removal of lead ions simultaneously, proving that the concept of multifunctional membrane was feasible and practicable.

(b) Extension of multifunctional membrane concept to other heavy metals

Further attempt was made to extend the concept of the multifunctional membrane to other heavy metal ions. As an illustration, 5,10,15,20-tetraphenolporphine tetrasulfonic acid (TPPS) functionalized CS/CA membrane was prepared and studied for its performance in Hg(II) detection and removal. The effects of various factors, including the amount of immobilized indicator, solution pH, solution ionic strength, initial Hg(II) concentration and the presence of interference ions, were investigated through a series of batch adsorption experiments. The performance of the prepared membrane was tested in both adsorption and filtration with synthetic Hg(II) water samples and real water samples dosed with Hg(II), respectively. The results showed

that the optimum TPPS immobilization amount appeared at 1.0mg (TPPS)/g (dry membrane) and the prepared membrane exhibited good performance for both visual detection and adsorptive removal of Hg(II) in solutions with initial pH ranging from 5 to 8. The influence of ionic strength in the solutions was not significant when the ion concentration was lower than 0.05M (as added NaNO₃). The interference study showed that the membrane possessed good selectivity and sensitivity towards Hg(II) with the presence of other cations, especially alkali and alkaline earth metal ions, even in their relatively high concentrations. Besides, the used membrane was found to be effectively regenerated by 0.01M EDTA and could be reused without significant loss of its functionality. This study has illustrated the potential prospect of the prepared membrane for the simultaneously warning and removal of mercury ions in water and wastewater treatment.

(c) Effect of organic pollutants on the performance of the multifunctional membrane

Followed the previous studies, a further work was directed to investigate the effect of organic contaminants in water on the performance of the multifunctional membrane. The ubiquitous existence of soluble humic substances in natural water, especially humic acid (HA), are suspected to affect the performance of the multifunctional membrane in real applications as HA may influence the speciation, solubility and transport of heavy metal ions in aqueous solutions; react with indicators and functional groups on the membrane; or cause fouling of the membrane. In this study, we investigated the effect of the presence of HA in solutions on the removal and visual detection of Hg(II) ions by the CS/CA-TPPS membrane prepared in the previous section. Experiments were conducted in three phases, i.e., batch adsorption and filtration of individual Hg(II) and HA solutions; sequential adsorption and

filtration of individual Hg(II) and HA solutions; co-adsorption and co-filtration of solutions containing both Hg (II) and HA. The results showed that the existence of HA would improve the removal of Hg(II) but the sensitivity of visual detection of Hg(II) by the multifunctional membrane would be compromised when HA existed in high concentrations. Therefore, the pretreatment for HA removal in the application of the CS/CA-TPPS membrane may be required if the visual detection of Hg(II) has a priority in the treatment of water or wastewater.

(d) Explore the advanced and more versatile method for the immobilization of indicators onto the base membrane

The immobilization of optical indicators onto the base membrane is a key and challenging step to prepare the multifunctional membranes with desired functions. In the fourth part of this study, a versatile post-grafting method - atom transfer radical polymerization (ATRP), was introduced to tackle this issue. 5,10,15,20-Tetrakis (1-methyl-4-pyridinio) porphyrin tetra (p-toluenesulfonate) (TMPyP), an optical indicator for cadmium ions which does not have intrinsic affinity to the CS/CA base membrane was selected as an example for illustration. TMPyP was successfully immobilized onto the CS/CA membrane via the ATRP method. The method was proven to be effective and efficient in modifying the membrane surface properties, which facilitated the immobilization of the optical indicator. Besides, the ATRP method was also found to improve the adsorption capacity of the membrane by introducing more functional groups through the grafted polymer brushes on the membrane surface. Therefore, this method is regarded as a facile and versatile strategy to design the surface of the membranes for the advanced development in multifunctional membrane technology.

CHAPTER 2 LITERATURE REVIEW

2.1 Heavy metal

Metals are defined chemically as “elements which conduct electricity, have a metallic luster, are malleable and ductile, form cations, and have basic oxides”. In order to clarify the individual properties for proper application, metals are usually subdivided into different classes based on their chemical, physical or biological properties, such as semimetal, light metal, heavy metal, essential metal and trace metal (Atkins and Jones 1997).

Over the past two decades, the term “heavy metal” has been used increasingly in various publications and legislations related to the chemical hazards and environmental safety. Many different definitions of “heavy metal” have been proposed, some based on density, some on atomic number or atomic weight, and some on chemical properties or toxicity (Duffus 2002). From the environmental and biological point of view, the term “heavy metal” refers to a group of metal and semimetals (metalloids) with a specific gravity that is at least 5 times of the specific gravity of water, which have been associated with contamination and potential toxicity or ecotoxicity (Hodgson et al. 1998; Webster 1976). This definition is applied in this study.

Appropriate intake of some heavy metals, e.g., iron, copper, manganese and zinc, in small quantity is essential in maintaining biochemical reaction of metabolism, which ensures an optimal health of living organism. These heavy metals are commonly found in foods, fruits, vegetables and commercially available multivitamin products in a small amount (International Occupational Safety and Health Information Centre 1999). Since 19th century, heavy metals have been largely applied in industries such as

battery manufacturing, metal electroplating, textile dying, alloys, steels and so on. Despite their undoubted contributions to the development of human society, heavy metals also pose a threat to the lives of human beings. More and more environmental and health issues related to excessive exposure or ingestion of heavy metals have emerged and become an acute global concern especially in developing countries (International Occupational Safety and Health information Centre 1999).

2.2 Heavy metal pollution

In the last few decades, the world has been undergoing a speedy process of great upheaval and we have seen numerous changes from every aspect of life. However, besides the exhilarating developments and improvements, we are also witnessing a deteriorated environment. Heavy metal contamination has been one of the greatest environmental issues induced. Ever since the first industrial revolution, the occurrence of heavy metal contaminants has dramatically increased as a result of extended industrial and urban activities. More and more people are or would be suffering from the exposure of significant levels of heavy metal contaminants. Heavy metal contaminants can be readily absorbed into living organisms in ions or soluble compound forms and would accumulate in the tissues. Once entering the human body, they will damage or reduce mental and central nervous functions, lower energy levels, and cause malfunction of lungs, kidneys, liver, and other vital organs. The symptoms of acute toxicity are usually severe and develop rapidly, including cramping, nausea, and vomiting; pain; sweating; headaches; difficulty breathing; impaired cognitive, motor, and language skills; mania; and convulsions (Al-Saleh et al. 2008; Ferner 2001). One of the major problems associated with heavy metal contaminants is their potential for bioaccumulation and biomagnifications through the food chain, thus

posing a lasting and pervasive threat to the living organisms. Long-term exposure to heavy metal contaminants may slowly and progressively lead to physical, muscular, and neurological degenerative processes that mimic Alzheimer's disease, Parkinson's disease, muscular dystrophy, multiple sclerosis, and some may even cause cancers (International Occupational Safety and Health Information Centre 1999).

Heavy metals can enter the water supply through industrial and domestic effluents, or from acidic rain that breaks down soils and releases heavy metals into streams, lakes, rivers and groundwater. Table 2.1 shows the national primary drinking water regulations on heavy metal contaminants from the U.S. Environmental Protection Agency (USEPA). Among all the heavy metal pollutants, mercury, lead and cadmium are the most frequently encountered species in industrial wastewater. They are highly toxic even at very low concentrations and have been listed in the USEPA's priority pollutants (Cameron and Sohn 1992). In cooperation with the USEPA, the Agency for Toxic Substances and Disease Registry (ATSDR, a part of the U. S. Department of Health and Human Services) has compiled a Priority List called the "Top 20 Hazardous Substances" in 2001; where lead, mercury and cadmium appear among the top 10. Therefore, in this study, lead(II), cadmium(II) and mercury(II) are selected as the research focus because of their high toxicity and prevalence. The following section provides a brief review of lead(II), cadmium(II) and mercury(II) in terms of their industrial applications, sources of pollution and toxicities to human health.

Table 2.1 Drinking water regulations on heavy metal contaminants (USEPA, NPDWR)¹

Contaminant	MCLG ² (mg/L)	MCL ³ or TT ⁴ (mg/L)	Potential Health Effects from Ingestion of Water
Antimony	0.006	0.006	Increase in blood cholesterol; decrease in blood sugar
Barium	2	2	Increase in blood pressure
Cadmium	0.005	0.005	Kidney damage
Chromium	0.1	0.1	Allergic dermatitis
Copper	1.3	TT ⁵ ; Action level=1.3	Short term exposure: Gastrointestinal distress; Long term exposure: Liver or kidney damage; People with Wilson's Disease should consult their personal doctor if the amount of copper in their water exceeds the action level
Lead	0	TT ⁵ ; Action Level=0.015	Infants and children: Delays in physical or mental development; children could show slight deficits in attention span and learning abilities; Adults: Kidney problems; high blood pressure
Mercury (inorganic)	0.002	0.002	Kidney damage
Selenium	0.05	0.05	Hair or fingernail loss; numbness in fingers or toes; circulatory problems
Thallium	0.0005	0.002	Hair or fingernail loss; numbness in fingers or toes; circulatory problems

1. USEPA (United States Environmental Protection Agency), NPDWR (National Primary Drinking Water Regulation) is a legally- enforceable standard that applies to public water systems. Primary standards protect drinking water quality by limiting the levels of specific contaminants that can adversely affect public health and are known or anticipated to occur in water. They take the form of Maximum Contaminant Levels or Treatment Techniques, which are described below.

2. MCL (Maximum Contaminant Level) - The highest level of a contaminant that is allowed in drinking water. MCLs are set as close to MCLGs as feasible using the best available treatment technology and taking cost into consideration. MCLs are enforceable standards.

3. MCLG (Maximum Contaminant Level Goal) - The level of a contaminant in drinking water below which there is no known or expected risk to health. MCLGs allow for a margin of safety and are non-enforceable public health goals.

4. TT (Treatment Technique) - A required process intended to reduce the level of a contaminant in drinking water.

5. Lead and copper are regulated by a Treatment Technique that requires systems to control the corrosiveness of their water. If more than 10% of tap water samples exceed the action level, water systems must take additional steps. For copper, the action level is 1.3 mg/L, and for lead is 0.015 mg/L.

2.2.1 Lead (Pb)

Lead appears as the number 2 on the ATSDR's "Top 20 List" and accounts for most cases of pediatric heavy metal poisoning (Roberts 1999). Lead pollutants are mainly from industries. Every year, industries produce about 2.5 million tons of lead throughout the world. Electroplating industries, metal furnishing industries, burning of leaded gasoline, mining and metallurgic industries, and trash incineration are by far the greatest sources of lead pollutants. Besides, lead has been used in pipes, drains, and soldering materials for many years. Millions of houses built before 1940 still contain lead (e.g., in painted surfaces), which is subject of causing chronic exposure of lead from weathering, flaking, chalking, and dust. Mild lead poisoning can cause anemia. The victim may have headaches and sore muscles, and may feel generally fatigued and irritable (Harrison and Laxen 1981). High levels of lead exposure may result in toxic biochemical effects in humans such as problems in the synthesis of haemoglobin, malfunction of the kidneys, pains in gastrointestinal tract and joints, and acute or chronic damage to the nervous system (International Occupational Safety and Health Information Centre 1999). It has also been reported that lead has an extensive history as a reproductive toxin, which exerts its effect either directly on the developing fetus after gestation begins, or indirectly on paternal or maternal physiology before and during the reproduction process (Silbergeld 1991). The USEPA has set an action level of lead in drinking water at 15 ppb (USEPA 2008).

2.2.2 Cadmium (Cd)

Cadmium is usually concentrated in argillaceous and shale deposits as greenockite

(CdS) or otavite (CdCO_3) and associated with zinc, lead or copper in sulfide form (Cameron 1992). It is only in the last twenty years that cadmium contamination has become a concern because of the extensive use in industrial applications including coating, steel plating, pigment, stabilizers and manufacturing of nickel/cadmium batteries (Hasan et al. 2006; Rorrer et al. 1993; Tatineni and El-Safty 2006). Cadmium has been listed as the number 7 on the ATSDR's "Top 20 list" and classified as a human carcinogen (Arisawa et al. 2007). Cadmium can produce many toxic effects such as damaging nephridium, causing sugar urine, bone loosening, and bone atrophy and bone distortion. Chronic cadmium exposure may lead to calcium metabolism disorders, renal dysfunction, and an increased risk of certain forms of cancers because cadmium can directly inhibit the remediation of DNA mismatch (McMurray and Tainer 2003). A recent study also showed that cadmium can cause dysfunction in the production of hormones, which leads to infertility (Al-Saleh et al. 2008). Besides, cadmium can be easily absorbed by agricultural crop such as rice. It has been reported that over 60% rice samples in southern region of China were found containing cadmium, which would eventually threaten the health of people who consume the rice. The U. S. Food and Drug Administration (USFDA) have set the limit of cadmium as 15 mg/L in food colors. Meanwhile, the limit for cadmium in drinking water is set at 5 ppb by the USEPA.

2.2.3 Mercury (Hg)

Mercury exists in the environment in three forms: elemental, inorganic and organic mercury. Elemental and ionic mercury contaminants are mainly released by the electrical industry, chloralkali industry, and through the burning of fossil fuels (coal, petroleum). Mercury can be dispersed across the globe by wind and return to the earth

in the form of rain, which then accumulates through the aquatic food chains (Clarkson 1990). The acute and long-term exposure of elemental and ionic mercury may cause gastrointestinal disturbance and renal damage, resulting in tubular dysfunction which leads to tubular necrosis in severe cases (Liu et al. 2003). Methylmercury is the most encountered organic mercury in the aquatic and terrestrial environment. It is formed from ionic mercury through biochemical reaction in the environment and can be easily absorbed by the organisms, accumulate in their bodies and eventually magnify the toxicity to human beings through the food chain. Therefore, even present at very low concentrations in the environment, Hg(II) can cause great potential threat to human health. The USEPA has established the drinking water criterion for mercury at 2µg/L, and the permitted discharge limit of mercury in wastewater at 10µg/L (USEPA 2001). In Europe, even more stringent limits have been set by the European Union at 1 and 5µg/L in drinking water and wastewater effluent, respectively (Ghodbane and Hamdaoui 2008).

2.3 Heavy metal removal technology

The remediation of heavy metal pollutants in environment has drawn great research interest over the last few decades. Numerous physical and chemical approaches have been developed and applied to remove heavy metal ions from contaminated water, such as chemical precipitation, solvent extraction, ion exchange, membrane separation and adsorption. Among all the efforts, adsorption and membrane separation have received a considerable research interests in recent years as effective, economical and environmentally friendly technologies.

Adsorption is generally described as the accumulation of components from a mixture

on the surface of a solid adsorbent. Adsorption has been increasingly used in various applications for purification and separation since the twentieth century and has been demonstrated good potential in water and wastewater treatment for its advantages of being cost-effective and user-friendly. Adsorption can be a physical or physicochemical process utilizing different interaction modes between adsorbents and adsorbates, such as electrostatic interaction, covalent bonding and complexation, and therefore it is efficient in removing pollutants, including heavy metal ions, even at low concentrations (Fu and Wang 2011). Furthermore, selective adsorption also provides the possibility to recover the targeted species for reuse, eliminating the need for their ultimate disposal and thus conserving resources.

Many of the adsorption behaviors are directly related to the physical or chemical properties of the adsorbents, such as surface morphology, porosity and functional groups. Current research interest has been put into the discovery of adsorbents with desired physical and chemical properties for the various applications. Naturally-occurring materials which come from the living or dead biomass are identified to be a desirable source of adsorbents due to their abundant availability, low cost and high bio-compatibility (Wang and Chen 2009). In the last two decades, many natural materials, such as seaweed, alginate, dead biomass, rice hulls, chitin and chitosan, have been widely studied and applied for heavy metal adsorption (Boddu et al. 2003; Deng and Ting 2005; Klimmek et al. 2001; Yun et al. 2001). Among the various natural materials, chitosan has received great research attention. Chitosan is a low-cost biopolymer derived from deacetylation of chitin, the second-most abundant natural biopolymer, which can be found in exoskeletons of crustaceans and insects (Kurita 2006). Normally, chitin is regarded as chitosan when the degree of

deacetylation is more than 70%. It has been reported that the market price for producing chitosan from fish and crustaceans is only US\$15.43/kg (Babel and Kurniawan 2003). The physical and chemical properties of chitosan depend on the degree of deacetylation, polymer mass and crystallinity. The deacetylation degree determines the amount of free amine groups that are mainly account for heavy metal adsorption (Brown and Thornton 1998). Commercial chitosan product normally has a degree of deacetylation from 75% to 95%. Fig. 2.1 shows the chemical structure of chitosan, wherein, the nitrogen atoms in the amine groups hold free electron doublets that can react with metal cations through the chelation mechanism. However, the crystallinity of the polymer affects the accessibility of the sorption sites. A usual practice for decreasing the crystallinity of chitosan is to dissolve it in an acid solution, and then coagulate it in a base solution (Guibal et al. 1998; Piron et al. 1997; Rorrer et al. 1993). Formic and acetic acids are two of the most commonly used acids for preparing chitosan solutions. Inorganic acids, such as hydrochloric acid, nitric acid, perchloric acid, and phosphoric acid, can also be used to dissolve chitosan but prolonged stirring and heating are required (Roberts 1992). Comparing with other adsorption materials such as activated carbon, zeolite, silica gel as well as synthetic polymer adsorbents, chitosan possesses the advantages of being non-toxic, easily biodegradable and highly hydrophilic; hence it is an ideal absorbent for heavy metal adsorption (Guibal 2004; Jang et al. 2004).

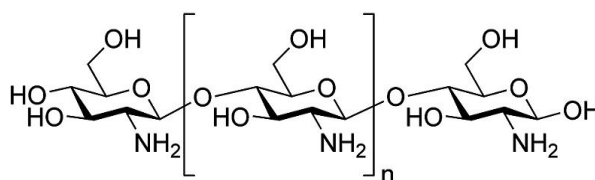


Fig. 2.1 Chemical structure of chitosan

Chitosan has been found to form surface complexes with many heavy metal ions, including Cd(II), Hg(II), Pb(II) and Cu(II) in aqueous solutions, and the binding capacity can be higher than 1mM metal/g chitosan, which is more effective than most commonly used ion exchange resins (Bailey et al. 1999). Besides, due to the existence of amino and hydroxyl functional groups, chitosan could also effectively adsorb various organic compounds including polychlorinated biphenyls, pesticides and dyes (Li et al. 2009; Maghami and Roberts 1988; Yoshizuka et al. 2000). Besides, the functional groups on chitosan make it easier for further functionalization by introducing other desired moieties. However, the use of chitosan in industrial waste treatment has been limited due to its poor mechanical strength.

Membrane separation has become one of the commercially attractive techniques in water and wastewater treatment due to its high removal, low footprint of installation and low reagent consumption (Kurniawan et al. 2006). Conventional membrane separation is based on the sieving mechanism which depends on the sizes of the target components to be separated and the membrane pores. Particles with larger size than the membrane pore size are retained while smaller particles can pass through the membrane. Based on the retaining particle size, membranes are usually classified as microfiltration (MF) membrane, ultrafiltration (UF) membrane, nanofiltration (NF) membrane and reverse osmosis (RO) membrane (Wagner 2001). MF and UF membrane could not eliminate heavy metal ions effectively from the water because the size of metal ions are too small as compared to the pore sizes of the membranes (Kagrananov et al. 2001; Lazaridis et al. 2004; Matis et al. 2004; Mavrov et al. 2003). Nanofiltration with membrane pore size in nanoscale may achieve removal of heavy metal ions at percentage as high as 90-98% (Mohammad et al. 2004; Tanninen et al.

2006; Yurlova et al. 2002); while RO can achieve even higher removal rate up to 99.5%. However, both NF and RO require high energy input in operation as a large pressure of up to 50-70 bars may be necessary for it to work. The high operation pressure must be applied to overcome the osmotic pressure of the feed solution (wastewater), resulting from solvent (water) permeation and retention of ionic compounds, and to drive the permeation flow through the membrane (Ozaki et al. 2002; Qin et al. 2002). Therefore NF and RO are generally not preferred because of the high operating cost and low productivity. Table 2.2 shows the typical energy consumption and product recovery values for various membrane systems; while Table 2.3 lists the advantages and disadvantages of each type of membranes.

Table 2.2 Typical energy consumption and product recovery values for various membrane systems (Metcalf and Eddy 2004).

Membrane Process	Operating pressure kPa	Energy consumption kWh per m ³	Product recovery %
Microfiltration	100	0.4	94-98
Ultrafiltration	525	3.0	70-80
Nanofiltration	875	5.3	80-85
Reverse Osmosis	2800	18.2	70-85

The major challenge in membrane separation technology for water and wastewater treatment now is to remove unwanted components in a more efficient and cost-effective way, especially where the pollutants are at low concentrations and of smaller sizes that conventional separation materials and technologies have reached their limits. In recent years, adsorptive membrane has been developed to mitigate the dilemma between high efficiency and high cost. Adsorptive membrane is an extension or special type of MF or UF membranes bearing functional groups or specific ligands on the membrane surface that could remove contaminants by selective surface adsorption

other than the size exclusion mechanism in the conventional membrane technology. The greater pore sizes of the adsorptive membranes allow the free passage of liquid and other dissolved components but selectively retain certain components to be removed from the passing liquid through the membrane matrix. Selective separation is achieved through specific chemical interactions between the targeted components and the functional groups of the membranes. Therefore, the pore size of the membranes is not crucial in this separation process, which overcomes the limitation of the conventional filtration membranes that depend entirely on pore sizes and work based on the size exclusion mechanism. Therefore, adsorptive membrane can obtain high removal efficiency of heavy metal ions and provide high permeate fluxes at low energy consumption.

Table 2.3 Advantages and disadvantages of membrane treatment technologies (Metcalf and Eddy 2004).

Advantage	Disadvantage
Microfiltration and ultrafiltration	
Can reduce the amount of treatment Chemicals	Uses more electricity, high-pressure systems can be energy-intensive
Smaller space requirement (footprint); Membrane equipment requires 50-80 percent less space than conventional plants	May need pretreatment to prevent fouling; pretreatment facilities increase space needs and overall costs
Reduced labor requirements; can be automated easily	May require residuals handling and disposal of concentrate
New membrane design allows use of lower pressure; system cost may be competitive with conventional waste-water treatment processes	Requires replacement of membranes about every 3 to 5 years
Removes protozoan cysts, oocysts, and helminth ova; may also remove limited amounts of bacteria and viruses	Scale formation can be a serious problem. scale-forming potential difficult to predict without field testing
	Flux rate (the rate of feed water flow through the membrane) gradually declines over time.

	Recovery rates may be considerably less than 100 percent
	Lack of a reliable low-cost method of monitoring performance
Reverse osmosis	
Can remove dissolved constituents	Works best on groundwater of low solids, surface water or pretreated wastewater effluent
Can disinfect treated water	
	Lack of a reliable low-cost method of monitoring performance
Can remove NDMA and other related organic compounds	May require residuals handling and disposal of concentrate
Can remove natural organic matter (a disinfection by-product precursor) and inorganic matter	Expensive compared to conventional treatment

A new trend for adsorptive membrane preparation is the application of naturally occurring biopolymers or their derivatives as the base materials. These biopolymers originally contain functional groups on their polymer backbones. Therefore, their use could greatly simplify the preparation process of adsorptive membranes because the surface modification or grafting of functional groups onto the conventional base membranes, which normally involves a number of steps and also requires harsh physical or chemical conditions, could be avoided or minimized (Beeskow et al. 1995; Randon et al. 1995; Wang et al. 2009; Zhu et al. 2009). Moreover, naturally occurring biopolymers can have many advantages over the synthetic polymers, including high hydrophilicity, good biocompatibility, nontoxicity, low cost and renewability. Chitosan has been studied for membrane preparation over years because it can be dissolved in weak acid solutions and can be easily processed into membranes with different configurations (e.g., flat sheet membrane, hollow fiber) for various applications. Although chitosan has many attractive properties, it has not been widely applied in industries. One of the major problems that affect its application is the poor

mechanical strength. In order to improve its mechanical strength, chitosan is usually blended with other polymers such as cellulose acetate (CA). In the study of Liu and Bai, chitosan/cellulose acetate (CS/CA) blend membrane was prepared by dissolving CS and CA polymers into formic acid, and then coagulated with sodium hydroxide (NaOH) solution (Liu and Bai 2005). Research has also shown that the membrane pore size, porosity and specific surface area of the membrane can be adjusted by controlling the ratio of CS to CA (Fig. 2.2, (Liu and Bai 2006b)). The prepared CS/CA blend membranes were found to possess good adsorption capacity, fast adsorption rates and short adsorption equilibrium times for heavy metal ions such as copper ions (Liu and Bai 2005). CS/CA blend membrane will be used as the base membrane in the present study.

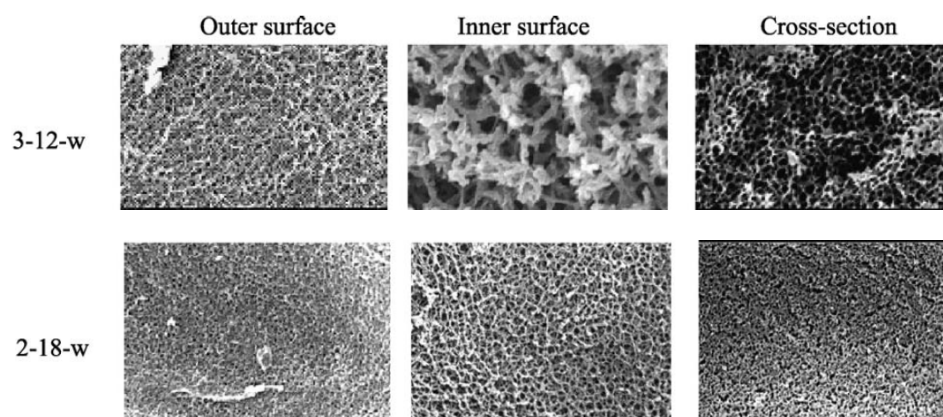


Fig. 2.2 Comparison of morphology of the CS/CA membrane with higher CS/CA ratio (3-12) as compared to that with a lower CS/CA ratio (2-18) (Liu and Bai 2006b).

2.4 Heavy metal monitoring technology

Improper discharge and incidental release of heavy metals to the environment would lead to long-lasting threat to human health (Clifford et al. 2005). Table 2.4 lists some incidents which are associated with heavy metals contamination and public health.

Table 2.4 Heavy metals contamination caused by natural or man-made disasters.

<p>1932, Minamata, Japan (Nishimura 1998)</p> <p>Sewage containing mercury was released by Chisso's chemicals works into Minamata Bay. Poisoning appeared in the population caused by consumption of fish polluted with mercury, resulting in over 500 fatalities.</p>
<p>1986, Sandoz, Switzerland (Güttinger and Stumm 1992)</p> <p>Water used to extinguish a major fire carried 30 ton fungicide containing mercury into the Upper Rhine. Fish were killed over a stretch of 100 km.</p>
<p>1998, Coto De Donana, Spain (Kraus and Wiegand 2006)</p> <p>5 million of mud containing sulphur, lead, copper, zinc and cadmium from a burst dam flowed down the Rio Guadimar. Europe's largest bird sanctuary, as well as Spain's agriculture and fisheries, suffered permanent damages from the heavy metal pollution.</p>
<p>2010, Ajka, Hungary (Schöll and Szövényi 2011)</p> <p>The Ajka alumina sludge spill freeing about a million cubic metres (35 million cubic feet) of liquid waste from red mud lakes containing heavy metals including arsenic, lead, cadmium and mercury. At least 9 people died, and 122 people were injured. About 40 square kilometres (15 square miles) of land were initially affected.</p>
<p>2011, Fukushima, Japan (Suminori 2012)</p> <p>The earthquake and tsunami on Mar. 11th disabled the reactor cooling systems of Fukushima Daiichi Nuclear Power Plant, leading to the leaking of fission products containing heavy metals.</p>
<p>2011, China (www.china-daily.org/China-News/Survey-shows-that-about-10-of-cadmium-in-rice-exceeded-the-disease-can-cause-pain)</p>

The New Century magazine in its Feb. 2011 edition reported that up to 10% of rice grown in China is contaminated by harmful heavy metals like cadmium, lead, mercury and arsenic due to years of pollution stemming from the nation's rapid economic growth.

In order to ensure the environment safety and security as well as safeguard the public health, we should always be vigilant to the heavy metal related industries and well prepared and equipped to manage the continuing effect of heavy metal contamination caused by the unforeseeable disasters. Thus, there is a dire need for advanced technologies that can instantly detect and adequately warn the existence of heavy metals in water that is suspected to be contaminated (Boiocchi et al. 2004; Oehme and Wolfbeis 1997).

2.4.1 Instrumental analysis

Instrumental analysis is a sophisticated technique that can detect the presence and the concentration of analytes in matrix. Various methods such as atomic absorption spectrometry (AAS) (Li et al. 2002; Tsalev et al. 2002), inductively coupled plasma (ICP) (Dias et al. 2005), and atomic fluorescence spectrometry (AFS) (Liu et al. 2003) are currently used to detect heavy metal ions. However, all the methods mentioned above are normally expensive, bulky, complicated to operate and require trained personnel, thus leading to high capital investment and costly maintenance, and yet not being suitable for on-site monitoring applications. Although X-Ray fluorescence (XRF) and electrochemical stripping analysis can be made “portable”, they are impractical in the field application as they require procedures to be carried out in laboratory such as pipetting. Therefore, reliable, easy-to-use and economical methods

are desired, especially the ones that are capable for real-time in-situ and on-site detection or identification of heavy metals without relying on sophisticated instruments and chemists as well as the complicated sample preparation procedures.

2.4.2 Chemical sensor

The growing need for on-site and in-situ monitoring of heavy metal pollutants has led to the development of chemical sensors. A chemical sensor is a device that can transform chemical information into an analytically useful signal. The chemical information, as mentioned above, may originate from a chemical reaction of an analyte or from a physical property of the system investigated (Hulanicki et al. 1991). Basically, a chemical sensor contains two major functional units: a receptor that could catch the analyte and induce a chemical signal; and a transducer that can translate the chemical signals into useful analytical signals (Fig. 2.3).

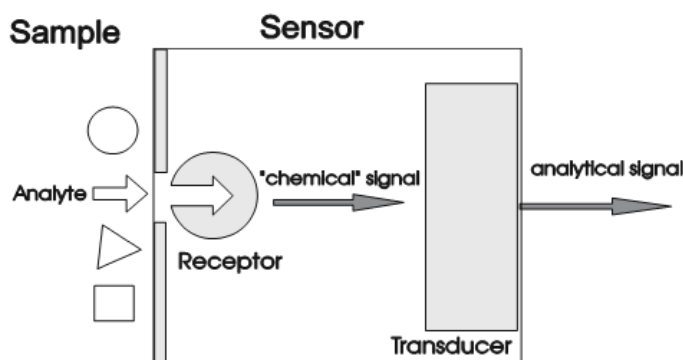


Fig.2.3 Schematic representation of the composition and function of a chemical sensor (Lobnik 2006).

The receptor of a chemical sensor may generate chemical signals of an analyte from different mechanisms, such as:

- Physical, where no chemical reaction takes place. Typical examples are those based upon the measurement of absorbance, refractive index, conductivity, temperature or mass change.
- Chemical, in which a chemical reaction will take place between the receptors and analyte accompanying with chemical signals. One common example is the measurement of pH based on the interaction of the hydronium ion with the glass electrode. Biosensor is a type of chemical sensor, in which biochemical reaction between analytes and receptors is the source of the analytical signal. Typical examples are microbial potentiometric sensors or immunosensors.

Normally, chemical sensors can be classified as optical, electrochemical, electrical, magnetic, thermometric and mass sensitive, according to the operating principle of the transducer (Fig. 2.4).

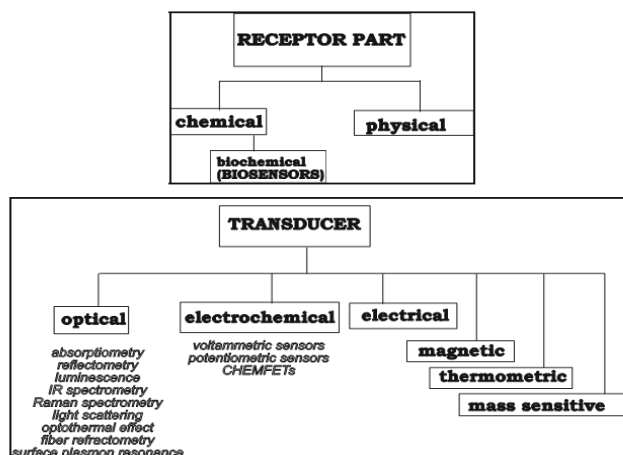


Fig.2.4 Classification of chemical sensor according to the operation principle of the receptor and transducer (Lobnik 2006).

The essential features of chemical sensors are

- (a) Sensitivity: it represents the detection capability with respect to the sample concentration or amount. A highly sensitive sensor can sense very low level of changes.
- (b) Selectivity: most chemical sensors are operated in complex environments, where various parameters change simultaneously. The sensor should have the ability to detect desirable physical quantity among a variety of other undesirable quantities.
- (c) Response time: this feature indicates how fast a sensor can react to changes and generate signals of chemical information depending upon environmental changes.
- (d) Operating life: this is the total lifetime of the sensor as measured by the repeatability of the measurement data within a specific threshold set by the application.

Various types of chemical sensors have been applied in many fields, such as environmental chemistry, waste management, bioremediation of radionuclide and clinical toxicology to protect the public health as well as the environment from unwanted contamination (Islam and Haider 2010). Particularly, many studies have been done to develop chemical sensors for heavy metals. A thin film chemical microsensor based on chalcogenide glass-sensitive materials was reported to exhibit Nernstian response with detection limit of 1×10^{-7} M to Cu(II) and Pb(II) ions; 4×10^{-7} M and 3×10^{-5} M to Cd(II) and Tl(I) ions, respectively (Mourzina et al. 2001). Besides, some amino acids, such as oligopeptides are found to be ideal sensor for heavy metals because of their highly specific complexation affinity towards certain heavy metal

ions. Chow et al. modified the gold electrodes with Asp-Arg-Val-Tyr-Ile-His-Pro-Phe-His-Leu and Gly-Gly-His to detect Pb(II) and Cu(II) respectively, where the oligopeptide-modified electrodes were coupled to cyclic voltammetry or Osteryoung square wave voltammetry to transduce the oligopeptide-metal binding events (Chow 2005). These electrodes can detect metal ions with high sensitivity and selectivity; and therefore receive considerable attention due to their potential for easy detection and quantification of the pollutant species. Silicon nanowires (SiNW) have also been applied as nanometer-scale sensors for the detection of metal ions ever since the discovery of their electrical properties. An attractive feature of the SiNW-based sensor is that the chemical binding can be monitored directly by using the changes in conductance or related electrical properties (Cui et al. 2001; Li et al. 2004). However, the mentioned electrochemical sensors are usually suffering from electrical interference and require a close connection of the reagent phase with the electrode body, which limits their application for on-site usage.

2.4.3 Optical chemical sensor with visual detection property

Among the many types of chemical sensors, the optical sensors which rely on optical detection of a chemical species represent a promising means as comparing with the traditional electrochemical sensors (Toth 1999). The recent years have seen an increasing activity in the development of optical sensors. Fiber optic chemical sensors (FOCSs) represent a subclass of optical sensor in which an optical fiber is used as part of the transduction element. Various fiber optic chemical sensors (optodes) for the determination of heavy metals have been reported in the literatures (Kirkbright et al. 1984; Valcarcel and Luque de Castro 1990). Most recently, there is a growing research interest on the development of non-fiber optic method for direct visual

detection, especially in terms of chromatic (color) change. This method is considered to be more convenient in application because the sensing results can be easily read out by naked eyes without involving any special transducers and substantial or complicated spectroscopic instrumentation (Chen et al. 2007; Zhang et al. 2004). It is regarded as a combination of sensitivity, selectivity, simplicity, low cost and easy data reading (Ensafi et al. 2008a; Ensafi et al. 2008b).

There are two basic sensing schemes for the visual detection of heavy metal ions:

➤ Detection based on intrinsic optical properties of heavy metals

In this case, quantification is accomplished via measurement of adsorption (ranging from the UV to the near infrared), or via luminescence. The respective laws of Lambert-Beer, Parker, or Kubelka-Munk are applicable to correlate absorbance, fluorescence or reflectance with analyte concentration. This sensing mechanism can be applied to heavy metals include copper (Freeman et al. 1985), cobalt, nickel, the lanthanide ions europium and terbium, and the radionuclides uranium (Boisde et al. 1991; Malstrom 1983), and plutonium (Boisde et al. 1991). However, such "sensors" lack specificity since they are interfered by other species absorbing at the same wavelength, and by sample turbidity and changes in refractive index. Besides, many of the above sensors are only applicable to detect heavy metals with relatively high concentrations because the molar optical absorptivities of heavy metals are relatively low for detection.

➤ Indicator (or label)-mediated sensing

Many compounds could bind with metal ions and generate changes in their light absorption accordingly, which make it possible to detect metal ions through the

optical changes of the compounds. These compounds are normally regarded as indicators (Fig. 2.5), which act as both receptors and transducers for the metal ions that cannot be determined directly by their intrinsic optical properties.

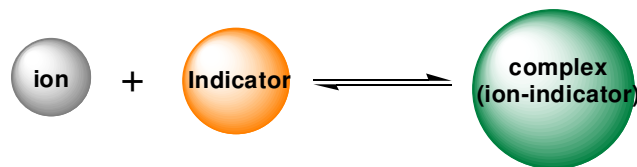


Fig. 2.5 Formation of ion-indicator complex

In the past few years, there have been increased activities to develop optical indicators for heavy metal ions. One of the achievements is the “chromogenic ionophore-based cation detection”. The term ionophore is used to describe a compound, normally an organic ligand, which selectively binds ions. Typically, ionophores are macrocyclic molecules with ion binding cavities. Chromogenic ionophores are designed by introducing chromogenic moieties into ionophores which could bring specific visible color change upon the interaction with the target metal cations, thus serving as chromatic indicators selectively for these metal ions. For the convenience of practical applications, the chromogenic ionophores are usually immobilized on or entrapped into a suitable solid matrix such as polymer membrane. For example, an optical chemical sensor for Ni(II) was developed by immobilizing 2-amino-1 cyclopentene-1 dithiocarboxylic acid (ACDA) onto transparent acetyl cellulose films (Steinberg et al. 2003). Besides, the selective determination of Cu(II) was accomplished by dissolving pyrocatechol violet indicator in plasticized PVC membrane as a lipophilic ion pair with tetraoctylammonium cation. The membrane obtained could respond to Cu(II) by changing color irreversibly from yellow to green (740nm) (Steinberg et al. 2003).

The selection of optical indicators, solid matrix and immobilization methods exerts a significant effect on the performance of the detection (Oehme and Wolfbeis 1997). The choice of optical indicators is usually based on its sensitivity, selectivity towards the target analytes; while the preference of solid matrix is governed by parameters such as permeability for the analyte, mechanical stability and its suitability for indicator immobilization (Oehme et al. 1998). Besides, the immobilization method is based on the physical and chemical properties of the selected optical indicator and solid matrix (Lobnik 2006). Extensive efforts have been made to discover and develop highly sensitive and selective optical indicators (Feng and Chen 2007; Li et al. 2006; Mohr 2006; Ng and Narayanaswamy 2006; Umemura et al. 2006). For example, Dithizone (DZ), diphenylcarbazide (DPC), 5,10,15,20-tetraphenylporphine tetrasulfonic acid (TPPS) and a,b,c,d-tetrakis(1-methylpyridinium-4-yl)porphine *p*-toluenesulfonate (TMPyP) were found to be highly sensitive and selective towards Pb(II), Cr(VI), Hg(II) and Cd(II), respectively (Balaji et al. 2006). Besides, a newly synthesized thioxanthone derivative, 1-hydroxy-3,4-dimethylthioxanthone has proven to be an excellent optical indicator for copper(II) ions because of the low detection limit (25.1 µg/L) and fast response time (<1min) (Yari and Afshari 2006). Meanwhile, considerable studies have been carried out to develop effective methods to immobilize optical indicators on the supporting materials. The immobilization can be achieved through different ways such as electrostatic interactions, van der Waals force, hydrogen-bonding interactions and ion exchange. Ensafi et al. immobilized 4-hydroxy salophen on triacetyl cellulose membrane through covalent bonding for the detection of Hg(II) and Cd(II) ions (Ensafi et al. 2008a; Ensafi et al. 2008b). Lerchi et al. dissolved methylen bis(diisobutyl dithiocarbamate) in a plasticized PVC membrane for the detection of Hg(II) (Lerchi et al. 1994); while Scindia et al. immobilized 1.5-

diphenylcarbazide (DPC) into cellulose acetate matrix through an anion exchanger (Aliquat-336) to determine Cr(VI) in aqueous samples (Scindia et al. 2004). In order to achieve a more stable immobilization, advanced approaches such as post-grafting and building-block methods were developed and applied. In the post-grafting technique, the cage solid carriers were first modified by silane- or thiol-coupling agents to enhance and tune the polarity of the solid carriers' surfaces. In the building-block methods, the same purpose was achieved by using certain surfactant to tune the polarity of the material surfaces before the indicator immobilization. Optical sensors obtained by these approaches were reported to be stable and robust without compromising the sensitivity and selectivity of the optical indicators towards target ions (El-Safty et al. 2008a). These studies on optical indicators and immobilization methods are essential references to the present work of developing multifunctional membrane for visual detection and adsorptive removal of heavy metal ions.

2.5 Significance of this study

Adsorptive membrane and optical sensor have been regarded as two promising techniques for the control of heavy metal contamination in their individual areas. There is a desire to combine the two technologies together to achieve heavy metal detection and removal simultaneously in a single membrane filtration process. This integration may have significant meaning in water and wastewater treatment as well as water quality and security monitoring. Besides, it will have other practical benefits in applications such as enhancing the overall treatment efficiency, simplifying the treatment system and reducing the environmental footprint. In this work, innovative attempts have been made to develop multifunctional membrane for visual detection and adsorptive removal of Pb(II), Hg(II) and Cd(II) respectively. The interdisciplinary

nature of the multifunctional membrane provides an innovative alternative to the conventional techniques, which would have a great prospect in heavy metal pollution remediation to safeguard water quality and security as well as public health.

**CHAPTER 3 DEVELOPMENT OF A NOVEL MULTIFUNCTIONAL
MEMBRANE FOR VISUAL DETECTION AND ADSORPTIVE REMOVAL
OF LEAD(II) IONS IN AQUEOUS SOLUTIONS**

SUMMARY

A multifunctional membrane for visual detection and enhanced adsorptive removal of lead ions in aqueous solution was prepared by immobilizing lead sensitive ligand, dithizone (DZ), onto chitosan (CS) /cellulose acetate (CA) blend membrane. The prepared membrane can display visible color change (from yellow to red) as a response to the presence of lead ions in aqueous solutions. At the same time, lead ions can be adsorptively removed by the functional groups on the membrane surface. Thus, this development demonstrated a truly multifunctional membrane technology that can achieve optical detection and adsorptively removal of lead ions simultaneously in a single membrane process.

3.1 Introduction

Anthropogenic activities have generated large amounts of industrial and domestic wastes that may contain pollutants with detrimental and even lethal effects to the environment and human beings. Lead pollution in water or wastewater for example has been one of the problems that cause a great concern to the living lives (Dias et al. 2005). Lead-containing pollutants are often introduced into the environment through the effluents discharged from industries such as electroplating, metal furnishing and mining. It is well known that lead ions could not be degrade into harmless end products during the metabolic pathway in the environment. It can accumulate in human body and may cause dysfunction of the kidneys, liver, brain and central nervous systems (Eiden et al. 1980; Jin and Bai 2002). Therefore, it is essential to develop high-performance technologies that can effectively warn the presence of lead ions in as well as remove them from the contaminated water.

Heavy metal sensing technology has attracted considerable attention in recent years. Among the many sensing techniques, optical sensor that provides instant visual indication is considered as one of the most advantageous methods because of its simple and instant on-site naked-eye recognition with less labor demands and lower cost, comparing with other methods such as atomic absorption spectrometry, fluorescent sensors and electrochemical techniques (Chatterjee et al. 2002; Hashem 2002; Yaman and Dilgin 2002). In order to make optical sensors more applicable, the chromophore indicators (e.g., indicator dyes) are usually immobilized on or entrapped into a suitable solid matrix (Che et al. 2003; Choi et al. 2006). Porous membrane could also be an ideal pedestal for carrying chromophore receptors as it provides a robust, open and tunable scaffold for the indicators.

In this study, a novel multifunctional membrane was designed to achieve visual detection and adsorptive removal of heavy metal ions, with a particular interest in lead ions. A lead-sensitive optical ligand, dithizone (DZ), was immobilized onto the chitosan (CS)/cellulose acetate (CA) blend membrane through a simple solution reaction. The prepared membrane was tested for its optical response as well as adsorption behavior towards lead ions. Unlike other developments that focused either on adsorbing or sensing heavy metal ions, the membrane obtained in this work can achieve both functions in a single membrane system. To the best of our knowledge, this is the first kind of multifunctional membrane prepared for on-site naked-eye detection and adsorptive removal of lead ions in aqueous solutions.

3.2 Materials and methods

3.2.1 Materials

CS flakes (85% deacetylated) were supplied by Sigma-Aldrich. CA, with acetyl content of 40%, was purchased from Fluka. Formic acid (98-100%) from Fluka was used as the co-solvent for both the CS and CA polymers. NaOH solution (2 wt.%) was used as the nonsolvent to coagulate the CS/CA blend membrane. DZ (>85%), from Sanland-Chem International Inc., was used as the optical indicator for lead ions. Ethanol (>99.9%) from Merck was used for the immobilization of DZ onto CS/CA blend membrane. $\text{Pb}(\text{NO}_3)_2$ standard solutions (1000 mg/L) from Merck was used in the adsorption experiments. Deionized (DI) water was used to prepare all test solutions as needed.

3.2.2 Preparation of porous CS/CA blend membrane

The general method for the preparation of CS/CA blend membrane was the same as

described elsewhere (Liu and Bai 2006a). In this study, the composition of CS/CA/FA was 2/16/82 by weight. CS and CA blend solution was prepared by stirring CS and CA together in formic acid (FA) at 200 rounds per minute (rpm) overnight at room temperature. The resulted homogenously blended solution was then degassed by a centrifuge at 8000rpm for 30min to free the air bubbles entrapped in the dope solution. The membrane was prepared by phase inversion in a wet process. The degassed solution was spread with an applicator (0.6mm slot) on a glass plate. The glass plate was subsequently immersed into a coagulation bath (2% NaOH solution). After peeling from the glass plate, the membrane was washed thoroughly with DI water, then dried and stored in a vacuum desiccator at room temperature (22-23°C) prior to further use for characterizations or performance tests.

3.2.3 Immobilization of DZ on CS/CA membrane

0.1g DZ was firstly dissolved in 50mL ethanol (>99.9%) in a flask. Then, 2g dry CS/CA membrane pieces were added into the solution. The mixture in the flask was stirred at room temperature for 30min, followed by a gentle evaporation of ethanol with a rotavapor (BUCHI Rotavapor R-210) at 40°C. The prepared membrane was finally washed thoroughly with DI water until no elution of DZ was detected by UV/Vis spectrometer. The membrane was then vacuum-dried at room temperature and stored in a vacuum desiccators for further uses. The obtained membrane is denoted as CS/CA-DZ in this thesis.

3.2.4 Experiments for chromatic response of the membranes in detection of lead ions in solutions

The tests were first done for lead solutions with different initial pH values. Lead

solutions with an initial concentration of 5mg/L were prepared by diluting the 1000mg/L standard lead solution with DI water and then adjusted to pH values in the range of 2 to 11 with dilute HCl or NaOH solutions. Membrane, cut into pieces, with a weight of around 0.06g, was added into a 50mL flask containing 20mL of a lead solution at a specific initial pH value. The contents in the flasks were shaken in an orbital shaker at 150rpm under room temperature for 20min. The membrane pieces were then taken out from the flasks, rinsed with DI water and used for the color assessments.

Next, the response time of the prepared functional membrane in the color change at different contact times was investigated. Pieces of the membrane with a weight of 0.06g were added respectively into each of the lead solution samples (initial concentration 5mg/L, solution volume 20mL, initial pH value 5, 22-23°C) with continuous shaking at 150rpm for different reaction times. Membrane samples at various reaction contact times were taken out for the color assessments.

The chromatic response of the functional membrane to lead solutions with different concentrations was also examined. The experiments were similarly conducted as above but at a different initial lead concentration ranging from 0 to 200mg/L with a contact time of 10min (initial pH value 5, 22-23°C).

3.2.5 Lead adsorption experiments

Adsorption kinetic study was carried out to characterize the uptake rates of lead ions and also the time to approach adsorption equilibrium. The experiments were conducted by adding 0.2g membrane pieces to 200mL lead solution with the initial

concentration of 10mg/L, at initial pH value 5 (22-23°C). The mixture was shaken on an orbit shaker at 150rpm for up to 600min. A 10mL amount of the solution was taken at each desired time interval, filtered through a 0.45µm Waterman membrane filter and then analyzed with an Inductively Coupled Plasma-Optical Emission Spectrometer (ICP-OES, Perkin Elmer Optima 3000DV) for determining the lead concentrations. The adsorbed amount of lead on the membrane at time t_i , $q(t_i)$ (mg/g), was calculated from the mass balance equation as:

$$q(t_i) = \frac{\sum (C_{t_{i-1}} - C_{t_i})V_{t_{i-1}}}{m} \quad \text{Eq. 3.1}$$

where C_{t_0} ($=C_0$) is the initial lead concentration, C_{t_i} (mg/L) is the lead concentration at time t_i ; V_{t_i} (L) is the volume of the solution at time t_i , and m (g) is the dry weight of the membrane pieces added.

Adsorption isotherm study was conducted to illustrate the adsorbed lead amounts versus the metal concentrations in the solutions. The experiments were conducted by adding about 0.06g membrane pieces to a number of 50mL flasks containing 20mL lead solution with different initial concentrations (in the range of 0-200mg/L) at initial pH value 5, 22-23°C. The contents in the flasks were shaken on an orbital shaker at 150rpm for a contact time of 300min (above the adsorption equilibrium time of about 200min). As predicted by the MINEQL+ software analysis, no lead precipitation would occur under the experimental conditions. The adsorbed amount at adsorption equilibrium, q_e (mg/g), was calculated by the following equation:

$$q_e = \frac{(C_0 - C_e)V}{m} \quad \text{Eq. 3.2}$$

where C_0 (mg/L) and C_e (mg/L) are the initial and final lead ion concentrations in the solution in each flask, respectively, V (L) is the volume of the solution in each flask,

and $m(g)$ is the dry weight of the membrane pieces added. For comparison, the same type of experiment was conducted with the CS/CA base membrane.

3.2.6 Experiments on interference study

The interference of other metal ions in the solution on the response and uptake of lead ions by the functional membrane was examined. The experiment was conducted by equilibrating the membrane pieces with solutions containing a fixed concentration of lead ions (1mg/L) at initial pH value 5, 22-23 °C with the presence of other metal ions, including K^+ , Na^+ , Ca^{2+} , Mg^{2+} , $Cd(II)$, Zn^{2+} and Ni^{2+} individually at different concentrations.

3.3 Results and discussion

3.3.1 Mechanisms of DZ immobilization and DZ interaction with lead ions

DZ has been reported as a spectrophotometric reagent for lead ions in the literatures (Deoliveira and Narayanaswamy 1992; Zaporozhets et al. 1999). It can change color in response to the interaction with lead ions in solutions. As reported, DZ can be immobilized onto different types of solid matrix such as silicas and Amberlite XAD-4 resin through van der Waals force or H-bonding interactions (El-Safty et al. 2008a). However, the immobilization of DZ on chitosan based membrane for visual detection and adsorptive removal of lead ions was never reported. In this study, DZ was immobilized on CS/CA membrane through a simple solution reaction. The mechanism of DZ immobilization and the binding event of lead ions on the obtained membrane were proposed in Fig. 3.1.

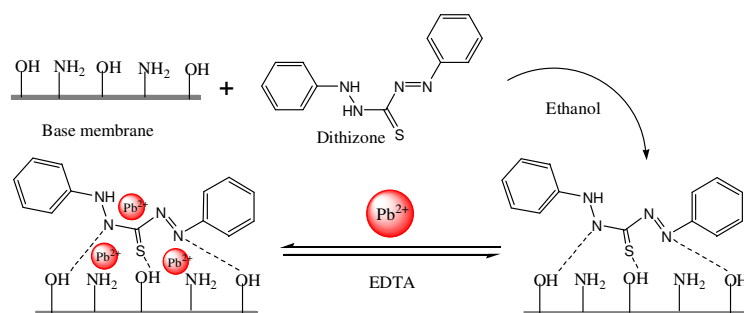


Fig. 3.1 Schematics showing the immobilization mechanism of DZ on CS/CA base membrane and the reaction with Pb(II) ions.

3.3.2 Effect of initial solution pH

The solution pH is usually an important parameter affecting the detection performance of heavy metal ions on sensitive materials, because it not only affects the form of metal species in solution but also influence the surface properties of the sensitive materials in terms of dissociation of functional groups and surface charges. Therefore, the influence of solution pH on the detection of lead ions with the prepared CS/CA-DZ membrane was investigated by emerging the membrane pieces in a solution containing 5mg/L lead at different initial pH values for a fixed time of 20min, As shown in Fig. 3.2, the results demonstrate that the CS/CA-DZ membrane exhibited obvious chromatic change when the initial solution pH was higher than 4, particularly in the initial pH range of 5-6. It is expected that the color change of the functional membrane at specific pH values depend on the feature of metal complex formation between lead ions and the DZ molecules on the membrane. The binding events of the nitrogen-containing DZ to lead ions may be optimum in the initial solution pH range of 5 to 6. In lower pH values, less Pb-DZ complex occurred due to the interaction of the protonated DZ molecules with positively charged lead ions (El-Safty et al. 2007b). However, with the increase of solution alkalinity (e.g., initial pH>10), the membrane showed lighter color than those were at initial pH value 5-6. This can be attributed to

the formation of $\text{Pb}(\text{OH})_2$ precipitate in the solution, which reduced the availability of free lead ions that can interact with the DZ molecules.

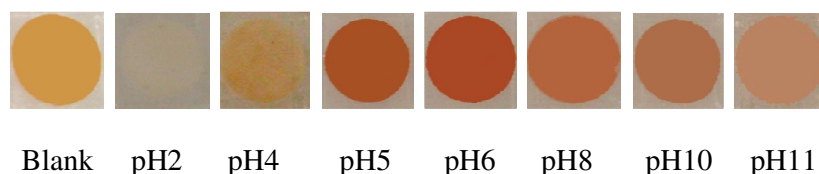


Fig. 3.2 Chromatic change of CS/CA-DZ in 5mg/L lead solutions at different initial pH values (22-23°C).

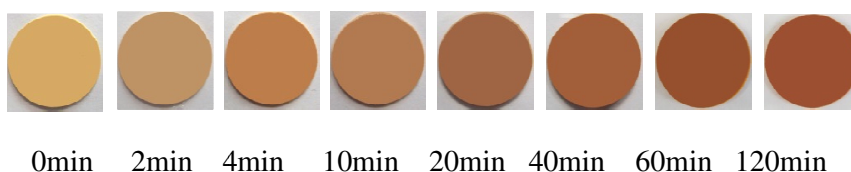
3.3.3 Effect of contact time

The response time of the prepared lead sensitive membrane was tested by adding the membrane into 5mg/L lead solutions at initial pH value 5 and 22-23°C. The time-evolution of the membrane color and the corresponding reflectance spectra of the membrane (measured with a UV/Vis spectrophotometer) are shown in Fig. 3.3. The results in Fig. 3.3(a) suggest that the CS/CA-DZ membrane had a quick visible color change response (within 5min) when it contacted with the lead ion in solution. The UV/Vis spectra in Fig. 3.3(b) exhibit a hypsochromic shift for the absorbance peak, λ_{max} , from 490nm to 440nm with the increase of the contact time. This result suggests that an overall color change of the membrane surface from yellow to red would occur, which is consistent with those observed from the photos in Fig. 3.3(a). The rapid and relatively sensitive detection of $\text{Pb}(\text{II})$ ions under the naked-eyes without using sophisticated instrument shows a great potential of the prepared membrane for practical and on-site application in water and wastewater treatment process.

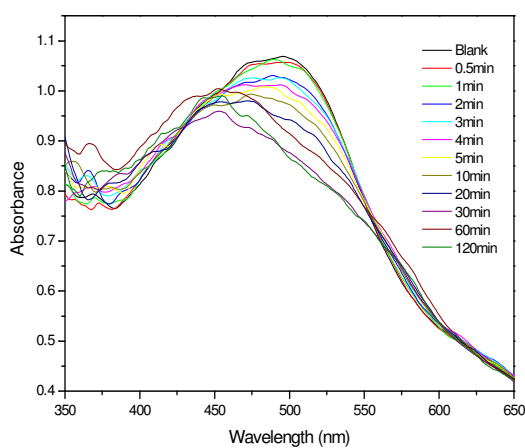
3.3.4 Effect of lead concentration

Fig. 3.4 shows the color-change pattern and the difference in absorbance intensity at 490nm of the prepared CS/CA-DZ membrane in response to lead ions with different concentrations. The results in Fig. 3.4(a) show that the color change increased with

the lead ion concentrations in the solution. In Fig. 3.4(b), the intensity difference at 490nm ($A_0 - A$) from the UV/Vis spectra was calculated. The intensity difference is found to increase with the increase of the lead ion concentrations from 0.01 to 5mg/L. Then, the saturation effect is gradually observed when the lead concentration is higher than 10mg/L. These results indicate that the color change is related to the amount of lead ions adsorbed or interacted with the immobilized DZ probes on the membrane.

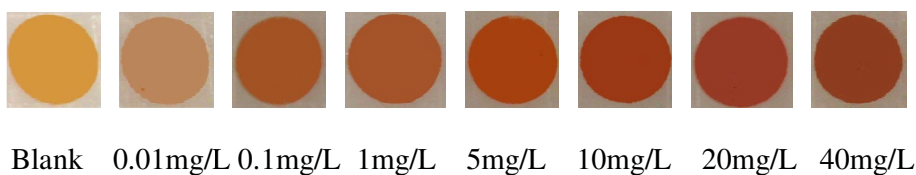


(a)

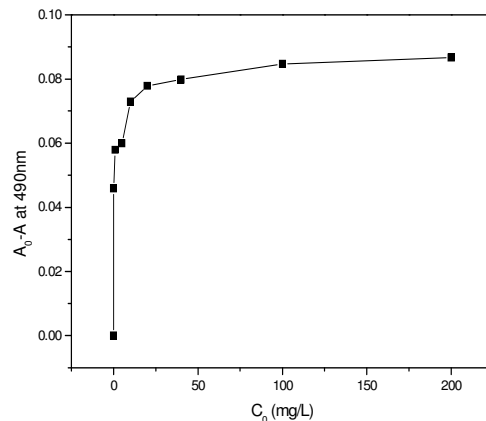


(b)

Fig. 3.3 The kinetic response of CS/CA-DZ membrane in the detection of 5mg/L lead solution at initial pH value 5, 22-23 °C. (a) Color transition pattern (b) UV/Vis spectra.



(a)



(b)

Fig. 3.4 (a) Color change and (b) UV/Vis spectra of CS/CA-DZ in response to Pb(II) ions with concentration ranging from 0.1mg/L to 200mg/L at initial pH value 5, 22-23 °C (A and A_0 are the absorption intensities of the CS/CA-DZ membranes at 490nm after and before reacting with Pb(II) ions).

3.3.5 Adsorption kinetics of lead ions on the membrane

Adsorption kinetic study was conducted to evaluate the uptake rate of lead ions on the prepared membrane. As shown in Fig. 3.5, the CS/CA-DZ membrane had both higher adsorption uptakes and shorter equilibrium time than the CS/CA base membrane. It is observed that lead ion uptake on the CS/CA-DZ membrane reached an adsorption equilibrium in around 100min with an adsorption amount up to 2.3mg/g in this case. In contrast, lead ion adsorption on the CS/CA base membrane underwent a slower process with a lower uptake amount (up to 0.5mg/g at around 300min). The enhanced performance of the CS/CA-DZ membrane can be attributed to the immobilized DZ probes that provide more functional groups ($-NH_2$, $-NH-$, $-N-$) on the prepared membrane to serve as adsorption sites for lead ions, thus providing a higher adsorption capacity and shorter equilibrium time than those of the CS/CA base membrane.

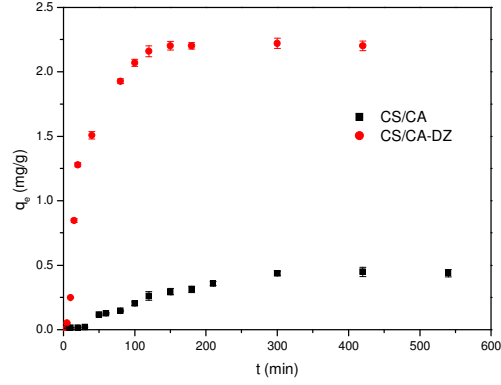


Fig. 3.5 Kinetic adsorption results of lead ions on CS/CA and CS/CA-DZ membranes ($C_0=10\text{mg/L}$, initial pH value 5; $22\text{-}23^\circ\text{C}$). Error bars are determined from three repeated tests, with errors $<5\%$.

3.3.6 Adsorption isotherms

The experimental adsorption isotherm data of the CS/CA base and the prepared CS/CA-DZ membranes were obtained, as shown in Fig. 3.6. To well understand the adsorption behaviors, the Langmuir and Freundlich isotherm models are applied to fit the experimental data respectively. The Langmuir equation can be expressed as:

$$q_e = \frac{q_m c_e}{K_L + c_e} \quad \text{Eq. 3.3}$$

where q_e is the amount of adsorption uptake (mg/g) at adsorption equilibrium, q_m is the maximum uptake capacity (mg/g), c_e is the equilibrium concentration of lead ions in the solution (mg/L), and K_L is the Langmuir adsorption constant (L/mg), reflecting the affinity of the adsorbate for the adsorbent.

The Freundlich equation, which is an empirical equation used to describe heterogeneous adsorption systems, can be represented as follows:

$$q_e = K_F c_e^{\frac{1}{n}} \quad \text{Eq. 3.4}$$

where q_e and c_e have the same definitions as before and K_F is the Freundlich constant

$[(\text{mg/g})(\text{L/mg})^{1/n}]$ which has a positive correlation with the adsorption capacity, and n is an empirical parameter, in general larger than 1. It will increase with the increasing degree of the heterogeneity.

The fitting of the Langmuir and Freundlich models to the adsorption data is also included in Fig. 3.6. The corresponding fitting parameters for the Langmuir and Freundlich isotherm models are given in Table 3.1. From the results in Fig. 3.6 and the correlation coefficients (R^2) in Table 3.1, it is found that the adsorption of Pb(II) ions on CS/CA and CS/CA-DZ membrane can be fitted by both Langmuir and Freundlich isotherm models, giving R^2 values higher than 0.98. The q_m value which represented the maximum adsorption capacity based on the Langmuir isotherm, was found higher for CS/CA-DZ than CS/CA base membrane. Meanwhile, the Langmuir constant (K_L) was found lower for CS/CA-DZ membrane. The value of K_L is related to the affinity of binding sites; a low value of K_L indicated a high affinity towards the adsorbate (Guibal et al., 1999). The K_L values in this study indicated that the CS/CA-DZ membrane had higher affinity towards Pb(II) ions than the CS/CA base membrane.

Based on the Freundlich isotherm, the adsorption capacity, K_F obtained for CS/CA-DZ membrane was higher than CS/CA base membrane. But, for both membranes the n values which represented the favorability of the adsorption were more than one, indicating that the adsorption intensity is good (or favorable) at high concentration. The parameter n is also related to the degree of surface heterogeneity. A higher n value indicates more heterogeneous surface whereas a value closer to or even one indicates the adsorbent has relatively more homogeneous binding sites (Chen et al., 2007). The heterogeneity factor n for the CS/CA-DZ adsorption system is calculated

to be 1.65 which is greater than that for the CS/CA adsorption system (1.339). This could be attributed to the existence of more functional groups ($-\text{NH}_2$, $-\text{NH}-$, $-\text{N}-$) on the CS/CA-DZ membrane from the immobilized DZ molecules, which could exhibit different binding energies for the adsorption.

From the Langmuir model fitting, the maximum adsorption capacity of lead ions on the prepared CS/CA-DZ membrane is predicted to be about 25mg/g, much higher than about 13mg/g for the CS/CA base membrane. In other words, the functionalization of CS/CA for the visual detection of lead ions also significantly increased the adsorption capacity of the prepared membrane for lead ions. The higher adsorption capacity of lead ions on the prepared CS/CA-DZ membrane is also supported by the greater value of K_F for CS/CA-DZ than that for CS/CA from the Freundlich model fitting analysis given in Table 3.1.

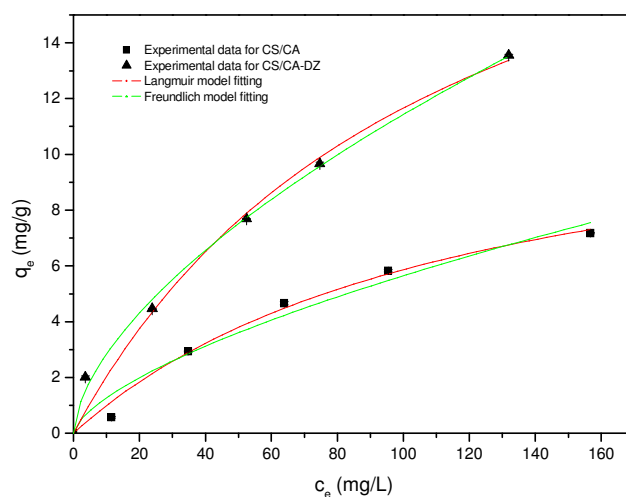


Fig. 3.6 Experimental adsorption isotherm data and the fitted results of the Langmuir and Freundlich isotherm models to the experimented data. Error bars are determined from three repeated tests, with errors < 5% (initial pH value 5; 22-23°C).

Table 3.1 Parameters of Langmuir and Freundlich isotherms for adsorption of Pb(II) ions on the membranes (CS/CA, CS/CA-DZ) at initial pH value 5, 22-23°C.










Membranes	Langmuir model			Freundlich model		
	$q_m(\text{mg/g})$	$K_L(\text{L/mg})$	R^2	n	$K_F(\text{mg/g})(\text{L/mg})^{1/n}$	R^2
CS/CA	12.9034	120.1239	0.9909	1.3385	0.2866	0.9877
CS/CA-DZ	24.7104	111.9256	0.9869	1.651	0.702	0.9985

3.3.7 Interference of other cations

The interference of other cations on the detection of lead ions by CS/CA-DZ was investigated. An ion was considered as interference when its presence produced a different color change or resulted in a variation in the absorbance of the analytes at greater than 5% (Ensafi et al. 2008a; Ensafi et al. 2008b). Cations including Na^+ , K^+ , Ca^{2+} , Mg^{2+} , Zn^{2+} , Ni^{2+} and Cd(II) were studied. The colormetric results are shown in Table 3.2. The experiment results indicate that species such as Na^+ , K^+ , Ca^{2+} , Mg^{2+} had little influence on both detection and adsorption of lead ions (1mg/L) even when their concentrations were 20-fold higher than that of the lead ions. In other words, those cations do not have specific interactions with the functional groups on DZ and CS of the membrane. However, Ni^{2+} , Zn^{2+} and Cd(II) cations were found to exert great interference on both detection and adsorption of lead ions. With these cations in presence, the membrane exhibited colors that were different from the one in the single lead ion system. Besides, adsorption of lead ions also decreased significantly. The reason was probably that those heavy metal cations could compete with Pb(II) ions to form complex with the DZ ligand and therefore interfered the recognition performance (Rinaudo 2006). However, a preliminary study has found that the influence could be mitigated by the addition of 2mmol/L $\text{Na}_2\text{S}_2\text{O}_3$ in the analyst solution (Zaporozhets et al. 1999). This is probably because sodium thiosulfate could

form stable complexes with those interfering cations (Van Sprang and Janssen 2001). Besides, no obvious influence on the detection and removal of lead ions was found with the addition of 2mmol/L $\text{Na}_2\text{S}_2\text{O}_3$ because lead ions are known to prefer the complex with nitrogen containing chelating groups that exist in both DZ and CS of the membrane (Mahmoud et al. 2010).

Table 3.2 color response of 1mg/L Pb(II) ions in presence of interfering cations in the solutions (initial pH value 5, 22-23 °C).

No.	Interfering cation [X]	Con. of Pb(II) (mg/L)	Con. of [X] (mg/L)	Addition of $\text{Na}_2\text{S}_2\text{O}_3$ (mg/L)	Color
1	-	0	0	0	
2	-	1	0	0	
3	Na^+ , K^+ , Ca^{2+} , Mg^{2+}	1	20	0	
4	Cd^{2+}	1	1	0	
5	Zn^{2+}	1	1	0	
6	Ni^{2+}	1	1	0	
7	Cd^{2+}	1	1	2	
8	Zn^{2+}	1	1	2	
9	Ni^{2+}	1	1	2	

3.3.8 Reusability of the prepared membrane

The reusability of the prepared CS/CA-DZ membrane is also of the interest in this study. EDTA (0.1%) has been found to be effective for the removal of lead ions from the saturated membrane. However, some influence of the stripping agent on the sensing functionality of the prepared membrane was noticed with gradually decreased sensitivity and delayed response-time during several cycles of regeneration experiments. Experimental results showed that after three regeneration/reuse cycles, the absorbance intensity of the regenerated membrane at 490nm was reduced to

around 40% of the freshly made CS/CA-DZ membrane; besides, around 30% reduction in lead ions adsorption capacity was observed. Therefore, there is a need to screen the more suitable desorption or stripping agent to regenerate and reuse the membrane without losing its functionality.

3.4 Conclusion

In this study, a simple and low cost multifunctional membrane for visual detection and adsorptive removal of Pb(II) ions was prepared by immobilizing lead sensitive chromophore DZ onto the CS/CA blend membrane. The obtained CS/CA-DZ membrane was able to show optical color changes when in contact with lead ions in solutions with a short response time (less than 5min). Besides, the membrane also showed enhanced adsorption performance towards lead ions. The DZ functionalized CS/CA membrane achieved truly multiple functions, including on-site naked-eye detection and effective adsorptive removal of lead ions from aqueous solution simultaneously. Thus, the multifunctional membrane concept has been proved feasible and achievable, which has a great prospect in water and wastewater treatment to minimize the environmental and health effects of the heavy metal pollutants.

**CHAPTER 4 SIMULTANEOUS DETECTION AND REMOVAL OF
MERCURY IONS IN AQUEOUS SOLUTIONS BY TPPS FUNCTIONALIZED
CS/CA MULTIFUNCTIONAL MEMBRANE**

SUMMARY

Simultaneously warning the existence of toxic substances and effectively removing them has a significant meaning in water safety and security. In this study, a multifunctional membrane was obtained by immobilizing an organic optical indicator (5, 10, 15, 20-tetraphenylporphine tetrasulfonic acid or TPPS in short) onto CS/CA membrane for visual detection and adsorptive removal of Hg(II) in aqueous solutions. The effects of various factors including the amount of immobilized indicator, solution pH, solution ionic strength, initial Hg(II) concentration and interference of other metal ions on the performance of the multifunctional membrane were investigated through a series of batch adsorption and filtration studies. The results showed that the optimum TPPS immobilization amount appeared at 1.0mg (TPPS)/g (dry membrane) and the resulted membrane exhibited good performance for both detection and removal of Hg(II) in solutions with initial pH ranging from 5 to 8 and at ionic concentration up to 0.05M (as added NaNO₃). The interference study demonstrated that the membrane possessed good selectivity and sensitivity towards Hg(II) ions with the presence of other cations, especially alkali and alkaline earth metal ions, even in their relatively high concentrations. Besides, the used membrane was found to be effectively regenerated by 0.01M EDTA and could be reused without the significant loss of its functionality. The study has illustrated the potential prospect of the prepared multifunctional membrane for the simultaneously warning and removal of mercury ions in water and wastewater treatment.

4.1 Introduction

Mercury contaminants have been a serious concern due to their high toxicity to living organisms, long persistence in the environment and frequent emission from various industrial sources (Li et al. 2010). Mercury may exist in the environment in different oxidation states, the most prevalent form of mercury contaminants in aquatic ecosystems is the soluble Hg(II) species. They are particularly toxic because they are highly reactive and can easily bind with cysteine proteins, therefore damage the living cells (Clarkson 1993). Besides, the biochemical conversion of Hg(II) would lead to a more toxic form-methylmercury (MeHg) that can be easily absorbed by the organisms, accumulate in their bodies and eventually magnify the toxicity to human beings through the food chain (Yan et al. 2011). Therefore, even present at very low concentrations in the environment, Hg(II) can cause great potential hazards to human beings. The USEPA has established the drinking water criterion for mercury at 2µg/L, and the permitted discharge limit of mercury in wastewater at 10µg/L (USEPA 2001). In the Europe, even more stringent limits have been set by the European Union at 1 and 5µg/L in drinking water and wastewater effluent, respectively (Ghodbane and Hamdaoui 2008).

One of the major sources of mercury pollution is the effluents from industries, such as chloralkali, mining, oil refining, electrical device manufacturing, rubber processing, where mercury concentrations have been reported in the range of 10-100mg/L (Zambrano et al. 2004). Improper effluent discharge, insufficient treatment and poor management of those wastewaters can lead to elevated mercury occurrence in natural waters. For example, the Great Lakes in North America, the Swedish forest lakes, the Mediterranean Sea and the North Sea are all found with some extents of mercury

pollution (Coquery and Cossa 1995; Dove et al. 2011; Kotnik et al. 2007; Lindstrom 2001). In addition, it has been reported that in some areas of the Delta water in California, the total concentration of mercury in various forms ever reached a thrillingly high level of 448pmol/L (89.8µg/L) (Conaway et al. 2008). Therefore, to minimize the impact to the environmental as well as the public health, it is of paramount importance to seek technologies that can instantly detect and effectively remove mercury contaminants from water in water supply or wastewater discharge.

In the previous chapter, we have developed a multifunctional membrane by immobilizing optical indicator dithizone onto a chitosan/cellulose acetate (CS/CA) blend membrane for the detection and removal of Pb(II) ions in aqueous solutions, (Zhang and Bai 2011). The previous study has demonstrated the feasibility and effectiveness of the multifunctional membrane concept. In the present study, the this concept was extended to the application on Hg(II) detection and removal, with a special focus on the effect of various preparation and experimental parameters on the performance of the membrane.

A commercially available organic optical indicator, 5, 10, 15, 20-tetraphenylporphine tetrasulfonic acid, denoted as TPPS, which has been known to show high sensitivity and selectivity towards Hg(II), was used in this study. TPPS can exhibit strong fluorescence in the visible light region of the electromagnetic spectrum, owing to the special conjugated double bond and the high mobility of its π -electrons (El-Safty et al. 2007b). When TPPS molecule is in contact with Hg(II), the formation of $[\text{Hg-TPPS}]^{n+}$ complex occurs, resulting in a batch chromic shift of light absorption from 410 to 450nm, which corresponds to a color change from pink to green in the light

reflectance spectrum (El-Safty et al. 2007b). The sulfonic acid groups on the central porphyrin structure of TPPS make it highly soluble in water and thus enable the possibility of TPPS being immobilized onto carrier materials via strong electrostatic interaction in an aqueous solution, leading to a stable sensor for the sensing assays of mercury ions (El-Safty 2009). Chitosan based adsorptive membrane provides an ideal platform for TPPS immobilization because chitosan has also been found to be an excellent adsorbent for anionic dyes containing sulfonic groups, attributed to the strong electrostatic attraction between the amine groups of chitosan and the sulfonate groups of the dyes (Sakkayawong et al. 2005). Upon the immobilization of TPPS on chitosan-based membranes, the remaining amine groups on chitosan and sulfonate groups on TPPS can contribute to the adsorptive capacity for mercury removal. Therefore, visual detection and adsorptive removal of mercury ions can be achieved simultaneously by a single membrane.

Some experimental factors, including the reaction time, the amount of immobilized indicators, solution pH and ionic strength, initial Hg(II) concentration and the existence of interference ions, are considered to affect the visual detection and adsorptive removal performance of the prepared membrane towards Hg(II) ions. In this study, a series of experiments was conducted to examine the possible effect of various process parameters on both visual detection and adsorptive removal of Hg(II) ions. Adsorption and filtration experiments were carried out with synthetic Hg(II) water samples and real water samples dosed with Hg(II) ions, respectively. Since many adsorbents reported so far did not show desired performance at low mercury concentrations, such as fast adsorption kinetics and high uptake amounts (Choong and Park 2005), the present study has purposely focused on Hg(II) solutions with

relatively low concentrations.

4.2 Materials and Methods

4.2.1 Preparation of multifunctional membrane

The base membrane was obtained from chitosan (CS) and cellulose acetate (CA) blend. The details on the materials and the general methods for the base membrane preparation can be found in Chapter 3. In this study, the specific ratio of CS: CA: FA in the cast solution was 2: 14: 84 by weight and the flat sheet membranes were cast using a motorized film applicator (K4340M10, Elcometer) with a casting thickness of 600 μ m. The cast membranes were then solidified in a diluted NaOH (2 wt %) solution for 24h and then rinsed with ultrapure water for several times, followed by keeping them in plenty of ultrapure water for sufficiently long time (more than three days) before further use.

The multifunctional membrane was prepared by immobilizing 5,10,15,20-tetraphenylporphine tetrasulfonic acid (TPPS) as an indicator onto the CS/CA blend base membrane through a solution reaction. TPPS supplied by Sigma-Aldrich with a purity of $\geq 95\%$ was dissolved in ultrapure water to make solutions with TPPS concentrations from 1mg/L to 10mg/L. The UV/Vis absorption intensity of the TPPS solution varied proportionally to its concentration, and hence a linear relationship was established between the concentration and the absorbance intensity of the solution at 434nm. A certain amount of CS/CA membrane (cut into about 0.95cm² disks) was placed into a TPPS solution at room temperature (22-23°C) and the reaction was allowed for a sufficient time of 24 hours. Then, the membrane disks were collected and washed thoroughly with ultrapure water in a flask for several rounds until no

obvious leaching of TPPS was observed in the washing elutes. The immobilized amount of TPPS on the membrane was quantified by mass balance from the concentration changes of TPPS in the reaction solution and in the washing elutes. Each batch used the membrane disks of a dry weight around 1g. TPPS concentrations in the solutions were determined from the UV/Vis absorption readings. TPPS immobilized CS/CA membrane generally showed a pink to red appearance, depending on the immobilized TPPS amounts. TPPS immobilized CS/CA membranes will be denoted as CS/CA-TPPS hereafter in this thesis. To get dried samples for analysis and adsorption study, the membranes were dried with a vacuum freeze drier (FreeZone 2.5Plus Labconco).

4.2.2 Performance evaluation through batch adsorption experiments

The effect of various factors, including the amount of immobilized TPPS, initial Hg(II) concentration, interference metal ions, initial solution pH and ionic strength on the performance of the multifunctional membrane in Hg(II) detection and removal was evaluated through a series of batch adsorption experiments. For the consistency and convenience of the experiments, the investigation of Hg(II) detection and adsorptive removal was conducted together in the same batch adsorption process. In each experiment, a type of CS/CA-TPPS membrane (varied in the amount of TPPS immobilized) in the disk form, with a dry mass around 0.02g, was added into 100mL of a Hg(II) solution in a flask and was shaken at 120rpm for 300min under room temperature (22-23°C). The Hg(II) solutions with various concentrations were prepared by diluting mercury nitrate [Hg (NO₃)₂] standard solution (1000mg/L, Merck) in ultrapure water. A sample of 10mL solution was taken at each desired time interval during the adsorption process. Mercury concentrations in the solutions were

determined by Inductively Coupled Plasma-Optical Emission Spectrometer (ICP-OES, Perkin Elmer Optima 3000DV) and Inductively Coupled Plasma-Mass spectroscopy (ICP-MS, Perkin Elmer ELAN6100) (for concentrations less than 50 μ g/L). Samples of the membrane disks were also taken out from the solution in the flask for the recording of color change with a digital camera (Panasonic LX-3) and the analysis of light absorbance change by a UV/Vis spectrometer (Jasco V-660) to evaluate their chromatic responses upon the exposure to Hg(II) ions at various extents. More specific information on the experimental conditions in each evaluation will be given later when the results are discussed.

4.2.3 Performance evaluation through batch filtration experiments

To simulate a more real membrane application process, the evaluation of the membrane performance was further carried out with a dead-end filtration system (Fig. 4.1). The tested membrane (around 11.8cm²) was mounted in a filtration cell (Advantec UHP-43, Japan) coupled with a magnetic stirrer. The pressure drop across the membrane was controlled by a pressure regulator installed on a compressed N₂ gas cylinder and was maintained at 1 bar in all runs. The permeate samples were collected at various time intervals for the analysis of mercury concentration. Color changes or light absorbance change of the membrane before and after a filtration experiment were also recorded with a digital camera or analyzed with a UV/Vis spectrometer.

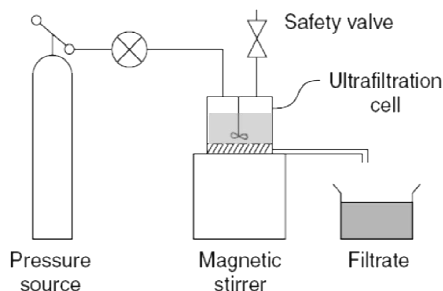


Fig. 4.1 Schematic of the unit used for filtration study

4.2.4 Other analyses

The mechanical property of the wet membranes was evaluated through the measurement of the tensile strength at maximum load and elongation ratio at break. Tests were conducted with an Instron-5542 (UK) Materials Testing Machine equipped with Bluehill (Instron) Ver. 2.5.391 software under the room temperature (22-23°C) and with a relative humidity of about 60%. A 10×70mm rectangular membrane sample was fixed vertically between two pairs of tweezers with a length of 30mm on the instrument. The membrane sample was then extended at a constant elongation rate of 10mm/min until it was broken. Three membrane samples were measured for each type of the membrane and the average value of the three measurements were taken to be the representative tensile strength and elongation rate for each type of the membranes.

The water content of a membrane was measured as an indication of the membrane's porosity. The determination was done by soaking a membrane in water for 24h. The membrane sample was then weighed after mopping the surface with a paper towel. Finally, the dry weight of the membrane sample was determined after placing it in a vacuum freeze drier (FreeZone 2.5Plus, Labconco) for 24h. The water content

percentage of the CS/CA base or CS/CA-TPPS multifunctional membrane is calculated as follows:

$$Watercontent = \frac{W_{wet} - W_{dry}}{W_{wet}} \times 100\% \quad \text{Eq. 4.1}$$

where W_{wet} and W_{dry} are the wet and dry weights of the membrane sample, respectively.

Pure water flux (PWF) measurements of the CS/CA and CS/CA-TPPS membranes were carried out in a dead end filtration set-up at room temperature (22-23°C). Pressure drop across the membrane was controlled by compressed N₂ gas and maintained at 1 bar in all runs. When the flux stabilized, the permeate quantity (Q) was collected over a time interval of ΔT (20min in this study). Then, the PWF was calculated by Eq. 4.2 below:

$$J_w = \frac{Q}{\Delta T \cdot A \cdot \Delta P} \quad \text{Eq. 4.2}$$

where J_w is the water flux (L/m²/h/bar), Q is the quantity of water permeated (L) during ΔT , ΔT is the sampling time (h), A is the membrane filtration area (m²), and ΔP is the pressure drop across the membrane (bar). Each type of membrane was tested three times and the average flux was reported in this thesis.

Filtration experiments were also carried out to determine the molecular weight cut-off (MWCO) of the CS/CA base and CS/CA-TPPS multifunctional membranes. The feed solution consisted of polyethyleneglycol (PEG) purchased from Fluka with different molecular weights ranging from 200 to 35,000 in ultrapure water with a concentration at 1000mg/L. The experiment was conducted in the procedure as described in the literature (Nidal et al. 2007). 10mL PEG permeate was collected and its concentration

was analyzed by a TOC meter (Shimadzu TOC-VCPH). The MWCO of the membrane was taken to be the molecular weight of the PEG with the retention of 90%.

The surface and cross-section morphologies of the membranes were examined with a Scanning Electron Microscope (SEM, JSM-5600LV). Membrane samples were first dried in a vacuum freeze drier (FreeZone 2.5Plus, Labconco) for 24h and then platinum-coated with a vacuum electric sputter coater (JEOL JFC-1300) before the SEM scanning. The membrane surface chemical composition was characterized by Attenuated Total Reflectance Fourier Transform Infrared Spectroscopy (ATR/FTIR). The analysis was conducted with a Shimadzu H8400 spectrophotometer (Japan) coupled with an ATR accessory (KRS-5 crystal, 45°) and in the wave number range of 600 to 4000cm⁻¹.

4.3 Results and Discussion

4.3.1 Membrane characteristics

The major physical properties of the CS/CA base membrane and CS/CA-TPPS functional membrane are given in Table 4.1. It appears clearly that the immobilization of TPPS indicators on CS/CA base membrane did not significantly alter the basic properties of the membrane. This is expected due to the mild reaction condition and it is also desired because the final membrane structure can be easily controlled by the selection of the base membrane structure. The typical surface and cross-section morphologies of the CS/CA and CS/CA-TPPS membranes are shown in Fig. 4.2. From the SEM image analysis, both CS/CA and CS/CA-TPPS membrane were found to be asymmetrical in the structure, with pore sizes ranging from about 0.01 on the top to 1μm on the bottom surface, respectively. Together with the result of PWF and

MWCO, the prepared membranes (CS/CA and CS/CA-TPPS) fall into the category of ultrafiltration membrane.

Table 4.1 Characteristic property of CS/CA and CS/CA-TPPS membranes

Membrane	CS/CA	CS/CA-TPPS
Parameter		
Tensile strength at maximum load	15.21 MPa	17.06 MPa
% Elongation at break	10.11%	10.45%
% Water content	77%	64%
PWF (1 bar)	7.8-16.8 L/m ² /h/bar	7.4-17.2 L/m ² /h/bar
MWCO	20,000Da	20,000Da

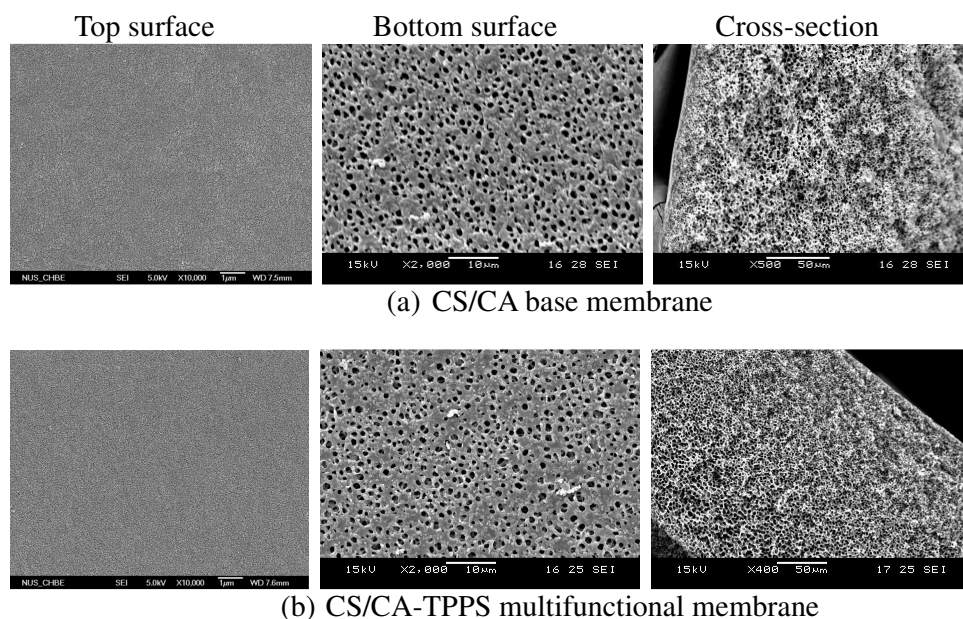


Fig. 4.2 SEM images showing the morphologies of CS/CA and CS/CA-TPPS membranes.

The interaction mechanism of TPPS with chitosan in aqueous solutions has been reported in the literature (Synytsya et al. 2006). In this study, FTIR analysis was conducted to verify the immobilization of TPPS on CS/CA membrane. The FTIR

spectra of TPPS powder, CS/CA base membrane and CS/CA-TPPS multifunctional membrane are shown in Fig. 4.3. For TPPS powder, the peaks appeared at 739, 795 cm^{-1} and 1485 cm^{-1} can be assigned to the C-H and C=C bonds in the aromatic groups; while peaks at 1030 cm^{-1} , 1114 cm^{-1} and 1225 cm^{-1} can be assigned to the asymmetric O=S=O stretching, symmetric O=S=O stretching, and S=O stretching vibrations of the sulfonate groups, respectively (Ismail et al. 2009; Xu et al. 2011). Peaks corresponding to the amine groups are identified at around 1640 cm^{-1} and 3340 cm^{-1} for both TPPS and the CS/CA base membrane (Nalva 1997). After TPPS immobilization, three new peaks at 739, 795 and 1485 cm^{-1} are observed for the CS/CA-TPPS membrane. These peaks are typically to represent the aromatic group in TPPS, which indicates a successful immobilization of TPPS onto CS/CA membrane.

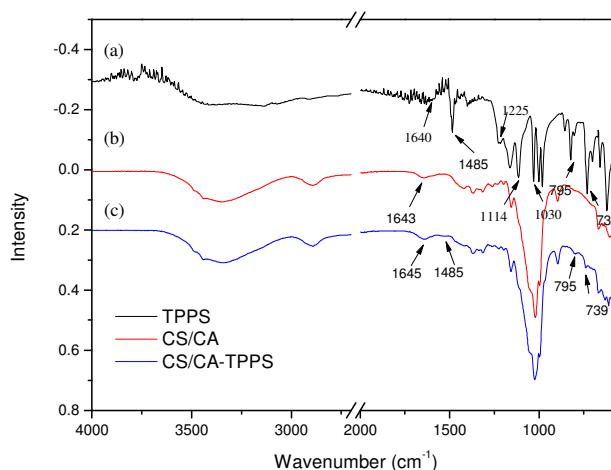


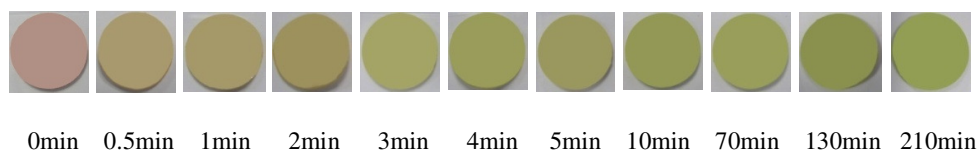
Fig. 4.3 FTIR spectra of (a) TPPS powder; (b) CS/CA base membrane; (c) CS/CA-TPPS multifunctional membrane.

In order to investigate the stability of immobilized TPPS molecules on CS/CA membrane, leaching test was conducted by adding 0.02g CS/CA-TPPS membranes to 100mL flasks, each containing ultrapure water but with initial pH being adjusted to a value in the range from 2 to 10. The contents in the flasks were shaken at 120rpm for

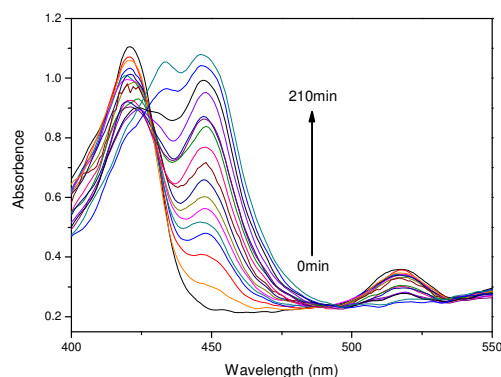
24h at room temperature (22-23°C). The concentrations of TPPS in the solutions were determined by the UV/Vis absorbance intensities at 434nm wavelength which is known to linearly change with TPPS concentrations (Tong et al. 1998). The results showed that only slight leaching of TPPS, up to 1.615%, was detected in the solution with initial pH value of 10 after 24h, but not in the solutions of other pH values. The tests indicated that the immobilized TPPS on the CS/CA membrane was of a chemical adsorption feature and was therefore reasonably stable.

4.3.2 Optical response of CS/CA-TPPS membrane to Hg(II) ions in water

Fig. 4.4 shows the color change and UV/Vis light absorbance spectrum variation of the CS/CA-TPPS membrane in contact with Hg(II) in aqueous solutions. As can be observed in Fig. 4.4(a), the CS/CA-TPPS membrane surface exhibited an obvious color change (pink to green) in response to the existence of Hg(II) in the solution, which can be easily noticed by the naked eye. Correspondingly, the UV/Vis light absorbance spectrum of the membrane in Fig. 4.4(b) was found to exhibit a bathchromic shift with increased peak intensities at 450nm, which corresponds to a color change from pink towards green (El-Safty 2009; Balaji 2006). The results in Fig. 4.4 confirms that the CS/CA-TPPS membrane has the desired functionality of quick optical response towards the existence of Hg(II) ions in solutions and the color change can be directly observed by naked eyes (The developed color of the membrane was found to be stable for even more than one year when kept in the desiccators). With the increase of the contact time, the developed green color was intensified, which attributed to more Hg(II)-TPPS complexes being formed on the membrane surface.



(a)



(b)

Fig. 4.4 Response of CS/CA-TPPS membrane to Hg(II) ions in a solution with the contact time: (a) optical color change and (b) variation of UV/Vis light absorbance spectrum versus wavelength (TPPS immobilized amount 1.0mg/g, 0.02g membrane, 100mL of solution, initial Hg(II) concentration 1mg/L, initial pH value 6, 22-23 °C).

4.3.3 Effect of TPPS immobilization amount on the performance of CS/CA-TPPS membrane

It is expected that the amount of TPPS immobilized on CS/CA membrane would affect the adsorption and the optical response of CS/CA-TPPS membrane to Hg(II) ions in a solution. The performance of CS/CA-TPPS membranes with different immobilized TPPS amounts was investigated. CS/CA base membrane disks were immersed into 100mL of TPPS solutions with different initial concentrations for 300min. The amount of TPPS immobilized on the base membrane was determined from mass balance calculation. Table 4.2 shows five sets of CS/CA-TPPS membranes with different amount of TPPS immobilized in the experiments. The adsorption and color response behaviors of the membranes to Hg(II) in a solution were examined and

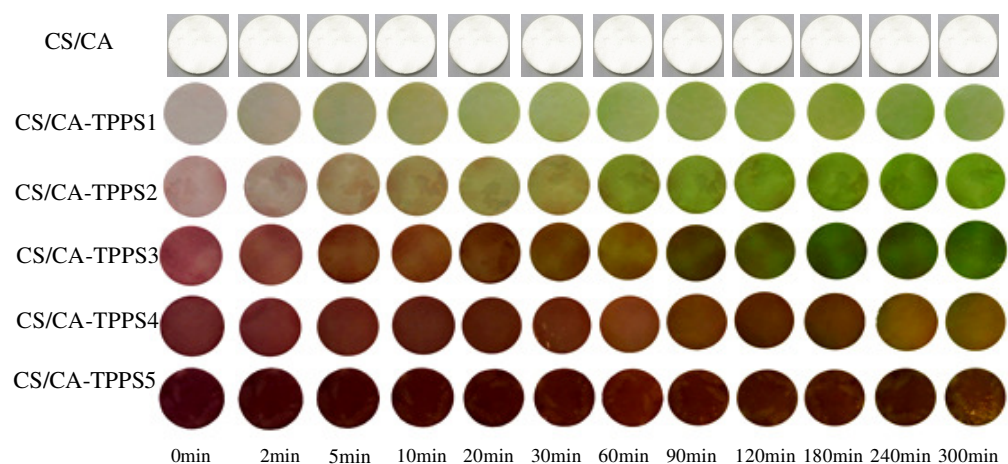
compared with those of the CS/CA base membrane.

Table 4.2 Immobilized TPPS amounts on various CS/CA-TPPS multifunction membranes.

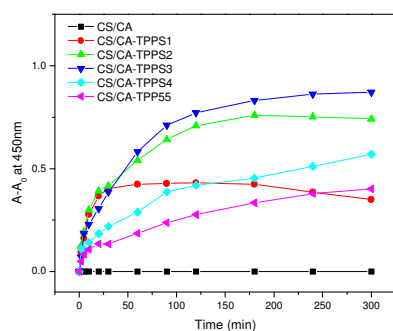
Membrane type	TPPS immobilization amount (mg/g)
CS/CA	0
CS/CA-TPPS1	0.5
CS/CA-TPPS2	1.0
CS/CA-TPPS3	3.2
CS/CA-TPPS4	5.7
CS/CA-TPPS5	8.3

Fig. 4.5 shows the effect of TPPS immobilized amount on the chromatic response and adsorption performance of the membranes to Hg(II) ions. The chromatic response was recorded as the developed color changes and the variations of the UV/Vis light absorption intensity (in terms of $A-A_0$) at 450nm with 300min of contact time. In Fig. 4.5(a), it is observed that the CS/CA base membrane did not show any color change and the increase of TPPS immobilized amount on CS/CA membrane was found to suppress the chromatic sensitivity of the membrane towards Hg(II) ions, which can be further proved by the UV/Vis spectra in Fig. 4.5(b). It can be seen that the curves of $A-A_0$ at 450nm versus time become less steep in the first 20min with the increased amount of immobilized TPPS, suggesting a higher insensitivity of the membrane color change towards the binding of Hg(II). This phenomenon may be due to the intensive array of TPPS molecules loaded on the membrane surface, which would shield the bond Hg(II) ions in the central porphyrin groups that are responsible for the optical sensory functions. In other words, very high TPPS immobilization amounts would lead to a high A_0 value, exhibiting as an intensified initial color; even if Hg(II)-TPPS binding events happened, the color change (quantified by $A-A_0$) was difficult to be detected. However, it is not reasonable to conclude that the lower the TPPS

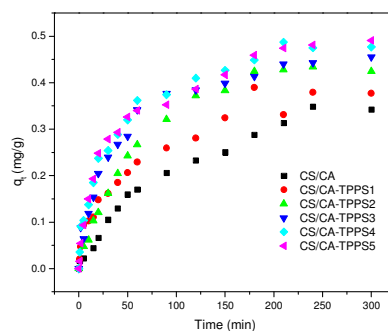
immobilization amount, the better the optical detection response. Although the CS/CA-TPPS1 membrane with least immobilized TPPS amount was noticed to show the quickest initial color response, its ultimate $A-A_0$ value was unfortunately small, indicating lower potential for color changes upon the exposure to mercury. On the other hand, the Hg(II) adsorption uptake amount was found to increase with the increase of the immobilized TPPS amounts; as shown in Fig. 4.5(c). The improvement of Hg(II) adsorption on the membrane could be attribute to the formation of metal- SO_4^{2-} complexes between Hg(II) ions and SO_4^{2-} groups in TPPS (e.g. $[\text{HgOH-SO}_4]^-$ and $[\text{Hg}(\text{OH})_2\text{-SO}_4]^{2-}$) (Krishnan and Anirudhan 2008; Eren and Afsin 2008). As shown in Fig. 4.6, the immobilization of TPPS molecules on the membrane could introduce more functional groups ($-\text{NH}-$, $-\text{SO}_3^-$) that have affinity towards Hg(II), hence increase the adsorptive removal of Hg(II). In order to achieve a balanced performance in both high detection sensitivity and good adsorption capacity, an appropriate or optimum TPPS immobilization amount is desired. From the present experimental results, the CS/CA membrane with TPPS immobilized amount of 1.0 mg/g, i.e., CS/CA-TPPS2, became a choice and hence it was used in further experimental studies described in the following sections.



(a)



(b)



(c)

Fig. 4.5 Performance of CS/CA-TPPS membranes with different amounts of TPPS immobilized in detection and adsorptive removal of Hg(II): (a) kinetic variation of color changes; (b) variation of UV/Vis light absorbance intensity (in terms of $A-A_0$) at 450nm; and (c) Hg(II) uptake amounts (initial Hg(II) concentration: $200\mu\text{g/L}$, initial pH value 6, $22-23^\circ\text{C}$, 100mL of solution volume, 0.02g membrane; A and A_0 are UV/Vis light absorbance intensity of the membrane at 450nm before and after in contact with Hg(II) ions in the solution).

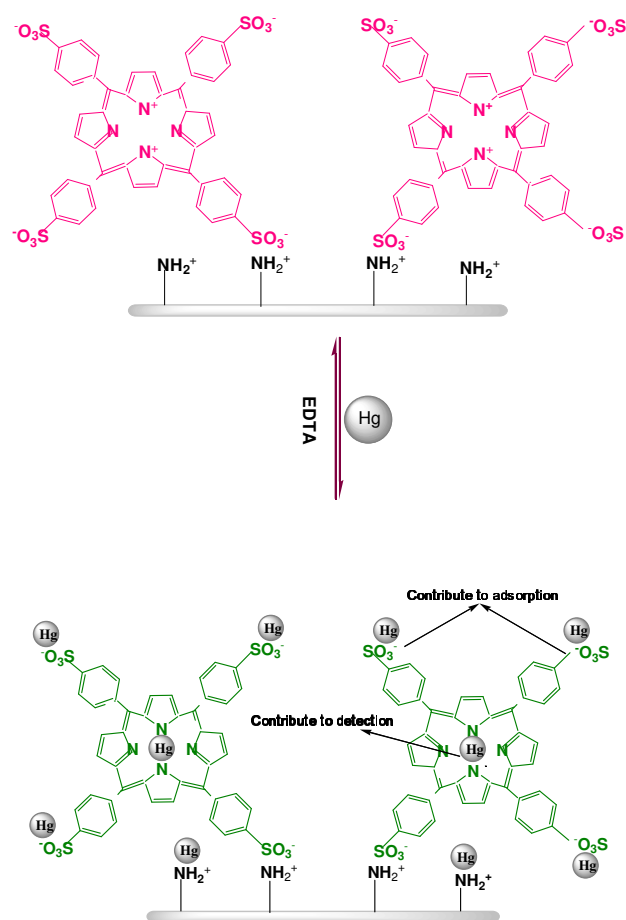


Fig. 4.6 Proposed detection (color change) and adsorption enhancement mechanism of Hg(II) by CS/CA-TPPS multifunctional membrane.

4.3.4 Effect of the initial solution pH value on the performance of CS/CA-TPPS membrane

Solution pH is often an important factor in an adsorption-based system as pH can affect the dissociation of functional groups, the conformational changes of molecular structure, stability of metal complexes and speciation of metal ions (Inbaraj et al. 2009). In this study, the influence of the initial solution pH value on visual detection and adsorptive removal of Hg(II) by the CS/CA-TPPS membrane was investigated by monitoring the membrane color change and Hg(II) uptake amount in the solutions

with initial pH from 4 to 8. According to the MINEQL+ analysis, no precipitation of Hg(II) would be formed at the examined concentration (200 μ g/L) in this pH range. The experimental results are presented in Fig. 4.7. From Fig. 4.7(a), it is clear that obvious membrane color change was observed within the studied pH range and the degree of color change enhanced with the increased initial solution pH. In all acid medium, the π -electron conjugated double bond system of TPPS would be disrupted and the coordination interaction between the protonated porphyrin and metal cations would become weak. Hence the color change was less obvious at a lower pH condition (Itoh et al. 1975). The adsorption of Hg(II) on the CS/CA-TPPS membrane was also improved with the increase of the solution pH value; as shown in Fig. 4.7(b). This may be attributed to the less competition between metal ions and protons for the sorption sites on the membrane at a higher pH. The result indicates that the prepared membrane was suitable for on-site detection and removal of Hg(II) ions in most of the surface waters that usually have a pH from 6 to 8. For wastewater treatment applications, pH adjustment can be done through pre-treatment if solution pH values become too high or too low.

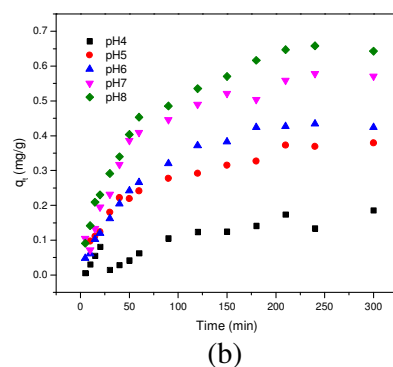
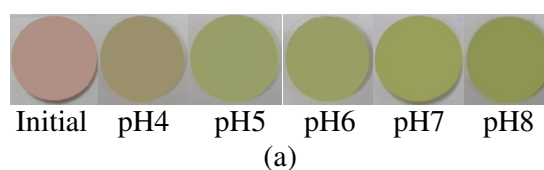


Fig. 4.7 Effect of initial solution pH on the performance of CS/CA-TPPS membrane. (a) Color change of the membrane after 20min contact time; (b) Hg(II) adsorption

uptakes from solutions with initial pH ranging from 4 to 8 (22-23°C, initial Hg concentration 200µg/L, 100mL of solution volume, 0.02g membrane).

4.3.5 Effect of ionic strength on the performance of CS/CA-TPPS membrane

Water or wastewater usually contains a certain amount of ions. Similar to solution pH, solution ionic strength can affect membrane surface property and heavy metal ion speciation, and therefore, affect the function and performance of the developed CS/CA-TPPS membrane. The influence of ionic strength on the performance of the membrane was investigated by adding different amounts of NaNO₃ into 200µg/L (10⁻⁶M) Hg(II) solution to make the ionic strength from 0 to 0.2M (NaNO₃). The solution pH was adjusted to 6 and was monitored during the experiment (the variation of the solution pH was found less than 5%). The experimental results are shown in Fig. 4.8. It can be found that both the detection sensitivity and Hg(II) uptake amount were not greatly affected when the solution ionic strength was below 0.05M of NaNO₃. However, further increase of the ionic strength from 0.05 to 0.2M NaNO₃ led to negative effects on both the detection and adsorption of Hg(II) ions. This is because at higher ionic strengths (high concentration of electrolyte ions, e.g. 0.2M NaNO₃), especially when the analyte concentration is low (e.g. 10⁻⁶M Hg(II)), the adsorption sites on the membrane would be surrounded by the overwhelming electrolyte ions, which could weaken the binding force in electrostatic interaction, reduce the contact likelihood of as well as compete with Hg(II) ions to the adsorption sites on the membrane. Therefore, the effectiveness of the membrane for detection and removal of Hg(II) ions might be compromised in the solution with high ionic strength.

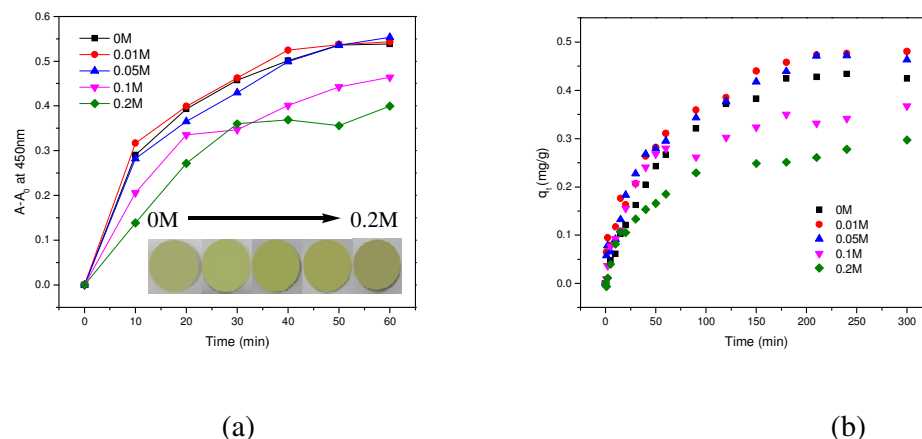


Fig. 4.8 Effect of ionic strength on the performance of CS/CA-TPPS multifunctional membrane: (a) variation of UV/Vis light absorbance intensity ($A-A_0$) of the membrane at 450nm and (b) adsorption uptakes of Hg(II) by the membrane ($200\mu\text{g/L}$ Hg(II) ions in the solutions with different ionic strength ranging from 0 to 0.2M NaNO_3 (initial pH value 6, $22-23^\circ\text{C}$, 100mL of solution volume, 0.02g membrane). Note: The photos in the insert of Fig. 4.8(a) were the membrane samples after 20min contact with the Hg(II) solutions.

4.3.6 Influence of initial Hg(II) concentration on the performance of CS/CA-TPPS membrane

The chromatic changes of CS/CA-TPPS membrane under different initial Hg(II) concentrations were recorded, with the results shown in Fig. 4.9. It is found that by allowing sufficient contact time, the membrane could detect Hg(II) by changing color in Hg(II) solutions with concentrations as low as $10\mu\text{g/L}$. The color response of the membrane became faster and more obvious with the increase of the initial mercury concentration. In the solutions with Hg(II) at 1mg/L and above, the color change could be instantaneously observed by the naked eyes. The influence of the initial Hg(II) concentrations on the adsorptive removal of Hg(II) was also examined, with the results given in Table 4.3. It can be seen that the adsorption amount also increased with the increase of Hg(II) initial concentrations. For the mercury solution with the initial concentration of $10\mu\text{g/L}$, after adsorption for 300min, the residual

concentration was lower than 5 μ g/L which is below the permitted discharge limit of wastewater established by the USEPA and European environmental regulations.

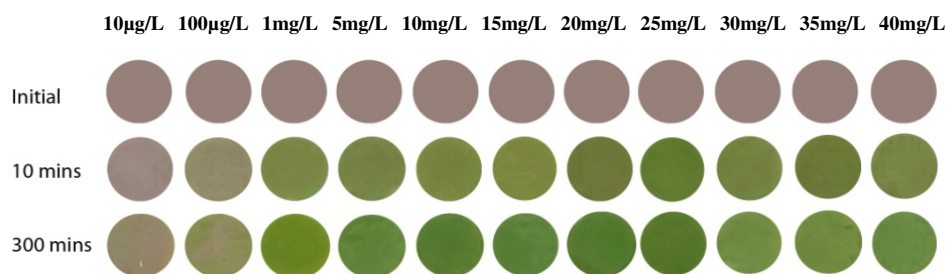


Fig. 4.9 Color change of CS/CA-TPPS multifunctional membrane in Hg(II) solutions with different initial Hg(II) ion concentrations (initial pH value 6, 22-23 $^{\circ}$ C, 100mL of solution volume, 0.02g membrane).

Table 4.3 Effect of initial Hg(II) concentrations on the adsorption amount of Hg(II) on the membrane (mg/g) and the residual Hg(II) concentration in the solution (initial pH value 6, 22-23 $^{\circ}$ C, 100mL of solution volume, 0.02g membrane, contact time 300min).

Initial concentration (mg/L)	Adsorption amount (mg/g)	Residual concentration (mg/L)
0.01	0.0287	0.0041
0.1	0.2903	0.0417
1	2.6338	0.46
5	12.986	2.38
10	23.2421	5.35
15	33.655	8.27
20	41.678	11.64
25	47.95	15.51
30	52.8	19.63
35	61.092	22.98
40	67.833	26.62

4.3.7 Interference of other metal ions on the performance of CS/CA-TPPS membrane

In the real situation, the water to be treated usually contains various other ion species. It is of interest to know whether the existence of other metal ions would affect the detection and removal of Hg(II) ions by the developed CS/CA-TPPS multifunctional

membrane. The experiments were particularly conducted at a low Hg(II) concentration of 10^{-6} mol/L (200 μ g/L), with other ions from the alkali, alkaline-earth and transition metal ions at relatively high concentrations (10^{-4} mol/L). The metal ions examined include Na^+ , K^+ , Ca^{2+} , Mg^{2+} , Cu^{2+} , Ni^{2+} , Zn^{2+} , Pb^{2+} , Cd^{2+} . Controlled experiments were also conducted to investigate whether these ions may have any independent effects on the chromatic response and affinity to the membrane. It has been found that the interferences of alkali and alkaline earth metals were minor, with the variation of $A-A_0$ values at 450nm to be less than 5% and the color changes to be so insignificant that cannot be noticed by the naked eyes; see Fig. 4.10 (a) and (b). In the controlled experiment with each single type of the cations, obvious signal responses of $A-A_0$ at 450nm in the UV/Vis spectra was noticed from Pb^{2+} , Cd^{2+} , Zn^{2+} and Cu^{2+} ions; see the dark cyan bars in Fig. 4.10(b). It indicates that these heavy metal cations may also form metal-complex with TPPS. When these cations co-existed with Hg(II) ions, the $A-A_0$ values at 450nm were higher than that of in single Hg(II) solution, as shown by the orange bars in Fig. 4.10(b). This can be attributed to the co-adsorption of these cations with Hg(II) by TPPS on the membrane that amplified the final light absorbance intensity and intensified the observed color. Whereas, the co-existence of Cu^{2+} ions was found to diminish the developed color (Fig. 4.10(a)). It indicates that Cu^{2+} ions are more preferable to couple with central porphyrin groups of TPPS on the membrane when its concentration is much higher than Hg(II) ions. However, in general, our findings show that the selective detection of Hg(II) was evident even in the existence of high interference ion concentrations at as high as 100 times to Hg(II) ion concentration.

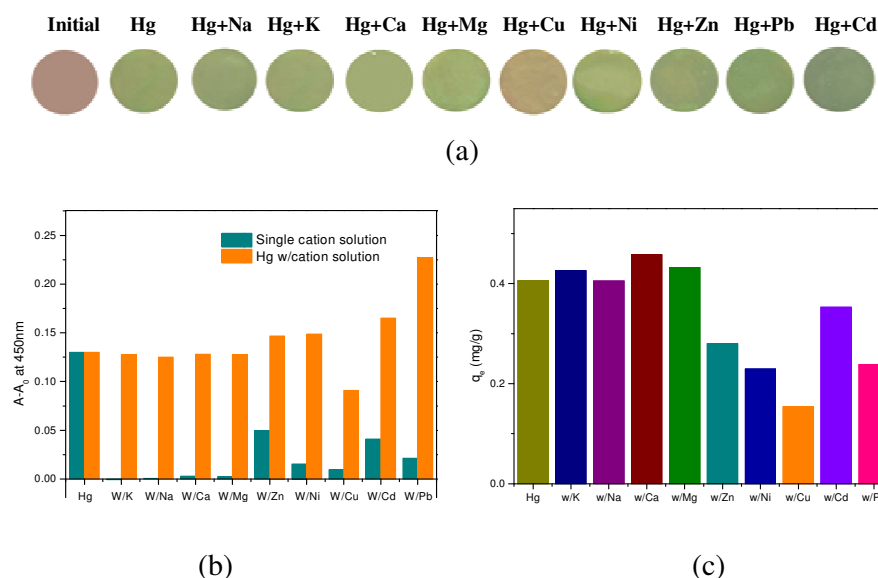


Fig. 4.10 Effect of interference metal ions on the performance of the CS/CA-TPPS membrane: (a) the developed color; (b) the UV/Vis light absorption difference (in terms of $A-A_0$) at 450nm after 5min of contact time with the Hg(II) solutions and (c) Hg(II) adsorption uptakes after 300min of contact time with the Hg(II) solutions (initial pH value 6, 22-23°C, Hg(II) concentration 10^{-6} M, other cation concentrations 10^{-4} M, 0.02g membrane).

The interference of other cations on mercury adsorption by the CS/CA-TPPS membrane was also investigated, with the results shown in Fig. 4.10(c). It is found that Hg(II) adsorption amount decreased with the presence of Pb^{2+} , Cd^{2+} , Zn^{2+} and Cu^{2+} ions. Since it has been reported that chitosan has affinity towards many heavy metal ions (Krajewska 2001), the reduction of Hg(II) adsorption in this case is expected due to the competitive adsorption exerted by these heavy metal ions. As both TPPS and chitosan have poor affinity towards alkaline and alkaline earth metals, the co-existence of Na^+ , K^+ , Ca^{2+} , Mg^{2+} ions do not exert great influence on Hg(II) removal by the CS/CA-TPPS membrane.

4.3.8 Desorption

The reusability of the developed multifunctional membrane is of interest for practical applications. Experiments were conducted to regenerate/reuse the membrane and

evaluate its performance in the desorption and re-adsorption cycles. Ethylenediamine tetra-acetic acid (EDTA) is a commonly used desorbing agent for metal ions. In this study, 200mL of 0.01M EDTA solution was used to strip Hg(II) from the membrane (0.02g) until the UV/Vis light absorbance intensity of the used membrane at 450nm reached the same value as the initial membrane. The membrane was then rinsed thoroughly with and conditioned in ultrapure water before reused in the next adsorption round. Chromatic changes of the membrane were monitored by a UV/Vis spectrometer in terms of light absorbance intensity in each desorption and adsorption cycle.

Fig. 4.11(a) shows the adsorption uptakes of the CS/CA-TPPS membrane in four consecutive rounds. The results suggest that the membrane can be reused after regenerated by the EDTA solution without deterioration of the adsorption capacity during the four rounds of adsorption/desorption cycles. Despite the regeneration resulted in a 50% reduction of the light absorbance intensity at 450nm after the first desorption, the color changes were still obvious for the naked eye detection and stabilized after the first cycle; as shown in Fig. 4.11(b). The decrease of the light absorbance intensity after the first cycle may be attributed to the intensive stripping effect of the EDTA agent on the TPPS functional groups on the membrane during the desorption process, in which the electronic configuration of some TPPS molecules might deform, and this may eventually result in some loss of the optical signal (Sayari et al. 2005). However, deformation of TPPS molecules by EDTA was not found to induce further deterioration in the detection during the following rounds.

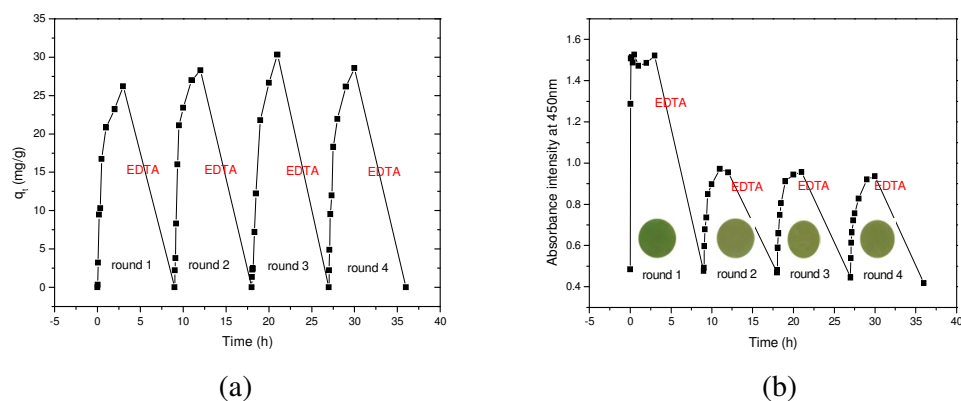


Fig. 4.11 Results from the adsorption and desorption experiments: (a) mercury uptake amount and (b) changes in the light absorbance intensity and developed color in the adsorption and desorption cycles (initial pH value 6, 22-23°C, initial Hg concentration 10mg/L, 0.02g membrane).

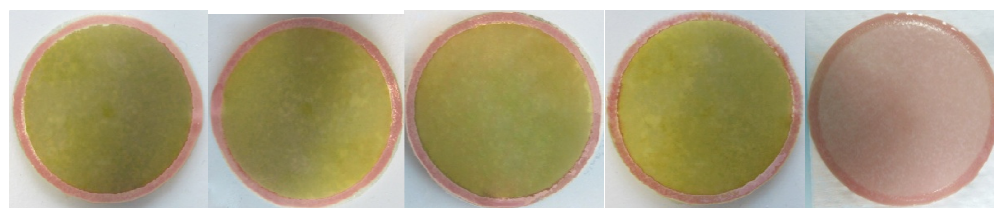
4.3.9 Application to real water samples

The CS/CA-TPPS membrane was also tested for its mercury detection and removal performance in a filtration process with various real water samples, including ultrapure water, reservoir water (MacRitchie Reservoir, Singapore), tap water (T-Lab in National University of Singapore), commercial bottled water (F&N, Singapore) and sea water (Labrador park beach, Singapore). No pre-treatment was done to remove any matrix component in the above water samples (Li et al. 2011). The main ions in the water samples were measured by ion chromatography and the results are given in Table 4.4. To simulate a Hg(II) contaminated water body, each water sample was “spiked” with mercury solution to make the concentration of 200µg/L. As shown in Fig. 4.12(a), the developed color of the membrane in reservoir water, tap water and commercial drinking water was almost the same as that in ultrapure water. However, no obvious color change was observed from the sea water sample, which may be due to the high ratio of background cations to Hg(II) ions ($>10^5$), which is consistent with the result in the effect of ionic strength. This result suggests that the obtained CS/CA-TPPS membrane has great potential to be applied for on-site and in situ detection of

Hg(II) ions in most of the possible water treatment applications. The removal rates of the 200µg/L Hg(II) concentration in different water samples by the CS/CA-TPPS membrane within 4h were shown in Fig. 4.12(b). It can be seen that the average removal rates are from 40% to 50%. The relatively low removal of mercury in this study can be attributed to the large pore size of the membrane and the short hydraulic retention time. Higher removal rate can be achieved by several approaches such as increasing the hydraulic retention time, or making the membrane with smaller pores.

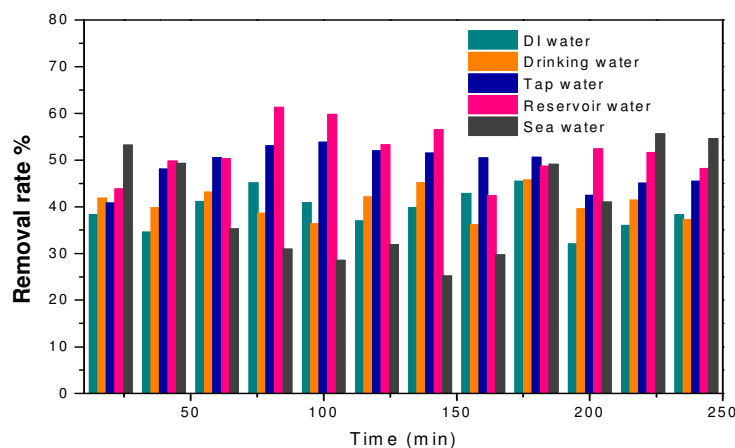
Table 4.4 The concentrations of major dissolved components in the various real water samples

Con. (mg/L)	Ultrapure water	Bottled water	Tap water	Reservoir water	Sea water
Na ⁺	0.01	22	14.39	1.52	11210
K ⁺	--	2	4.51	0.57	250
Mg ²⁺	--	7	0.51	0.13	590
Ca ²⁺	0.1	34	13.44	1.03	210
Cl ⁻	0.15	3	19.64	19.64	20010
NO ₃ ⁻	--	--	24.7	0.2	50
PO ₄ ³⁻	0.1	--	61.72	7.04	180
pH	4.63	7.68	8.12	6.9	8.02



Ultrapure water Tap water Bottled water Reservoir water Sea water

(a)



(b)

Fig. 4.12 (a) Color change of the membrane after filtration of and (b) removal rate of Hg (II) from the various simulated Hg(II) contaminated natural water samples (initial mercury concentration $200\mu\text{g/L}$; $22\text{-}23^\circ\text{C}$; membrane area 11.8cm^2 ; applied pressure 1bar).

4.4 Conclusion

In this study, CS/CA-TPPS multifunctional membrane was prepared for visual detection and adsorptive removal of mercury ions in aqueous solutions. The influences of preparation and experimental factors on the performance of the membrane were investigated. The results demonstrated that the obtained membrane can be applied in solution with initial pH ranging from 5 to 8 with good stability of the immobilized TPPS indicators. The immobilization amount of $1.0\text{mg (TPPS)}/\text{g}$ (dry CS/CA membrane) appeared to provide a balanced performance in both the detection sensitivity and adsorption uptake amount. There was no significant

influence on the performance of the membrane when the solution ionic strength was below 0.05M (NaNO_3), but very high ionic strength may have negative effect on both detection and adsorption performance. The interference study showed that the membrane possessed good selectivity towards mercury ion in the presence of alkali and alkaline earth metal ions. However, the existence of a large amount of Cu^{2+} ions would impose negative effect on both detection and adsorption of Hg(II) ions. In general, the prepared CS/CA-TPPS multifunctional membrane showed good performance of simultaneous visual detection/warning and adsorptive removal of mercury ions in aqueous solutions. It has a great potential prospect in water and wastewater treatment process, especially for the remote areas where there is a lack of or not convenient to use sophisticated analytical instruments.

**CHAPTER 5 THE EFFECT OF HUMIC ACID ON THE DETECTION AND
REMOVAL OF HG(II) FROM AQUEOUS SOLUTIONS BY THE CS/CA-
TPPS MEMBRANE**

SUMMARY

In the previous study, a multifunctional membrane for mercury detection and removal has been developed by immobilizing tetraphenylporphine tetrasulfonic acid (TPPS), onto chitosan/cellulose acetate (CS/CA) membrane. The resulting CS/CA-TPPS membrane can achieve filtration, adsorption and visual detection of mercury ions simultaneously. The influence of factors such as TPPS immobilized amount, solution pH and ionic strength on the performance of membrane was revealed. Besides, the interference of other metal ions was also studied in terms of the sensitivity, selectivity and uptake amount of mercury ions.

In realistic situation, the matrix composition of environmental water samples is highly variable. The dissolved organic matters (DOM), especially humic acid (HA), are suspected to affect the performance of the membrane. In this study, we investigated the removal of Hg(II) and humic acid (HA) by the CS/CA-TPPS membrane, with a special focus on the effect of HA on the removal efficiency and visual detection sensitivity of Hg(II) ions in solutions. Experiments were conducted in three phases, i.e., batch adsorption and filtration of individual Hg(II) and HA solutions; sequential adsorption and filtration tests of Hg(II) and HA solutions; and co-adsorption and co-filtration of solutions with both Hg (II) and HA. The results showed that the visual detection sensitivity of the membrane towards Hg(II) ions may be reduced with the presence of HA, especially at high concentrations. The previously adsorbed or filtered HA on the membrane surface was found to improve the removal of Hg(II) by providing more adsorption sites. When HA co-existed with Hg(II) in the solutions, the removal of Hg(II) by the membrane was reduced due to the formation of less

adsorptive complex HA-Hg(II). However, in the filtration test, the removal rates of Hg(II) were found to be significantly improved with the presence of HA in the feed solutions, and the removal mechanism was greatly attributed to the size exclusion or interception rather than adsorption. The results in this study suggested that the prepared multifunctional membrane were effective for both Hg(II) and HA removal. Although the presence of HA may improve Hg(II) removal in most examined phases, the visual detection of Hg(II) was injured in terms of delayed response time and decreased degree of final developed color. Therefore, the effect of HA should be taken a great consideration in the real application of the multifunctional membranes.

5.1 Introduction

The presence of mercury in surface waters has been a concern in many parts of the world because mercury is a neurotoxin that could bio-accumulate in organisms and eventually affect human health adversely. In regions with soils of high organic matter content, such as the Sacramento-San Joaquin Delta (Delta) in California, USA, elevated Hg concentration in surface water is an ongoing issue that challenges the State's intention for ecosystem restoration (Conaway et al. 2008; Henneberry et al. 2011). In the previous chapter, simultaneous visual detection and adsorptive removal of mercury ions was successfully achieved by immobilizing an optical indicator, 5, 10, 15, 20-tetraphenylporphine tetrasulfonic acid (TPPS), onto chitosan/cellulose acetate (CS/CA) blend membrane. The membrane, denoted as CS/CA-TPPS, is able to perform filtration separation, plus adsorptive removal and visual detection of mercury ions in aqueous solutions, simultaneously in a single membrane process. The development showed a great potential for practical applications in on-site and in-situ control of mercury contamination, especially for remote locations where the sophisticated analysis instruments and treatment systems are not available.

Many studies have shown that the properties of heavy metal ions in surface waters are strongly associated with dissolved organic matters (DOM) (Lamborg et al. 2003; Schuster et al. 2008). An important part of DOM in surface waters is humic acid (HA) that mainly come from the breakdown and biodegradation of dead or decaying plant and animal matters during the process of humidification by microorganisms (Liu and Gonzalez 1999). Especially in systems with high concentration of DOM such as wetlands and other peat derived water bodies, HA plays a significant role in the solubility and transport phenomenon of heavy metal ions (Davies et al. 1995;

Stevenson 1982). HA usually consists of macromolecules that contain conjugated olefinic, aromatic, phenolic; semiquinone or quinone structures, with various functional groups such as carboxyl, phenolic and amine groups that enable HA to easily complex with heavy metal ions in solutions. Among all the heavy metal ions, Hg(II) has been reported to be the most easily complexed species by HA (Benegas et al. 2003; Liu and Gonzalez 1999; Oshea and Mancy 1978; van den Hoop et al. 2002).

The ubiquitous presence of HA in surface waters has caused many water quality concerns. It could serve as the food for bacterial growth, produce undesirable color and taste, and act as a vehicle trapping heavy metal ions, thus increasing their concentrations in water supply. In addition, it is also well known that HA can be the principal precursor of halogenated disinfection byproducts (DBP), such as trihalomethanes (THMs) and haloacetic acids (HAAs) that are potentially carcinogenic to humans (Lorenc-Grabowska and Gryglewicz 2005; Nie et al. 2010; Rostad 2000; Wang et al. 2008; Xue et al. 2011).

Adsorption has been one of the technologies commonly used for HA removal (Nayak et al. 1990; Varadachari et al. 1991; Varadachari et al. 1995; Varadachari et al. 1994). For example, biopolymer chitosan has been reported as an effective absorbent for HA because the amine groups in chitosan could interact with the carboxyl or phenolic groups in HA to form organic complexes such as $-\text{NH}_3^+ \cdots \text{OOC-R}$ or $-\text{NH}_3^+ \cdots \text{O-C}_6\text{H}_4\text{-R}$ (Zhang and Bai 2003). It has also been reported that HA was able to form supramolecular complexes with compounds containing porphyrin structures such as TPPS, via oxidative coupling (Piccolo et al. 2005; Fukushima et al. 2007). Therefore, the CS/CA-TPPS multifunctional membrane can also be expected to adsorptively

remove HA. In this study, we investigated the removal of Hg(II) and HA by the multifunctional membrane (CS/CA-TPPS), with a special focus on the effect of HA on the detection effectiveness and removal efficiency of Hg(II) ions. Experiments were conducted in three phases:

Phase I- Batch adsorption and filtration tests of individual Hg(II) and HA solutions;

Phase II- Sequential adsorption and filtration tests of individual Hg(II) and HA solutions; and

Phase III- Co-adsorption and co-filtration tests of solutions containing both Hg(II) and HA.

These experiments may also provide an estimation of the contribution of adsorptive removal during the filtration operation of the Hg(II) and HA solutions by the membrane (Cari et al. 2000; Ognier et al. 2002).

Literatures have shown that the mean values of HA in natural waters are at the level around 6mg/L (de Wuilloud et al. 2003; Michalowski et al. 2001) and the pH values of the waters are in the range of 6.5 to 8.5 (Michaud 1991; Moore 1989). A study by Lim and Bai demonstrated that the HA in surface waters of Singapore was in the range from 0.8 to 12.8mg/L and the pH is from 6.9 to 8.6 (Lim 2004). Taking all the above information into account, we carried out the experiments with the HA concentration in the range of 2 to 15mg/L and solution pH values in the range of 6.5 to 8.5 in this work.

5.2 Methods and Materials

5.2.1 Materials

The detailed information on the materials and the method for the preparation of the CS/CA-TPPS multifunctional membrane can be found in Chapter 4. Mercury nitrate [$\text{Hg}(\text{NO}_3)_2$] standard solution (1000mg/L) purchased from Merck and humic acid (HA) (in sodium salt with C: 39.03%, H: 4.43% and N: 0.68%) supplied by Aldrich Chemical Co. were used as the sources of mercury ions and humic acid compounds in the study. Ultrapure water was used to prepare various test solutions as needed.

5.2.2 Experiments

5.2.2.1 Batch adsorption test

Phase I: Individual adsorption of Hg (II) or HA by CS/CA-TPPS membrane

A number of Hg (II) solutions with a volume of 100mL and an initial Hg(II) concentration of 800 $\mu\text{g/L}$ were prepared by diluting the 1000mg/L Hg (II) standard solution with ultrapure water. The initial pH values of the solutions were adjusted to 6.5, 7.5, and 8.5 respectively with diluted HNO_3 or NaOH solutions. Membrane samples in disk form of about 1.1cm diameter and a weight of 0.02g were added into each of the Hg(II) solutions with different initial pH values in the flasks. The contents in the flasks were shaken in an orbital shaker at 120rpm under room temperature (22-23 $^{\circ}\text{C}$) for 300min. A 2mL amount of solution was taken from each of the flasks at various desired time intervals to determine the mercury concentration. Solution pH values in the flasks were monitored through the process and no significant changes were observed (<5%). Color changes of the membrane samples at a desired time interval were examined by taking out a membrane disk and recording its color by a digital camera (Panasonic LX-3) and its light absorbance by a UV/Vis spectrometer

(Jasco V-660). The membrane disk after the analysis was returned into the flask to maintain a constant mass of membrane in the experiments. The membrane samples after the Hg(II) adsorption (300min) are denoted as CS/CA-TPPS-Hg. The adsorption tests of HA by the membrane was done similarly at an initial HA concentration of 15mg/L. The membrane samples after the HA adsorption tests are denoted as CS/CA-TPPS-HA. Hg(II) concentrations in the solutions were determined by an Inductively Coupled Plasma-Optical Emission Spectrometer (ICP-OES, Perkin Elmer Optima 3000DV). Humic acid concentrations in the samples were quantified by measuring the UV/Vis light absorbance at the wavelength of 400nm with an UV/Vis spectrometer (Jasco V-660). Since the light absorbance varied slightly with different initial solution pH values at this wavelength (Liu and Gonzalez 1999; Yan and Bai 2005), individual light absorbance calibration curves were prepared from solutions of known HA concentrations (in the range of 5–30 mg/L) with initial pH at 6.5, 7.5, and 8.5, respectively. The concentrations of HA in the solutions were then obtained from the calibration curve at each pH value.

Phase II: Sequential adsorption of Hg(II) and HA by CS/CA-TPPS membrane

CS/CA-TPPS-HA membrane samples obtained after HA adsorption tests at pH6.5, pH7.5 or pH8.5 were mopped with paper towel and then immersed into an Hg(II) solution at pH 6.5, pH7.5 or pH8.5 for further Hg(II) adsorption. Similarly, the CS/CA-TPPS-Hg membrane samples after Hg(II) adsorption tests at pH6.5, pH7.5 or pH8.5 were placed into an HA solution at pH6.5, pH7.5 or pH8.5 correspondingly for the further HA adsorption. The experimental conditions of the Hg(II) and HA solutions were the same as those described in the individual adsorption tests in Phase I.

Phase III: Co-adsorption of Hg(II) and HA in the same solutions by CS/CA-TPPS membrane

Solutions containing Hg(II) at a concentration of 800 μ g/L and HA at a concentration of 2mg/L, 8mg/L or 15mg/L were prepared, with the initial pH values adjusted to 6.5, 7.5 or 8.5, respectively. In order to ensure a sufficient equilibrium time between HA molecules and Hg(II) ions to form HA-Hg complexes, the solutions containing both Hg(II) and HA were stirred in flasks under room temperature (22-23°C) for 24h before conducting the adsorption tests with CS/CA-TPPS membranes. Membrane disks of a weight about 0.02g were then added into each of the solutions in the flasks. The contents in the flasks were shaken in an orbital shaker at 120rpm for 300min for the co-adsorption or competitive adsorption of Hg(II), HA and HA-Hg(II) complexes. The adsorbed amounts of Hg(II) and HA as well as the color change of the membrane were analyzed at various time intervals.

5.2.2.2 Filtration tests

The filtration tests of the membrane were carried out with a dead-end filtration system at 1 bar transmembrane pressure in all runs. The tested membrane sample of a diameter of 3.9cm was mounted in the same filtration apparatus as described in the previous chapter. Permeate samples were collected at various time intervals for the analysis of mercury, HA or both concentrations. The permeate flux of the membrane sample was determined from the collected mass of the permeate versus the filtration time. The color change of the membrane before and after a filtration test was also recorded in terms of the photos by a digital camera or light absorbance by a UV/Vis spectrometer. The filtration tests were also conducted in three phases.

Phase I: Individual Filtration

The filtration tests were conducted for a Hg(II) solution (800 μ g/L) or a HA solution (15mg/L) at an initial pH6.5 for 150min.

Phase II: Sequential filtration

The filtration tests were conducted for a Hg(II) solution first (or a HA solution first) and then followed with a HA solution (or Hg(II) solution) in sequence.

Phase III: Co-filtration

The filtration tests were conducted with solutions containing both Hg(II) and HA. The preparation of solutions used in the filtration tests was the same as those used in the adsorption tests. All filtration tests were carried out for 150 min.

5. 3 Result and discussion

5.3.1Batch adsorption

Phase I: Individual adsorption of Hg(II) or HA by CS/CA-TPPS membrane

Fig. 5.1(a) shows the results of individual Hg(II) adsorption under different initial solution pH values. Obvious membrane color change from initially pink to final green was observed in the Hg(II) solutions from less than 5min contact time under all pH conditions; as shown in the inserted photos in Fig. 5.1(a). Hg(II) adsorption on the membrane is found to achieve greater uptake amounts at higher solution pH values, which is consisted with the results we obtain in Chapter 4. For individual adsorption of HA, changes in the membrane color were not detected by the naked eyes; as evidenced by the inserted photos in Fig. 5.1(b) under each pH condition. Besides, the adsorption uptakes of HA by CS/CA-TPPS membrane did not show a clear difference with the increase of solution initial pH value from 6.5 to 8.5; see Fig. 5.1(b). This may be due to the narrow pH range examined in this study (Yan and Bai, 2005). The final

uptake of Hg(II) on the membrane after 300min adsorption was in the range of 2-3mg/g and that of HA was at around 2.2mg/g. The results of individual adsorption confirm that the CS/CA-TPPS membrane could adsorb both Hg(II) and HA species in the aqueous solutions, but only show color change as the response to the presence of Hg(II).

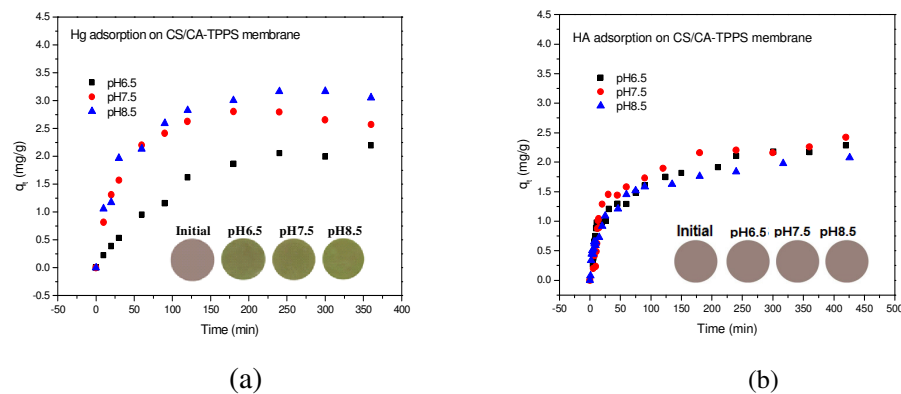


Fig. 5.1 Results of individual (a) Hg(II) (800 μ g/L) and (b) HA (15mg/L) adsorption on CS/CA-TPPS membrane in solutions with initial pH from 6.5 to 8.5. (22-23 $^{\circ}$ C, 0.02g membrane and 100mL solution for each adsorption, inserted photos were obtained after the contact time of 5min for Hg(II) solution and 300min for HA solution).

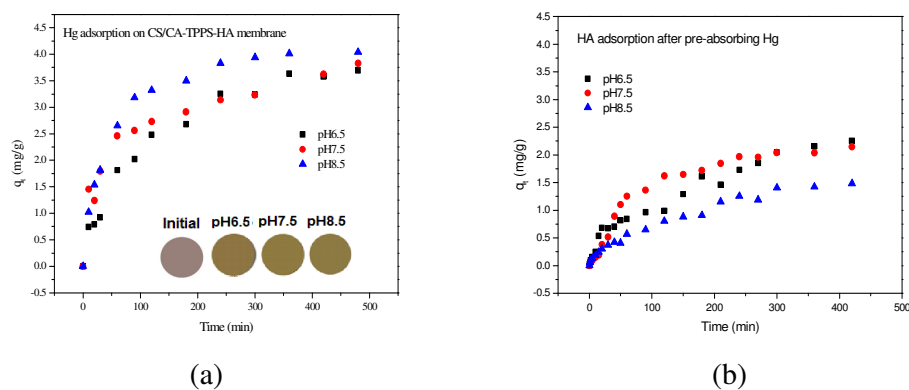


Fig. 5.2 Results of sequential adsorption. (a) Hg(II) (800 μ g/L) adsorption on CS/CA-TPPS-HA membrane; and (b) HA (15mg/L) adsorption on CS/CA-TPPS-Hg membrane in solutions with initial pH from 6.5 to 8.5 (22-23 $^{\circ}$ C, 0.02g membrane and 100mL solution for each adsorption, the inserted picture was obtained after 30min of contact time).

Phase II: sequential adsorption of Hg(II) and HA

CS/CA-TPPS-HA membranes after HA adsorption were further used for the sequential adsorption of Hg(II). Fig. 5.2(a) shows the sequential adsorption results of Hg(II) on CS/CA-TPPS-HA membrane under different initial solution pH values. It was found that the optical response of CS/CA-TPPS-HA membrane towards Hg(II) became less sensitive as the obvious color change from pink to green was only observed after 30min of contact time (see the inserted photos in Fig. 5.2(a)). According to El-Safty (2009), the variations of the UV/Vis light absorption intensity difference ($A-A_0$) of the surface at 450nm before and after contact with Hg(II) ions can be an indication to the extent of the formation of $[\text{Hg-TPPS}]^{n+}$ complex and the degree of color change. As shown in Fig. 5.3, it has been found that the $A-A_0$ curves of the CS/CA-TPPS-HA membranes at 450nm versus time were less steep than that of CS/CA-TPPS membranes. This suggests a reduced binding of Hg(II) ions with TPPS indicators on the CS/CA-TPPS multifunctional membrane, which led to a less significant color evolution in the process.

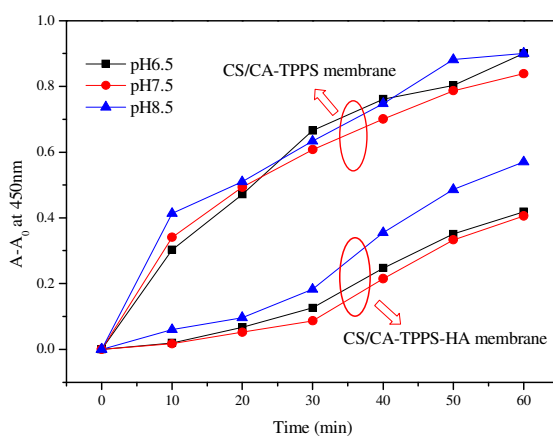


Fig. 5.3 Changes of developed membrane colors in terms of UV/Vis light absorbance intensity difference ($A-A_0$) at 450nm (A_0 and A are the light absorbance intensities of the membrane surface at 450nm before and after Hg(II) adsorption).

However, the mercury uptake amounts of the CS/CA-TPPS-HA membrane were higher than those of CS/CA-TPPS membrane (see Fig. 5.2(a) and in comparison with Fig. 5.1(a)). The adsorption kinetics of Hg(II) on both CS/CA-TPPS and CS/CA-TPPS-HA membranes were found to be well fitted to a pseudo second-order kinetic model which is often given as:

$$\frac{t}{q_t} = \frac{1}{K q_e^2} + \frac{1}{q_e} t \quad \text{Eq. 5.1}$$

where q_e (mg/g) is the amount of the adsorbate adsorbed at adsorption equilibrium, q_t (mg/g) is the amount of the adsorbate adsorbed at time t (min), and K ($\text{g} \cdot \text{mg}^{-1} \cdot \text{min}^{-1}$) is the rate constant of pseudo second-order kinetic model.

From the experiment results, the rate constant K , q_e and the regression coefficient R^2 were obtained; as given in Table 5.1. The results suggest that the adsorption of Hg(II) on both CS/CA-TPPS and CS/CA-TPPS-HA membranes was predominated by chemical interaction between the Hg(II) ions in the solution and the functional groups on the surface of the membranes (Ho and McKay 1999). The greater q_e values of CS/CA-TPPS-HA than that of CS/CA-TPPS indicate that the previously adsorbed HA on the membrane surface provided more adsorption sites for the uptake of Hg(II) ions. Desorption of previously adsorbed humic acid during the sequential Hg(II) adsorption was not detected in the solutions.

Table 5.1 Results of pseudo second-order kinetics model fitted to experiment data of Hg(II) adsorption on CS/CA-TPPS and CS/CA-TPPS-HA at different initial solution pH values.

	CS/CA-TPPS			CS/CA-TPPS-HA		
	K	q_e	R^2	K	q_e	R^2
pH6.5	0.0026	2.9967	0.9839	0.0025	4.3573	0.9884
pH7.5	0.0207	2.8224	0.9927	0.0057	3.9603	0.9887
pH8.5	0.0109	3.391	0.996	0.0061	4.3879	0.9992

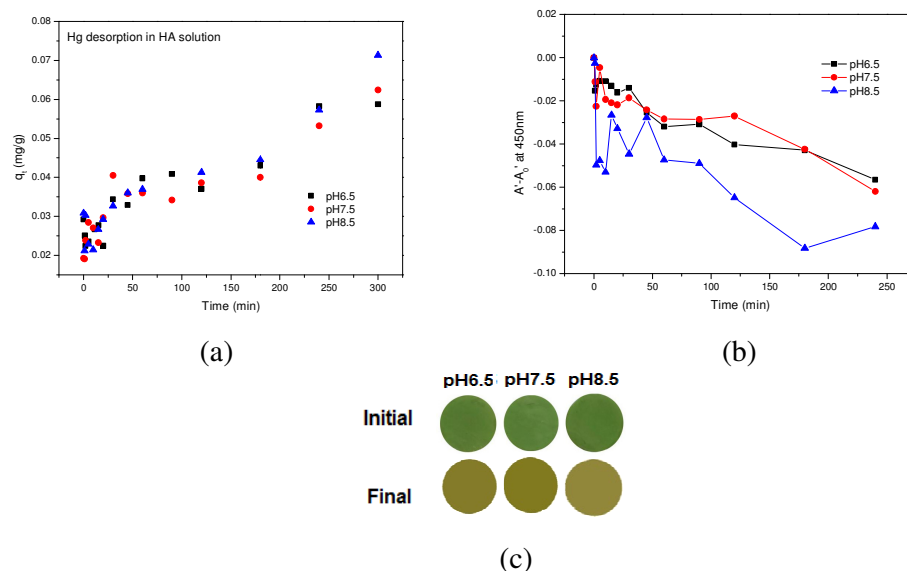


Fig. 5.4 Desorption results of Hg(II) ions from CS/CA-TPPS-Hg membrane during sequential adsorption of HA. (a) Hg(II) desorption amount and (b) changes in absorbance intensity ($A' - A_0$) at 450nm and (c) the color change of CS/CA-TPPS-Hg membrane after sequential HA adsorption (22-23°C, initial HA concentration 15mg/L, 100mL, 0.02g membrane).

For the sequential HA adsorption by the CS/CA-TPPS-Hg membrane, the final HA uptake amounts were found to be reduced and the adsorption equilibrium time was found to be prolonged, in comparison with that by the CS/CA-TPPS membrane (see result in Fig. 5.2(b) and Fig. 5.1(b)). In addition, a desorption of previously adsorbed Hg(II) was detected in the solutions during the sequential HA adsorption. For example, the concentration of desorbed Hg(II) in the HA solution was up to 70 μ g/L at pH8.5 after 300min, which indicates that an about 10% of previously adsorbed Hg(II) has leached from the membrane. The concentrations of desorbed Hg(II) ions in HA solutions is shown in Fig. 5.4(a). The membrane color was found to fade from green to yellowish-green; and the measured UV/Vis light absorbance intensity difference ($A' - A_0'$) at 450nm was reduced gradually during the sequential HA adsorption; see Fig. 5.4(b) and (c) (where A_0' and A' are the UV/Vis absorbance intensity of CS/CA-TPPS-Hg membrane at 450nm before and after the adsorption of HA), which also

indicates the desorption of Hg(II) ions from the CS/CA-TPPS-Hg membrane surface. The effect of pH on the sequential adsorption of Hg(II) or HA showed similar trends as in the individual adsorption of Hg(II) or HA.

From the results in the sequential adsorption study, the sequence of adsorption affected the detection and adsorption performance of the CS/CA-TPPS functional membrane greatly. In the literature, HA is reported to be a good complex agent for Hg(II) ions (Gu et al. 2011; Lu and Jaffe 2001; Rocha et al. 2003; Wallschlager et al. 1996; Zhai et al. 2010), and its binding with mercury ion can be through complexation with the carboxyl and/or phenolic groups in HA molecules (Wallschlager et al. 1996; Zhai et al. 2010; Yan and Bai 2005). Based on the study of Yan and Bai (2005), there are three possible ways that the previously adsorbed HA on the membrane may affect the detection and adsorption of Hg(II) in this study: (i) the previously adsorbed HA may take up the functional sites for the detection and adsorption of Hg(II) ions on the membrane surface, which could suppress both functions towards Hg(II); (ii) the attachment of HA onto the CS/CA-TPPS membrane surface did not consume the functional sites for the detection or adsorption of Hg(II), but may create a steric barrier that would hinder Hg(II) ions approaching to the available functional sites. In this case, the adsorption capacity will not decrease, but both the adsorption kinetics and detection response may be delayed; and (iii) the attached HA through either (i) or (ii) or both provided additional sites for mercury adsorption. Although the total amount of mercury adsorption may increase, the amount of Hg(II) available to TPPS indicators on the membrane surface can be decreased, and thus the detection response would be reduced. The above three mechanisms may function together in the adsorption process (Yan and Bai 2005). In this study, the delayed optical response

time and the increased mercury adsorption uptake by the CS/CA-TPPS-HA membrane indicate that the mechanisms of (ii) and (iii) have most probably taken place. The mechanisms may be schematically shown in Fig. 5.5(a).

On the other hand, the sequential adsorption of HA by the CS/CA-TPPS-Hg membrane showed decreased uptake amount and prolonged adsorption equilibrium time, which indicated that the previously adsorbed Hg(II) may influence the sequential HA adsorption by type (i) or (ii). The desorption of Hg(II) from CS/CA-TPPS-Hg could be attribute to the stripping effect of HA during its sequential adsorption, where some weakly bonded Hg(II) might be taken off or replaced by HA molecules from the bulk solution (see Fig. 5.5(b)). Two possible adsorption structures for the adsorption of metal and organic compounds on solid surfaces have been proposed by Stumm (Stumm 1992). One is the S-Me-HA and the other is the S-HA-Me, where S represents the adsorption site on the solid surface, Me is the adsorbed metal ion, and HA is humic acid. According to the experimental results, the S-HA-Me structure may be more stable than the S-Me-HA structure in this study.

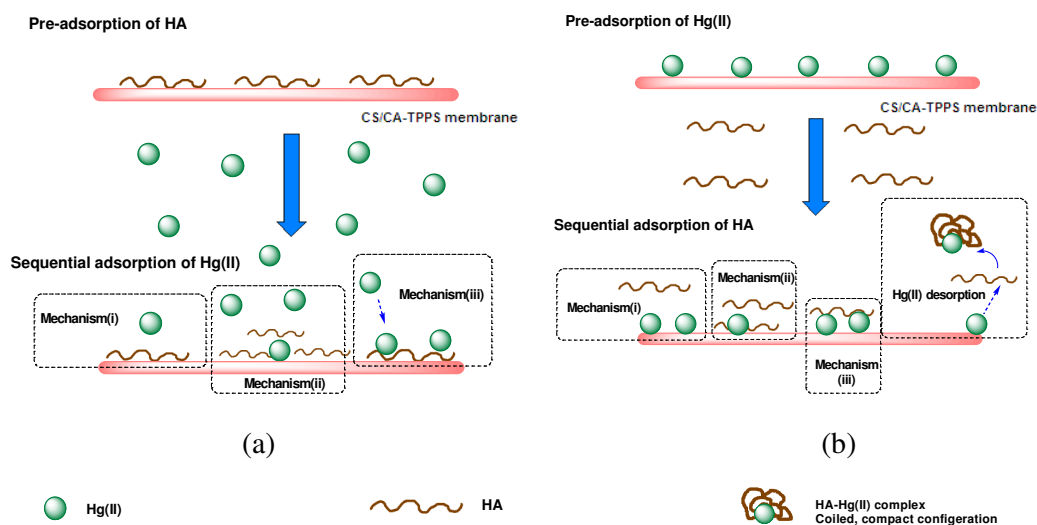


Fig. 5.5 The proposed mechanisms of sequential adsorption of (a) Hg(II) and (b) HA on CS/CA-TPPS membrane.

Phase III: Co-adsorption

In the real situation, HA may be more likely to co-exist with Hg (II) in surface water. This necessitates the investigation on the effect of co-existed HA on the adsorption and detection of Hg (II) ions by the CS/CA-TPPS membrane. Solutions containing both HA (15mg/L) and Hg (II) (800 μ g/L) at initial pH 6.5, 7.5 and 8.5 were tested. Fig. 5.6 shows the results of the adsorption behaviors for Hg(II) and HA in the mixed solutions. As can be found from the figure, the adsorption for both HA and Hg(II) were greatly reduced, particularly for Hg(II). No color change of the membrane surface was observed even after 300min of adsorption time (see Fig. 5.6(c)). In order to further investigate the effect of co-existed HA, experiments were conducted with solutions of the same Hg(II) concentration (800 μ g/L) while the HA concentrations were in the range of 2-15mg/L. As shown in Fig. 5.7, both visual detection and adsorption of Hg(II) was spoiled with the increases of the co-existed HA concentrations, which may be attributed to the formation of less-adsorbable HA-Hg(II) complexes (Lai and Chen 2001). The test solutions in this experiments were prepared 24h before the addition of membrane samples and hence, the interaction between HA and Hg(II) to form HA-Hg(II) complexes was expected to be fully established before the commencement of adsorption by the membrane. With the increase of HA/Hg ratios, more Hg(II) may exist in the form of HA-Hg(II) complexes. As the HA-Hg(II) complexes were less affinitive towards the membrane, the adsorption of Hg(II) on the membrane was reduced. Besides, the excessive free HA molecules in the solutions may compete with the HA-Hg(II) complexes for adsorption sites, and the adsorbed HA may create steric hindrance and electrostatic repulsion, which could further reduce the adsorption of Hg(II) (Hong and Elimelech 1997; Nystrom et al. 1996; Yan and Bai 2005).

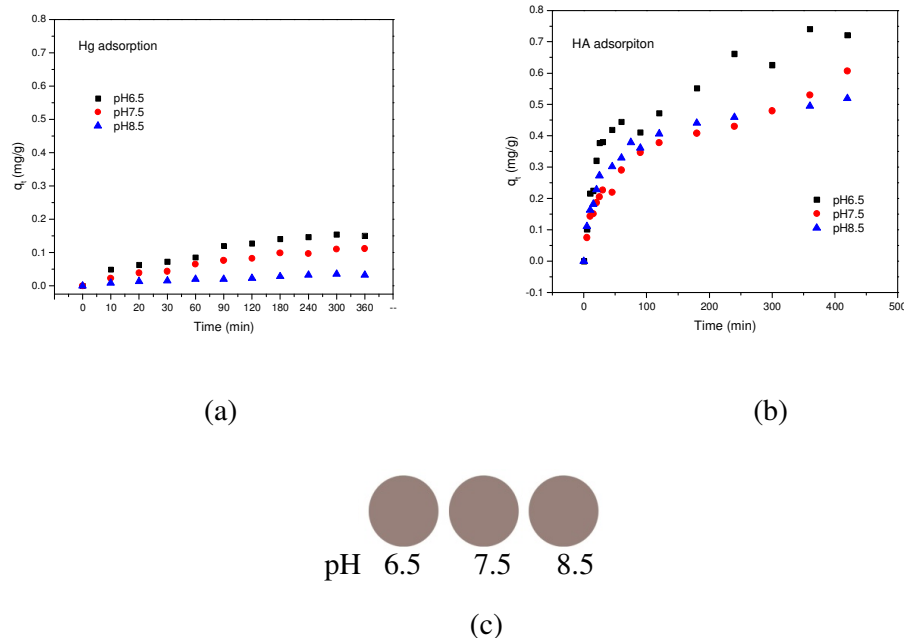


Fig. 5.6 Result of co-adsorption of 800g/L Hg(II) and 15mg/L HA in the same solution. (a) Hg(II) adsorption (b) HA adsorption; (c) membrane color after adsorption 300min (22-23°C, 100mL solution, initial pH6.5-8.5, 0.02g membrane).

From the batch adsorption study, we found that the effect of HA on the detection and adsorption of Hg(II) ions showed the same trend within the examined pH range (6.5 to 8.5) in all three phases. Previously adsorbed HA on the membrane can improve the adsorption of Hg(II) by providing additional adsorption sites to Hg(II). However, the detection sensitivity of the membrane towards Hg(II) ions may be reduced by the previously adsorbed HA on the membrane surface. On the other hand, leaching of Hg(II) from the CS/CA-TPPS-Hg membrane was noticed during the subsequent adsorption of HA. In the co-adsorption study, co-existence of HA with Hg(II) in the solutions reduced both adsorption uptakes and the detection sensitivity towards Hg(II), perhaps due to the formation of less-adsorbable HA-Hg(II) complexes. The effect was found to become more significant with the increase of the HA/Hg(II) ratio.

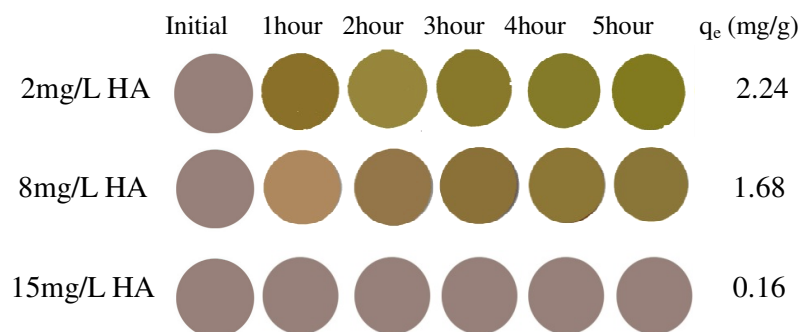


Fig. 5.7 The color response and Hg(II) uptake amount (q_e) of CS/CA-TPPS membrane in Hg(II) and HA mixed solution (22-23°C, initial Hg concentration 800 μ g/L, initial HA concentration from 2, 8, or 15mg/L, initial pH6.5, 100mL solution, 0.02g membrane).

5.3.2 Filtration performance

In the batch adsorption experiments, the target components were detected and removed mostly by the adsorption sites on the surface of the membrane. However, under a filtration mode, the applied pressure would produce a convective flow that transports the target components to the surface of the membrane, which may be expected to cause differences in the performance of the membrane (Ognier et al. 2002). In addition, the prepared CS/CA-TPPS multifunctional membrane is also targeted for separation in a filtration system for water treatment. Therefore, it is of practical interest to investigate its performance during filtration. Similar to the batch adsorption study, the experiments were also carried out for three phases, namely, filtration of individual type of Hg(II) or HA solutions, sequential filtration of Hg(II) and HA solutions and filtration of solutions containing both Hg(II) and HA.

Phase I: Individual filtration of Hg (II) or HA solutions by CS/CA-TPPS membrane

As shown in Fig. 5.8(a), the filtration of Hg(II) solution at a concentration of 800 μ g/L achieved a removal of Hg(II) in the range of 50 to 60% during the 150min filtration experiment. The color change of the membrane before and after the Hg(II) solution

filtration was very obvious (see Fig. 5.8(b)). For HA solution filtration, the removal rate of HA was at around 70%, slightly higher than that of Hg(II) (see Fig. 5.9(a)). Apart from adsorption removal, the membrane could also remove a portion of HA through size exclusion or the filtration mechanism. Besides, the attached HA on the membrane surface may further enhance the interception of the approaching HA in the feed solution, resulting in a cake layer on the membrane surface, as evidenced in Fig. 5.9(b) (Cheremisinoff 2002). It has been reported that HA can cause severe fouling of the membranes at concentrations as low as 10mg/L (Nystrom et al. 1996). This phenomenon was very obvious in this experiment with HA concentration at 15mg/L as the permeate flux was found to drop by about 36% from 11.5L/m²·h in the beginning of the filtration to 7.4 L/m²·h after 150min of filtration.

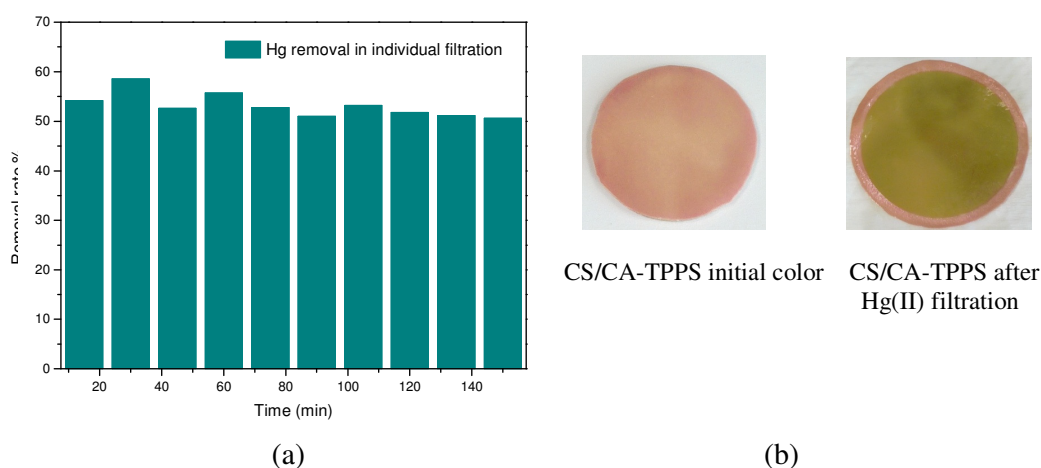


Fig. 5.8 Result of Hg(II) solution filtration by CS/CA-TPPS membrane. (a) Removal rate of Hg(II) and (b) membrane color change after filtration of Hg(II) (22-23°C, initial Hg concentration 800µg/L, initial pH6.5, membrane area 11.8cm², applied pressure 1 bar, filtration duration 150min, permeate flux 12.3L/m²·h).

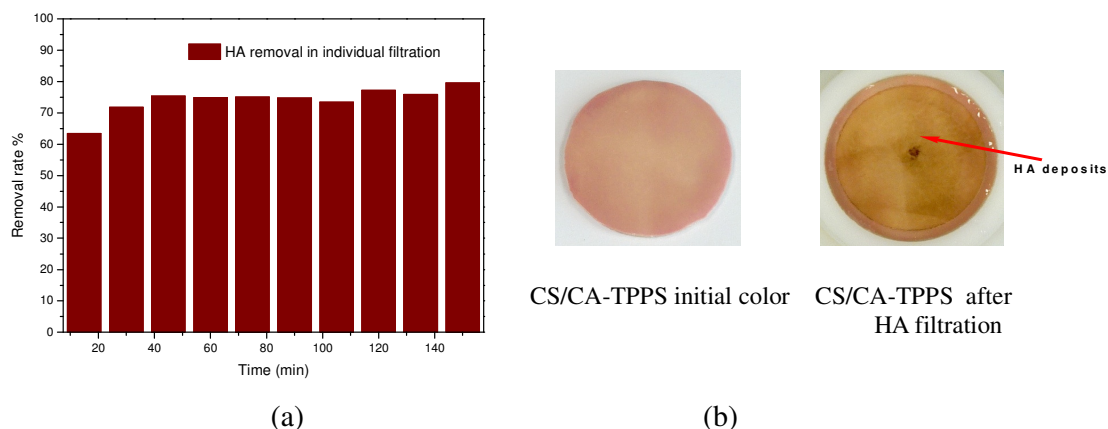


Fig. 5.9 Result of HA solution filtration (a) Removal rate of HA and (b) membrane colors after filtration of HA by CS/CA-TPPS membrane (22-23°C, initial HA concentration 15mg/L, initial pH6.5, membrane area 11.8cm², applied pressure 1 bar, filtration duration 150min, permeate flux dropped continuously from 11.5L/m²·h to 7.4 L/m²·h).

Phase II: Sequential filtration of Hg(II) and HA solutions

(i) Filtration of HA solution followed by Hg(II)solution

The CS/CA-TPPS membrane after the filtration of 15mg/L HA solution as in Phase I was then used for the filtration of 800μg/L Hg(II) solution. The result on the removal rate of Hg(II) are shown in Fig. 5.10(a). It can be observed that the removal rate attained was as high as up to 95%, about 45% higher than that achieved in the filtration of individual Hg(II) solution. As suggested in the batch adsorption study, the HA adsorbed on the membrane surface during the HA solution filtration would provide more adsorption sites that allowed more Hg(II) ions to be removed. This effect can be further enhanced by the formation of the HA cake layer occurred before the filtration of the Hg(II) solutions, which greatly improved the removal of Hg(II), possibly due to HA providing more adsorption site for Hg(II) ions. Although the attached or retained HA on the membrane improved the removal of Hg(II), the detection sensitivity of the membrane to Hg(II) was reduced (see Fig. 5.10(b)) as no

obvious color change can be observed. This may be attributed to the masking effect imposed by the adsorbed or retained HA cake layer on the membrane surface. As a large fraction of Hg(II) ions removal during the filtration may be attributed to the adsorption in the HA cake layer and only a small fraction in the feed can reach and be in contact with the TPPS indicators on the membrane surface, less TPPS-Hg(II) complexes would therefore be formed, which resulted in a reduced degree of color change for the visual detection of Hg(II).

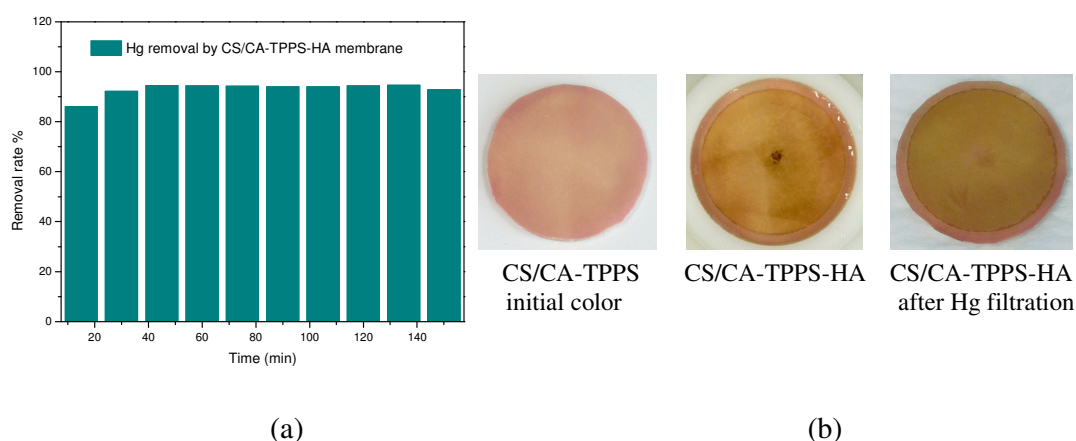


Fig. 5.10 Filtration of Hg(II) solution by CS/CA-TPPS-HA membrane. (a) Removal rate of Hg(II) and (b) the membrane colors before and after sequential Hg solution filtration (22-23°C, initial Hg(II) concentration 800µg/L, initial pH6.5, membrane area 11.8cm², applied pressure 1 bar, filtration duration 150min, permeate flux around 7.3L/m²·h).

(ii) *Filtration of Hg(II) solution followed by HA solution*

The CS/CA-TPPS-Hg membrane obtained from the filtration of Hg(II) solution (800µg/L) was then used for the filtration of 15mg/L HA solution. The results obtained are shown in Fig. 5.11. The removal of HA was in the range of about 70 to 80%, similar to that attained in the individual HA solution filtration test (see Fig. 5.11(a) and Fig. 5.9(a)). According to the results in the batch adsorption study, the pre-adsorbed Hg(II) ions may reduce HA adsorption by consuming the adsorption sites available for HA on the membrane surface (Nakamura and Matsumoto 2006).

However, in the sequential filtration study, the HA removal obtained was similar to that in the individual HA solution filtration, which indicates that the HA removal during the filtration largely relied on the interception mechanism rather than the adsorption mechanism (Cheremisinoff 2002). Leaching of previously attached Hg(II) on the membrane was detected at up to 0.052mg/L in the permeate (see Fig. 5.12). Besides the stripping effect imposed by HA, it could also be attributed to the flushing action by the convective flow under the applied pressure. When HA solution was passing through the membrane matrix, the permeating HA might replace some physically adsorbed or weakly bonded Hg(II) ions on the membrane surface, contributing to Hg(II) leaching in the permeate. The color of CS/CA-TPPS-Hg membrane changed from green to yellowish green after the subsequent filtration of HA solution (see Fig. 5.11(b)). This could be attributed to the leaching of adsorbed Hg(II) ions and the mask effect of retained HA layers on the membrane surface.

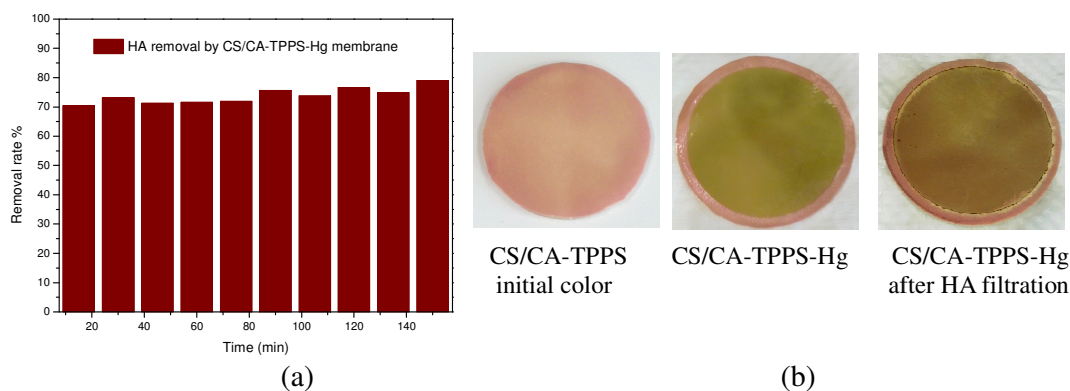


Fig. 5.11 Filtration of HA solution by CS/CA-TPPS-Hg membrane. (a) Removal rate of HA and (b) the developed color after HA filtration (22-23°C, initial HA concentration 15mg/L, initial pH6.5, membrane area 11.8cm², applied pressure 1 bar, filtration duration 150min, permeate flux dropped continuously from around 12.1L/m²·h to 8.3L/m²·h).

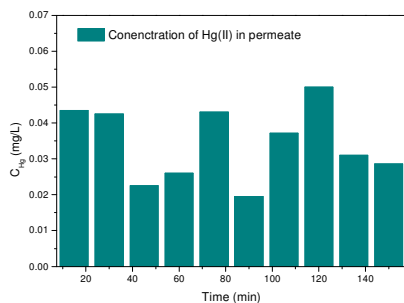


Fig. 5.12 Desorption of Hg(II) from CS/CA-TPPS-Hg membrane in the sequential filtration of 15mg/L HA solution.

Phase III: Filtration of the solutions containing both Hg(II) and HA

Similar to the batch adsorption tests, the feed solution containing both 15mg/L HA and 800 μ g/L Hg(II) was prepared 24h before commencing the filtration experiments. The results on the removal of Hg(II) and HA during the filtration and the membrane surface color before and after the filtration are shown in Fig. 5.13.

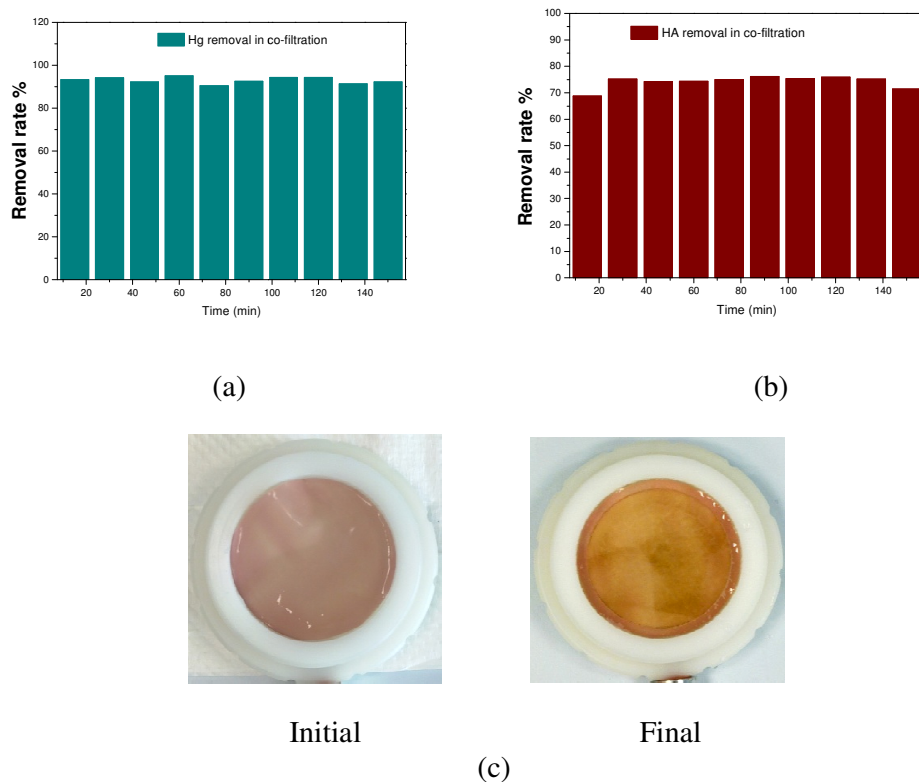


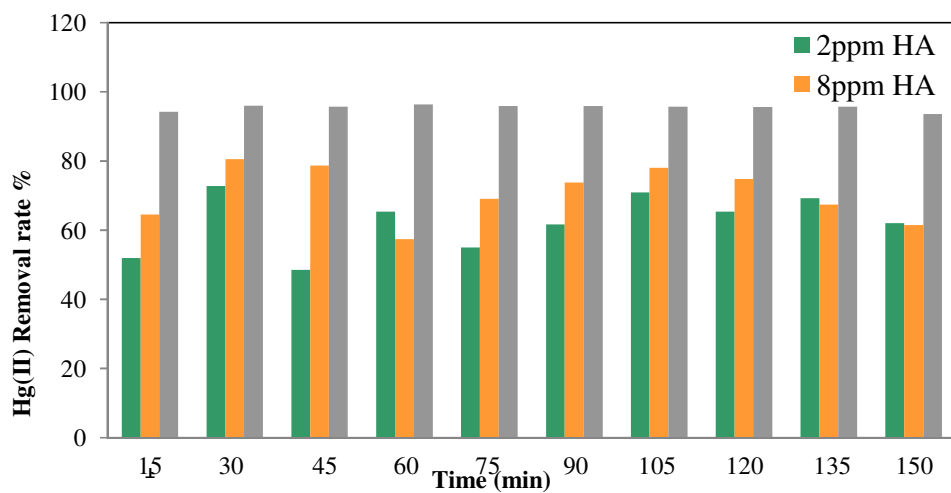
Fig. 5.13 Filtration of the solution containing 800 μ g/L Hg and 15mg/L HA. Removal rate of (a) Hg(II); (b) HA and (c) the membrane color before and after the filtration

(22-23°C, initial pH6.5, membrane area 11.8cm², applied pressure 1bar, filtration duration 150min, permeate flux continuously dropped from 11.2L/m²·h to 6.7L/m²·h).

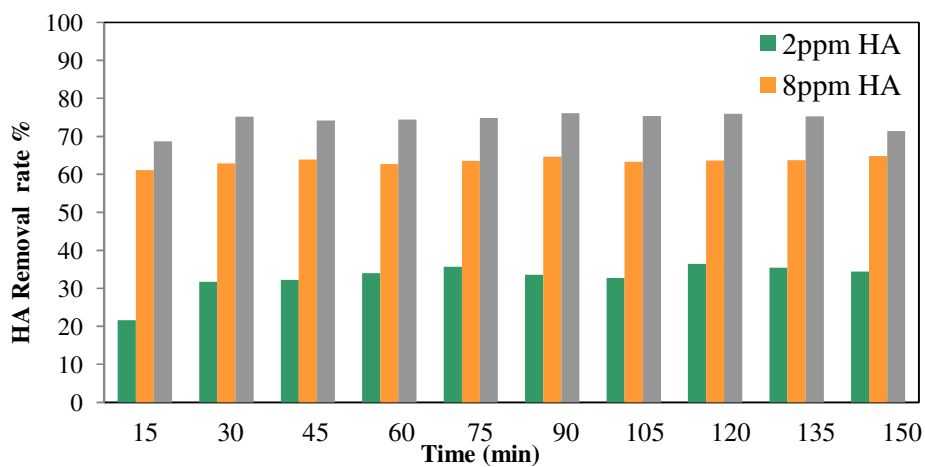
It can be found that the removal of Hg(II) appeared to be considerably high at more than 90% (Fig. 5.13 (a)), similar to those in the sequential filtration of Hg(II) solution by CS/CA-TPPS-HA membrane. Recalling the result in batch adsorption that the Hg(II) uptake in co-adsorption tests was low, it indicated a poorer affinity of the HA-Hg(II) complex to the adsorption sites on the membrane surface. However, during filtration, other than the adsorption of Hg(II) or HA-Hg(II) complex, the removal of Hg(II) could also be achieved by the interception of the HA-Hg complexes, which was not relied on the availability of and the affinity to the adsorption sites on the membrane surface. The removal of HA in the filtration appeared to be in the same range as those in the individual and sequential HA solution filtration tests (see Fig. 5.13 (b)). This further supports the assumption that the removal of HA during filtration was mainly attributed to the interception mechanism (Cheremisinoff 2002).

The membrane surface before and after filtration of the Hg(II) and HA solution, as shown in Fig. 5.13(c), demonstrate a color change from pink to brown instead of green. This was mainly attributed to the deposit of HA or HA-Hg(II) complex on the membrane surface. The permeate flux of the membrane was found to continuously drop from initially 11.2L/m²·h to 6.7L/m²·h after 150min of filtration. In order to further investigate the effect of co-existed HA on the detection and removal of Hg(II), experiments were conducted with different HA/Hg(II) ratios. The results in Fig. 5.14 show that the removal rates of HA and Hg(II) both increased with the increase of the HA/Hg(II) ratio, suggesting that more HA deposited on the membrane surface could further enhanced the removal rate of HA and Hg(II) during the filtration. However,

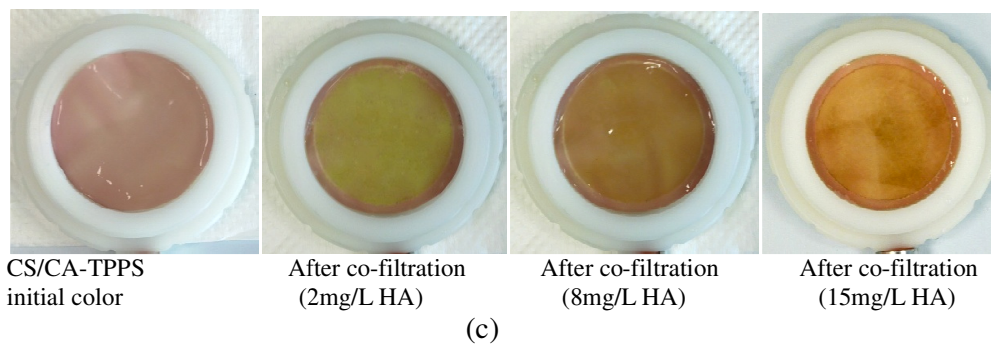
the visual detection sensitivity to Hg(II) was compromised at higher HA/Hg(II) ratios; see Fig. 5.14(c).



(a)



(b)



(c)

Fig. 5.14 Filtration of solutions containing both HA and Hg(II) at different HA/Hg(II)

ratios. Removal rate of (a) Hg(II), (b) HA and (c) the membrane color changes before and after the filtration runs (22-23°C, initial Hg(II) concentration 800µg/L, initial HA concentration 2mg/L, 8mg/L and 15mg/L, respectively, initial pH6.5, membrane area 11.8cm², applied pressure 1 bar, filtration duration 150min).

In summary, the results in the filtration experiments indicated that the presence of HA can also affect the performance of the CS/CA-TPPS membrane during the filtration operation. The visual detection sensitivity for Hg(II) was found deteriorated by the presence of HA under all examined filtration conditions. However, the removal of Hg(II) was improved when HA was pre-loaded on the membrane or co-existing with Hg(II) in the feed solutions. However, leaching of the pre-adsorbed Hg(II) ions from the membrane surface was observed during the sequential filtration of HA. The removal rates of HA were found in the same range in the three types of filtration tests, indicating that the removal of HA in the filtration was mainly through the interception mechanism.

5.4 Conclusion

In this study, the influence of HA on the detection sensitivity and removal efficiency of Hg(II) by a multifunctional membrane (CS/CA-TPPS) was examined under both batch adsorption and batch filtration conditions in three different phases. Generally, the presence of HA in solutions could improve Hg(II) removal; but impose a negative effect on Hg(II) detection by the CS/CA-TPPS membrane. In the batch adsorption experiments, the membrane was found to be able to adsorb both Hg(II) and HA. When the adsorption was in sequential order, previously adsorbed HA may improve the removal of Hg(II) by providing more adsorption sites, however, the detection sensitivity towards Hg(II) in terms of developed color change was reduced. When Hg(II) and HA co-existed in the same solution, both HA and Hg(II) removal by

adsorption was decreased due to the formation of less-adsorbable HA-Hg(II) complexes. In the filtration study, the removal rate of Hg(II) was found to be significantly increased by either the pre-loaded HA on the membrane surface or the co-existing HA in the solutions. Similar to that in the adsorption study, when the HA/Hg ratio was increased, the detection of Hg(II) by the membrane became less sensitive. Based on our experimental results, there is a great potential for the practical application of CS/CA-TPPS membrane for Hg(II) removal and visual detection in water treatment process if the interfering HA concentrations are relatively low; otherwise, suitable pre-treatment processes are suggested to reduce HA/Hg(II) ratio in water to ensure a sensitive detection of Hg(II) ions.

**CHAPTER 6 A VERSATILE METHOD FOR THE IMMOBILIZATION OF
OPTICAL INDICATORS ON THE BASE MEMBRANE: APPLICATION TO
CADMIUM(II)**

SUMMERAY

The immobilization of optical indicators onto the base membrane is a key factor to develop high performance multifunctional membrane for visual detection and adsorptive removal of heavy metal ions. In the previous chapters, indicators for lead (DZ) and mercury (TPPS) has been successfully immobilized onto CS/CA membrane through simple solution reactions. However, some indicators may not have intrinsic affinity towards the base membrane, thus cannot be directly immobilized onto the membrane via adsorption. In this study, a versatile post-grafting method - surface-initiated atom transfer radical polymerization (ATRP) is introduced to solve this issue. ATRP is a fixable approach that can adjust the membrane surface property according to the requirements, thus facilitate and consolidate the immobilization of various optical indicators. Besides, the results in this study also indicated that the ATRP method could also improve the adsorption capacity by providing more functional groups through the grafted polymer brushes.

6.1 Introduction

Due to the surface properties of the base membranes, some indicators cannot be directly immobilized onto the membrane through adsorption-based simple reaction; therefore, advanced methods are required to facilitate the immobilization. Surface grafting is one of the most commonly used methods to achieve the purpose (Coronado et al. 2005; Liu and Lu 2004). El-Safty et al. has reported several grafting strategies by using hard or soft modifier coupling agents (El-Safty et al. 2007a; El-Safty et al. 2007b). However, there are some challenges in the above grafting techniques including the sophisticated immobilization procedures, the potential leaching of indicators, and the retention of the specific activity of the indicators, as well as the decrease of the intrinsic mobility of the immobilized indicators, all of which can obstruct the generation and transducing of the optical signals in response to the metal binding events.

In this study, we introduced a versatile method, surface-initiated atom transfer radical polymerization (ATRP), to assist the immobilization of optical indicators that do not have intrinsic affinities towards CS/CA base membrane. The ATRP method is one of the most facile grafting methods, but, it has only been used for membrane surface modification in recent years (Balachandra et al. 2003; Husson et al. 2008; Singh et al. 2005; Sun et al. 2005; Sun et al. 2006). It is a catalyst-activated process where catalyst initiates the polymerization by reversible abstraction of halogen atom from the surface, and the polymer chains then grow by the monomer addition from the surface (Granel et al. 1996; Haddleton et al. 1997; Kato et al. 1995; Xia et al. 1998a; Xia and Matyjaszewski 1997; Xia and Matyjaszewski 1999; Xia et al. 1998b). An ATRP catalyst normally consists of three parts: a transition metal species, for example Cu^{I} ,

which can expand its coordination sphere and increase its oxidation number; a complexing ligand; and a counterion (Y) which can form a ionic or covalent bond with the transition metal species. The transition metal complex ($\text{Cu}^{\text{I}}\text{-Y/Ligand}$) is responsible for the cleavage of alkyl halogen bond (R-X), which could generate a higher oxidation state metal halide complex $\text{X-Cu}^{\text{II}}\text{-Y/Ligand}$ (rate constant k_{act}) and an organic radical R^\bullet (Kamigaito et al. 2001; Matyjaszewski and Xia 2001). The organic radical R^\bullet can then propagate with monomers (k_{p}) and the reaction will be terminated by either coupling or disproportionation (k_{t}), or be reversibly deactivated (k_{deact}) in the equilibrium by $\text{X-Cu}^{\text{II}}\text{-Y/Ligand}$ to form a halide-capped dormant polymer chain. The proposed mechanism is shown in Fig. 6.1 (Braunecker and Matyjaszewski 2007).

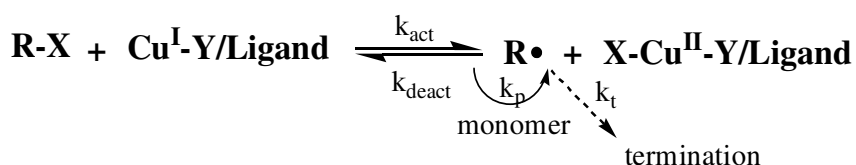


Fig. 6.1 Mechanism of ATRP.

Through the ATRP method, a highly accessible, flexible, and finely tuned surface can be created for the sequential immobilization of desired indicator molecules. Besides, the grafting of polymer brushes on the membrane surface could also provide more adsorption sites for heavy metals, which can lead to an improved adsorption performance. In this study, the ATRP method was used to modify the CS/CA membrane surface properties specifically with negatively charged polymer brushes. A cadmium optical indicator, 5,10,15,20-Tetrakis (1-methyl-4-pyridinio) porphyrin tetra (p-toluenesulfonate) (TMPyP), which does not have intrinsic affinity towards CS/CA membrane, was then successfully immobilized onto the membrane through the electrostatic interaction with the grafted polymer brushes.

6.2 Materials and methods

6.2.1 Materials

The materials for the CS/CA base membrane preparation were obtained as described in pervious chapters. Tetrahydrofuran (THF, HPLC grade), triethylamine (TEA), and α -bromoisobutyryl bromide (98%) supplied by Sigma-Aldrich were used in the introduction of polymerization initiator on the CS/CA membrane surface during the ATRP process. Other chemicals used for the surface-initiated ATRP, including 3-Sulfopropyl methacrylate potassium salt (SMP, to form negatively charged polymer brushes), methanol (99%), copper(I) bromide (CuBr, 99%), copper(II) bromide (CuBr₂, 99%), 2,2'-Bipyridyl (BPY, >99%) and EDTA (disodium salt-ethylenediaminetetraacetic acid, 0.1M) were from Sigma-Aldrich. The optical indicator, 5,10,15,20-Tetrakis(1-methyl-4-pyridinio) porphyrin tetra (*p*-toluenesulfonate) (TMPyP, $\geq 95\%$) was also supplied by Sigma-Aldrich. Cd(NO₃)₂ standard solution (1000 mg/L) from Merck was used in the adsorption study. Ultrapure water was used to prepare all test solutions as needed.

6.2.2 Preparation of CS/CA blend base membrane

The general method for the preparation of CS/CA blend base membrane was the same as described in previous chapters. Since a 2% NaOH solution was used to coagulate the membrane in the preparation process, the cellulose acetate molecules on the membrane surface were converted to cellulose, which made the membrane insoluble in the THF mixture that was used for the grafting of polymer brushes in the following preparation process.

6.2.3 Grafting of polymer brushes on CS/CA base membrane for indicator immobilization

To achieve satisfactory immobilization of the indicator molecules, surface initiated ATRP method was used to graft negatively charged polymer brushes onto the membrane surface. The advantage of the ATRP process lies in its controllability for the polymerization degree or extent (Patten and Matyjaszewski 1998). Before the ATRP process, α -bromoisobutyryl bromide was first introduced onto the CS/CA membrane as the polymerization initiator. This was done through the following processes in this work. A 100mL three-neck flask containing 50mL THF was purged with nitrogen gas for 30min. A 2g of the dry CS/CA membrane was then added into the flask, followed by the addition of 1mL dehydrated TEA. The contents in the flask were gently stirred under nitrogen gas for another 30min to eliminate any oxygen that may exist in the flask. After that, 2mL of α -bromoisobutyryl bromide was added into the solution and the reaction in the flask was allowed to proceed for 24h at room temperature (22-23°C) under the protection of nitrogen gas in the headspace. Finally, the CS/CA membrane with the introduced initiators was rinsed with THF, methanol and DI water in sequence and then dried and stored in a vacuum desiccator for further use.

The grafting of the negatively charged polymer brushes from SMP on the surface initiated CS/CA membrane was realized through the ATRP method. The process was demonstrated as the followings. Amount of 1g surface initiated CS/CA membrane was added into a 100mL three-neck flask containing 10mL DI water and 40mL methanol. The contents in the flask were sealed by glass stoppers and purged with nitrogen gas for 1h to remove any possible oxygen in the flask. Then, 1g SMP was

added into the flask. After the SMP monomer was completely dissolved in the solution, 321.4mg (2.05mM) 2'2-bipyridyl (BPY), 55.8mg (0.25mM) CuBr₂ were added into the system in sequence. The contents in the flask were gently stirred under nitrogen gas again for another 30min to eliminate any remaining oxygen that may exist in the flask. Then, 144mg CuBr (1mM) was added into the flask and the reaction was allowed to proceed for a desired reaction time (the reaction time was fixed at 3h and no variation in the polymerization degree was examined in this study) at room temperature for the SMP polymer brushes to grow. Finally, the membrane was removed from the reaction mixture and washed thoroughly with 0.1M EDTA first, followed by excess DI water. The membrane from this process, denoted as CS/CA-SMP in this study, was dried and then stored in a vacuum desiccator for further use.

6.2.4 Coupling of cadmium indicator (TMPyP) onto CS/CA-SMP membrane

The coupling of TMPyP on the CS/CA-SMP membrane was achieved by adding the membrane into 100mL TMPyP solution with a concentration at around 7mg/L. The mixture was shaken in an orbit shaker at 150rpm under room temperature for 8h. The final product, denoted as CS/CA-SMP-TMPyP membrane, was taken out from the TMPyP solution and then washed extensively in a series of 100mL DI water until no apparent TMPyP was found in the spent liquid (analyzed by a UV/Vis spectrophotometer, Jasco V660, Japan). Finally, the obtained membrane was dried and then stored in a vacuum desiccator for further use. In order to compare the affinity of TMPyP molecules to CS/CA base membrane and CS/CA-SMP membrane, the UV/Vis absorption measurement for TMPyP in the solution before and after equilibrated with each type of the membranes were also measured. The amount of TMPyP immobilized on the CS/CA-SMP membrane was estimated through mass

balance analysis from the measured TMPyP concentrations in the TMPyP solution before and after the coupling process as well as in the washing solutions.

6.2.5 Characterization of membranes

The surface chemical compositions of the membranes were characterized by attenuated total reflectance Fourier transform infrared spectroscopy (FTIR/ATR). The analysis was done through a Shimadzu H8400 spectrophotometer (Japan) equipped with an ATR cell (KRS-5 crystal, 45°) in the wave number range of 600-4000cm⁻¹.

The surface morphologies of the various membranes were observed with a Scanning Electron Microscope (SEM, JSM-5600LV). Samples were platinum-coated with a vacuum electric sputter coater (JEOL JFC-1300) before the SEM scans and the analysis was done by following the standard operation procedures (Li and Bai 2005). Pure water flux (PWF) measurements for each type of the membranes were carried out with a dead-end filtration system as described in previous chapters. The assessments on color changes of the membrane samples with adsorbed cadmium species were made by taking photos with a digital camera (Canon Digital IXUS 1101S) as well as by obtaining UV/Vis light absorbance spectra with a UV/Vis spectrophotometer (Jasco V660, Japan).

6.2.6 Experiments for examining chromatic response of the membranes in detecting cadmium ions in solutions

First, the response time of the prepared membranes in their color change at different contact times was monitored. Samples of a specific type of membrane with a weight of about 0.06g were added respectively into a number of cadmium solutions (initial

concentration 50mg/L, solution volume 20mL, initial pH value 8, 22-23°C) with continuous shaking on a shaker at 150rpm. The membrane samples at various contact times with the cadmium solutions were taken out for the color assessments.

The tests were then done for cadmium solutions with different initial pH values. Cadmium solutions with an initial concentration of 50mg/L were prepared by diluting the 1000mg/L standard cadmium solution with ultrapure water and then adjusted to different initial pH values in the range of 4 to 10 with dilute HCl or NaOH solutions. Membrane samples with a weight of around 0.06g were added into each of a number of 50mL flasks containing 20mL of a cadmium solution (50mg/L) with different initial pH values. The contents in the flasks were shaken in an orbital shaker at 150rpm and room temperature for 20min. The membranes were then taken out from the flasks, rinsed with DI water and used for the color assessments as mentioned early.

Finally, the chromatic response of the prepared membranes to cadmium solutions with different concentrations was also investigated. The experiments were similarly conducted as above but at a different initial cadmium concentration ranging from 0 to 120mg/L (initial pH value 8, 22-23°C, contact time: 20min).

6.2.7 Cadmium adsorption performance experiments

Adsorption kinetic study was carried out to characterize the uptake rates of cadmium ions on the prepared membranes and also the time for the membranes to approach adsorption equilibrium. The experiments were conducted by adding about 1.2g membrane in small pieces (each around 0.95cm²) to 400mL of a cadmium solution with the initial concentration at 50mg/L and initial pH at 8 in a 500mL flask under

room temperature. The mixture in the flask was shaken in an orbital shaker at 150rpm for a period of up to 10h. 10mL solution was taken at each desired time interval, filtered through a 0.45 μ m Waterman membrane filter and then the filtrate was analyzed with an Inductively Coupled Plasma-Optical Emission Spectrometer (ICP-OES, Perkin Elmer Optima 3000DV) for the cadmium concentration in the solution. The pH of the solution was not controlled during the adsorption process in order not to introduce any additional ions (the final pH was found to slightly drop from 8 to 7.94). The adsorbed amount of cadmium on the membrane at time t_i , $q(t_i)$ (mg/g), was calculated from the mass balance equation (Eq. 3.1).

Adsorption isotherm study was conducted to illustrate the adsorbed cadmium amount versus the metal concentrations in the solutions at adsorption equilibrium. The experiments were conducted by adding about 0.06g membrane in small pieces to each of a number of 50mL flasks containing 20mL of cadmium solution with different initial concentrations (in the range of 1-260mg/L) at initial pH value 8. The contents in the flasks were shaken in an orbital shaker at 150rpm and under room temperature for a contact time of up to 300min (well above the adsorption equilibrium time of about 200min). Cadmium ion concentrations in the initial and final solutions were analyzed using the ICP-OES instrument. Before the analysis, each sample was filtered through a 0.45 μ m Waterman membrane filter to remove any possible suspended particles in the sample. As predicted by the MINEQL+ software analysis, no cadmium precipitation would occur under the experimental conditions (Schecher and McAvoy 2003). The adsorbed amount at adsorption equilibrium, q_e (mg/g), was calculated by the equation Eq. 3.2.

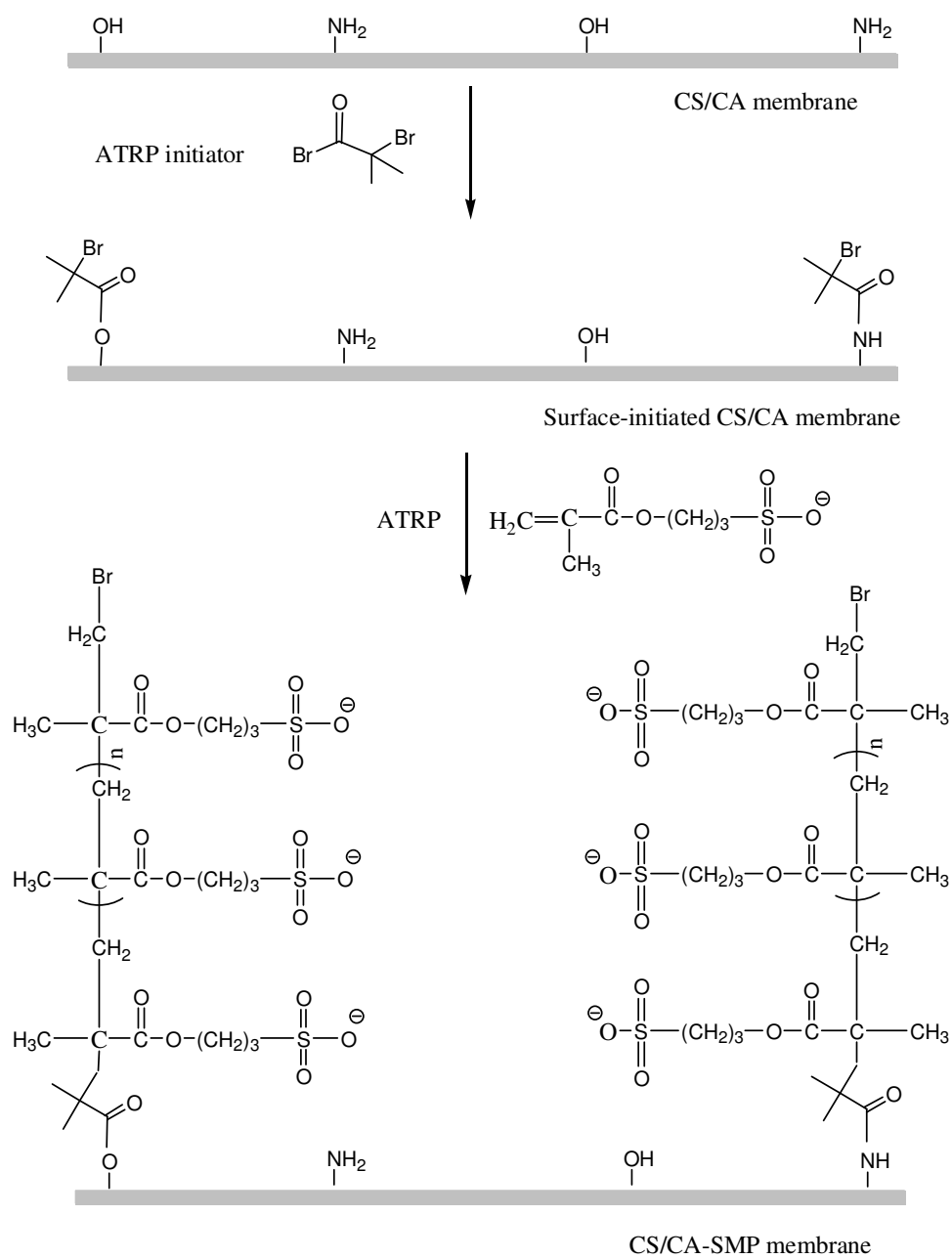
6.2.8 Experiments on interference study

The interference of other metal ions in the solution on the response and uptake of cadmium to the prepared functional membrane was examined. The experiments were conducted by equilibrating the membrane samples with solutions containing a fixed concentration of cadmium ions (10^{-4}M) at initial pH value 8 under room temperature with the presence of different amounts of interfering metal ions. The interfering metal ions used in the experiments included K^+ , Na^+ , Ca^{2+} , Mg^{2+} , Co^{2+} and Ni^{2+} ions.

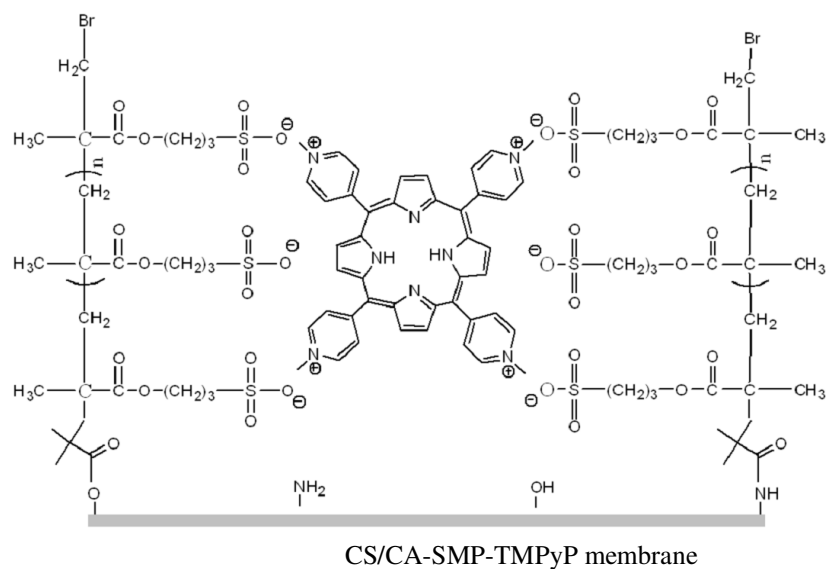
6.3. Results and discussion

6.3.1 Functionalization of membrane surface for cadmium ions

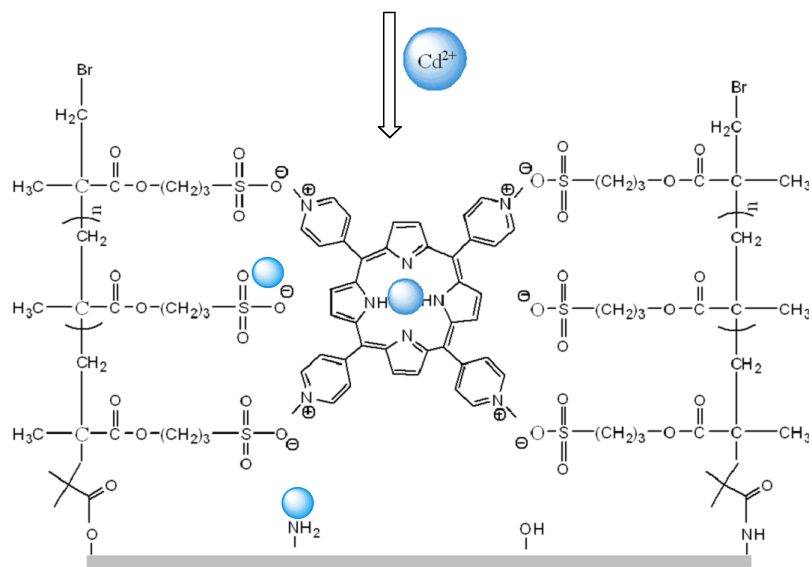
TMPyP has been studied as an optical indicator for cadmium ions due to its unique chromatic response to the presence of cadmium ions in solutions. It has been desirable to immobilize TMPyP as a probe onto a solid matrix for sensor applications (Balaji et al. 2006). As the CS/CA base membrane does not have the affinity to the TMPyP probes, negatively charged polymer brushes were first grafted onto the CS/CA base membrane surfaces in this study through a surface initiated ATRP method, which provided an effective way to immobilize TMPyP probes onto the CS/CA base membrane through strong electrostatic interactions. The pathway of immobilizing TMPyP probes onto the CS/CA base membrane for cadmium detection and removal in this work is outlined in Fig. 6.2.



(a)



(b)



(c)

Fig. 6.2 Schematic representation of the processes to obtain the multifunctional membrane. (a) Immobilization of the surface initiator and the polymerization of negatively charged monomer (SMP) on CS/CA base membrane surface; (b) coupling of TMPyP molecules to obtain CS/CA-SMP-TMPyP; (c) interaction between cadmium ions and CS/CA-SMP-TMPyP membrane.

In order to graft the negatively charged polymer brushes, the initiator of α -bromoisobutryl bromide was introduced to the CS/CA membrane surface through the

reaction with both the hydroxyl and amine groups (Kang et al. 2009; Li et al. 2005). Tetrahydrofuran (THF) was used as the solvent for the reaction and organic alkali triethylamine (TEA) was added as the catalyst. Then, the polymerization of SMP on to the membrane surface from the ATRP process was carried out in a water/methanol solution. 2,2'-bipyridyl was selected in this study as an effective ligands for copper-based ATRP in forming a complex with Cu(I) halides powerfully. A certain amount of CuBr₂ was also applied as the deactivating species to control the reaction (Patten and Matyjaszewski 1998). After a desired polymerization time, the ATRP process was stopped and the membrane surface with polymer brushes containing -SO₃⁻ groups was obtained (denoted as CS/CA-SMP). The introduction of the initiator and the growth of polymer brushes in the ATRP process are illustrated in Fig. 6.2(a).

When the prepared membrane was added into the TMPyP solution, the TMPyP indicator molecules were immobilized onto the CS/CA-SMP membrane through strong ion-pair electrostatic interaction between the TMPyP molecules and -SO₃⁻ groups on the membrane surfaces [Fig. 6.2(b)]. The finally obtained membrane is denoted as CS/CA-SMP-TMPyP in this paper. The interaction between cadmium ions and the obtained CS/CA-SMP-TMPyP membrane is shown in. Fig. 6.2(c).

Fig. 6.3 shows the FTIR/ATR spectra of the TMPyP powder, CS/CA base membrane, CS/CA membrane with surface initiator, CS/CA-SMP membrane, and CS/CA-SMP-TMPyP. For the spectrum of TMPyP powder [see Fig. 6.3(a)], the broad absorption band centered at 3468 cm⁻¹ is the characteristic stretching vibration of the N-H groups and the sharp peak at around 1640cm⁻¹ can be attributed to the N-H bending vibration in the TMPyP structure. For the spectrum of CS/CA base membrane [see Fig. 6.3(b)],

the peaks at around 889 and 1153 cm^{-1} typically represent the saccharide structure while the peak at around 1643 cm^{-1} is attributed to the N-H bending vibrations in chitosan (Nalva 1997). The broad absorption band centered at 3336 cm^{-1} is the characteristic stretching vibration of the O-H and N-H groups in chitosan. After the surface initiation, new peaks at 1730 cm^{-1} and 1525 cm^{-1} appeared respectively for the membrane surface [see Fig. 6.3(c)]. The peak at 1525 cm^{-1} may be assigned to the amide (II) deformation vibration, suggesting that the immobilization of the initiator on the CS/CA base membrane was also through the reaction with the amine groups in chitosan and formed the amide groups (Li and Bai 2006; Nalva 1997), as indicated in Fig. 6.2(a). Meanwhile, the peak at 1730 cm^{-1} is usually representative of the -C=O- groups which were generated due to the reaction between the initiator and the -OH or -NH₂ on the CS/CA base membrane; as also shown in Fig. 6.2(a). After the ATRP polymerization process [see Fig. 6.3(d)], new peaks at 1199 cm^{-1} and 794 cm^{-1} are observed. These peaks are attributed to the stretching vibrations of S=O and S-O in the sulfonate groups of SMP. Besides, increased absorbance at around 1730 cm^{-1} for the -C=O- was also observed in the spectrum. These results confirm the successful polymerization of SMP on the membrane surface to obtain CS/CA-SMP. There are no significant changes in the absorption bands after the immobilization of TMPyP on CS/CA-SMP [see Fig. 6.3(e)]. This may be due to the overlaps of the features of TMPyP with those of CS/CA-SMP. In summary, the FTIR spectra in Fig. 6.3 support the reaction steps given in Fig. 6.2(a).

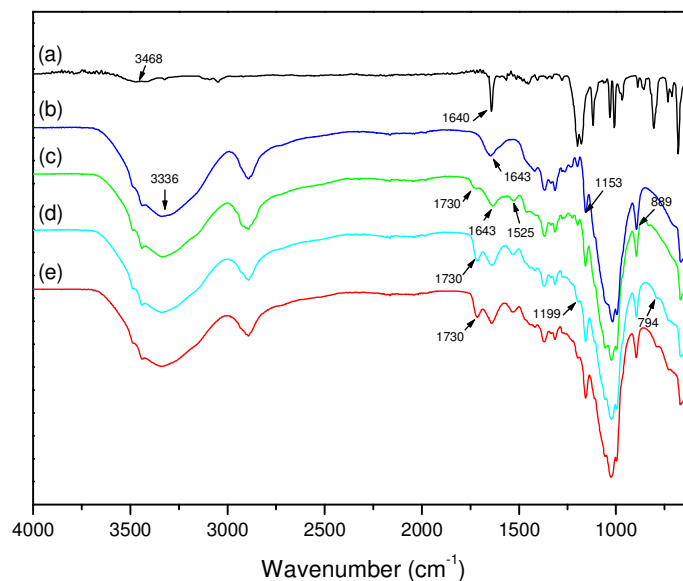


Fig. 6.3 FTIR spectra of (a) TMPyP powder; (b) CS/CA base membrane; (c) surface initiated CS/CA membrane; (d) CS/CA-SMP membrane; (e) CS/CA-SMP-TMPyP membrane.

Fig. 6.4 shows the UV/Vis absorption spectra of TMPyP solution before and after equilibrium with CS/CA and CS/CA-SMP membranes. The absorbance intensity at 420nm wavelength is positively proportional to the TMPyP concentration in the solution (Takagi et al. 2006). It is found that the absorbance intensity of TMPyP solution at 420nm remarkably decreased after the equilibrium with CS/CA-SMP membrane while little decrease was observed in the case of CS/CA base membrane. The results indicate that, by grafting negatively charged polymer brushes, the surface affinity of the membrane towards TMPyP molecules was greatly improved. From the mass balance analysis, it was found that the amount of TMPyP immobilized on the CS/CA-SMP membrane was about 0.12 mg/g, as compared to 0.006 mg/g on the CS/CA base membrane.

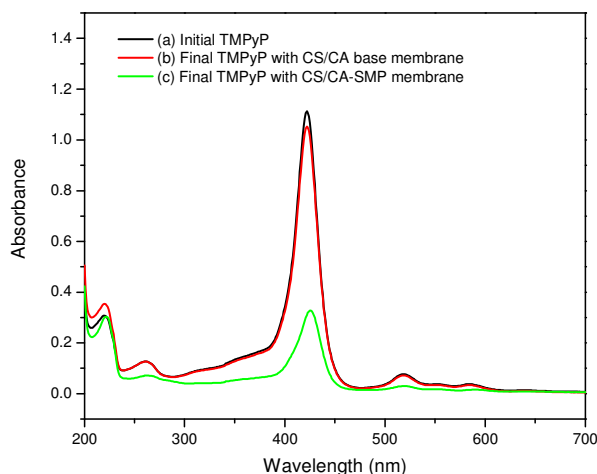


Fig. 6.4 UV/Vis spectra of (a) initial TMPyP solution; and final TMPyP solution after adsorption equilibration with (b) CS/CA base membrane; and (c) CS/CA-SMP membrane

6.3.2 Morphology and permeability of prepared membranes

Surface images of the different types of membranes prepared in the process were obtained by Scanning Electron Microscope (SEM); as shown in Fig. 6.5. It can be found that the prepared membranes were highly porous and the surface initiation and the grafting polymerization of SMP indeed reduced the pore sizes of the membranes from CS/CA to CS/CA-SMP. However, as indicated by the SEM images, the introduction of TMPyP molecules onto CS/CA-SMP did not seem to affect the membrane surface morphology and structure significantly. The result can be supported by the permeability experiments with pure water. Table 6.1 shows the measured pure water fluxes of the different types of membranes. The average water flux of CS/CA membrane under 1 bar was reduced from $15.21 \text{ L/m}^2 \cdot \text{hr}$ to $8.51 \text{ L/m}^2 \cdot \text{hr}$ for CS/CA-SMP membrane but only slightly changed to $7.72 \text{ L/m}^2 \cdot \text{hr}$ after the immobilization of TMPyP molecules. Nevertheless, the flux of $7.72 \text{ L/m}^2 \cdot \text{hr}$ under 1 bar can be considered to be reasonably good for an adsorptive membrane.

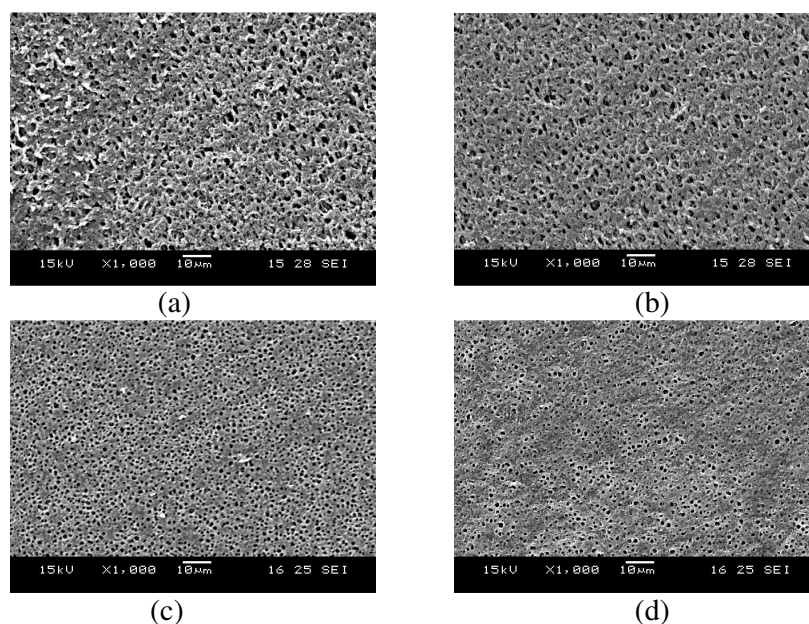


Fig. 6.5 SEM image of (a) CS/CA base membrane; (b) surface initiated CS/CA membrane; (c) CS/CA-SMP membrane; (d) CS/CA-SMP-TMPyP membrane.

Table 6.1 Pure water fluxes (PWF) of CS/CA, CA/CA-SMP and CS/CA-SMP-TMPyP membranes (1 bar, 22-23°C).

Samples	PWF (L/m ² ·hr· bar)
CS/CA	15.21
CS/CA-SMP	8.51
CS/CA-SMP-TMPyP	7.72

6.3.3 Response time of CS/CA-SMP-TMPyP membrane to cadmium detection

Fig. 6.6(a) shows the color changes of CS/CA-SMP-TMPyP responding to the times of the membrane in contact with the cadmium solution (50mg/L, initial pH value 8, 22-23°C). The results indicate that the CS/CA-SMP-TMPyP membrane showed a quick response in color change that can be observed with the naked eyes within 2min when the membrane was in contact with cadmium ions in the solution. The color change also intensified with the increase of the contact time, probably due to the increase in the adsorbed amount of cadmium. The UV/Vis spectra of the membrane

corresponding to different contact times were also obtained (Fig. 6.7). The UV/Vis spectrum of the CS/CA-SMP-TMPyP membrane initially shows five absorption bands in the visible region: the Soret band at around 420nm and four Q-bands from 500 to 700nm (Takagi et al. 2006). With the increase of contact time, the Soret band was found to undergo a gradually bathochromic shift from 420nm to 445nm. In addition, hyperchromic effect at 580nm and hypsochromic effect at 520nm also took place with the increase of the contact time; and finally, at 60min only two Q-bands could be observed. These specific spectral changes indicate a molecule symmetry change of TMPyP from D_{2h} (orthorhombic-bipyramidal) to D_{4h} (ditetragonal-dipyramidal) due to the metallation of core nitrogen atoms (Takagi et al. 2006; Vandamme et al. 1978). These changes in the absorption bands suggests an overall color change from yellow to green, which is consistent with those observed from the photos in Fig. 6.6(a). The phenomenon could be explained by the ligand-to-metal charge-transfer (LMCT) transition between TMPyP molecules and cadmium ions (Tarr and Miessler 1991). The excitation energy in forming TMPyP-Cd complex occurred in the visible region of the UV/Vis spectrum, which led to changes in the optical absorption bands, and, accordingly, the color change of the CS/CA-SMP-TMPyP membrane was observed (Kalyanasundaram 1992; Vogler and Kunkely 2000). This rapid and sensitive response of the prepared membrane to cadmium ions under naked-eyes without using other sophisticated instrument shows a great potential advantage in practical and on-site application of the prepared membrane in water and wastewater treatment.

6.3.4 Effect of initial solution pH on cadmium detection by the prepared membrane

The results of the influence of initial solution pH on the detection of cadmium ions

with CS/CA-SMP-TMPyP membrane (solution contained 50mg/L cadmium, membrane contact time was 20min) are shown in Fig. 6.6(b). As seen in Fig. 6.6(b), the CS/CA-SMP-TMPyP membrane exhibited obvious chromatic changes when the initial solution pH was from 5.6 to higher values. Correspondingly, a sharp increase in the light absorption at 445nm wavelength was observed for initial solution pH from 5.6 to 8; see Fig. 6.8(a). The greater color change at a higher pH value may be attributed to more surface complexes formed between the cadmium ions and the TMPyP molecules, which induced the increase of the color intensity. The binding of the nitrogen-containing TMPyP to cadmium ions may be enhanced in alkaline solutions, but reduced at lower pH values, because of the protonation and deprotonation of the TMPyP molecules (El-Safty et al. 2007b).

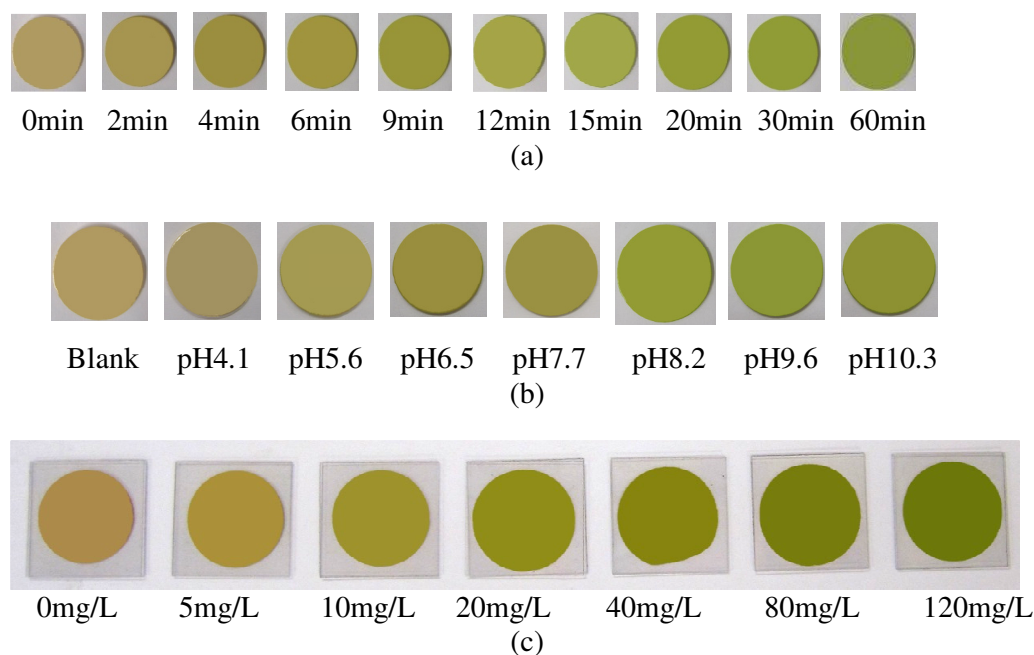


Fig. 6.6 Color change of CS/CA-SMP-TMPyP membrane in responding to Cd(II) ions with (a) different contact time ($C_0=50\text{mg/L}$, initial pH value 8, $22-23^\circ\text{C}$); (b) different initial solution pH values ($C_0=50\text{mg/L}$, $22-23^\circ\text{C}$); (c) different initial concentrations (contact time: 20min, initial pH value 8, $22-23^\circ\text{C}$).

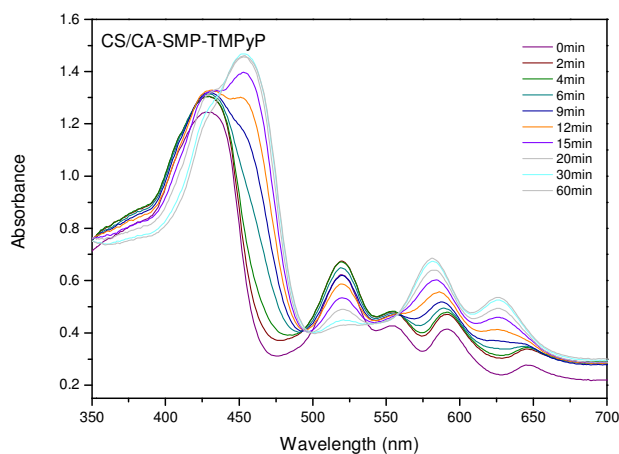


Fig. 6.7 UV/Vis spectra in time response of CS/CA-SMP-TMPyP membrane for detecting Cd(II) ions ($C_0=50\text{mg/L}$, initial pH value 8, $22-23^\circ\text{C}$).

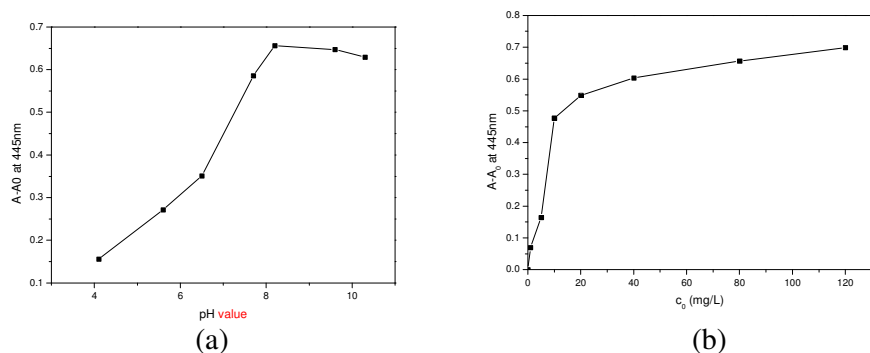


Fig. 6.8 Difference in the absorbance intensity at 445nm for CS/CA-SMP-TMPyP membrane in response to cadmium solution with (a) different initial pH values; (b) different initial concentrations. The A_0 and A are the absorption signal responses of the CS/CA-SMP-TMPyP membranes at 445nm before and after equilibrating with Cd(II) ions.

6.3.5 Response of CS/CA-SMP-TMPyP membrane in detecting cadmium ions with different concentrations

The response of the prepared membrane to cadmium ions over a concentration range from 0 to 120mg/L was examined, with the results shown in Fig. 6.6(c). As expected, color change of the membrane was clearly observed for all the initial cadmium concentrations tested and the change in color intensity increased with the increase of the initial cadmium concentration in the solutions. Since the changes in the Soret bands at 445nm could indicate the extent of cadmium chelation with TMPyP molecules (Takagi et al. 2006), the differences in the absorption intensity at 445nm were recorded for the prepared membrane at various initial cadmium concentrations (see Fig. 6.8(b)). The results show that the membrane absorption intensity at 445nm increased sharply with the increase of the initial cadmium concentration from 0 to 10mg/L. Further increase in the initial cadmium concentration from 10 to 120mg/L only gradually and moderately increased the absorption intensity, which is consistent with the developed color change pattern of the CS/CA-SMP-TMPyP membrane shown in Fig. 6.6(c), where obvious color change from yellow to light green was observed first and then followed by color intensification from light green to green.

The results suggest that the formation of charge-transfer complexes between Cd(II) ions and the TMPyP probes was enhanced by increasing cadmium ion concentration in the solution but the effect eventually stabilized as the formed complexes approached the saturated state.

6.3.6 Adsorption performance

Adsorption kinetic results are useful to predict the uptake rates as well as to possibly suggest the nature of adsorption. The experimental adsorption kinetic results were obtained for the CS/CA base membrane and the prepared CS/CA-SMP-TMPyP membrane (at initial cadmium concentration of 50mg/L, initial pH8, 22-23°C); as shown in Fig. 6.9. It can be found that the prepared CS/CA-SMP-TMPyP membrane had a significantly higher adsorption uptake amount and a shorter equilibrium time than the CS/CA base membrane. The results indicate that the approach to obtain the cadmium sensor membrane of CS/CA-SMP-TMPyP from the CS/CA base membrane also significantly enhanced the adsorption performance of the prepared sensor membrane. The enhanced adsorption performance of CS/CA-SMP-TMPyP may be attributed to the much more functional groups ($-NH_2$, $-NH-$, $-SO_3^-$) on it than those on the CS/CA base membrane.

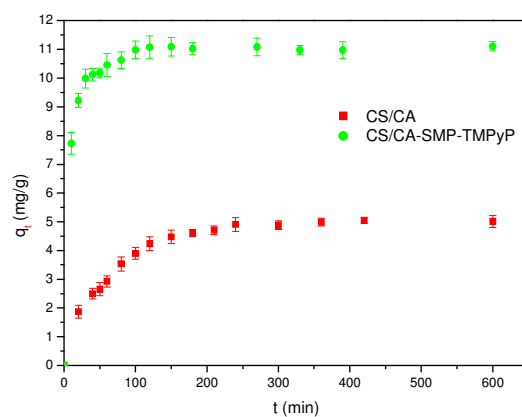


Fig. 6.9 Kinetic adsorption results of cadmium ions on CS/CA and CS/CA-SMP-

TMPyP membrane ($C_0=50\text{mg/L}$, initial pH value 8, $22-23^\circ\text{C}$). Error bars are determined from three repeated tests, with errors $<5\%$.

The pseudo first-order and pseudo second-order adsorption kinetic models have often been used to characterize the adsorption process and reveal whether the overall adsorption process is dominated by a typical physical or chemical attachment phenomenon (Tien 1994). The pseudo first-order (Eq. 6.1) and pseudo second-order (please refer to Eq. 5.1) adsorption kinetic models are often given as below:

$$\log(q_e - q_t) = \log q_e - \frac{k_1}{2.303} t \quad \text{Eq. 6.1}$$

$$\frac{t}{q_t} = \frac{1}{k_2 q_e^2} + \frac{1}{q_e} t \quad \text{Eq. 5.1}$$

where q_e (mg/g) is the adsorption uptake amount at adsorption equilibrium, q_t (mg/g) is the amount of adsorption uptake at adsorption time t , k_1 (min^{-1}) and k_2 (g/mg·min) are the rate constants of the pseudo-first-order and pseudo-second-order adsorption kinetic models, respectively. An analysis for the experimental adsorption kinetic data in Fig. 6.9 with Eq. 6.1 and Eq. 5.1 was carried out. As shown in Fig. 6.10, cadmium adsorption on both the CS/CA base membrane and the prepared CS/CA-SMP-TMPyP membranes in this study meets the pseudo second order model with the $R^2 > 0.99$. The experimental adsorption capacity for CS/CA base membrane and functionalized membrane are 5.01mg/g and 11.11mg/g ; while the theoretical adsorption capacity based on Eq. 5.1 are 5.13mg/g and 11.09mg/g . The results therefore suggest that chemical interaction between the cadmium ions to be adsorbed in the solution and the functional groups on the membrane surfaces dominated the overall adsorption rate. It is found that the pseudo second-order rate constant k_2 has a much higher value of $0.0268\text{g/mg}\cdot\text{min}$ for the CS/CA-SMP-TMPyP membrane than $0.0045\text{g/mg}\cdot\text{min}$ for the CS/CA base membrane, suggesting that cadmium adsorption on CS/CA-SMP-

TMPyP was much faster than on CS/CA. In general, adsorption process dominated by chemical interaction is faster than physical interaction and hence is preferred for achieving quick adsorption and detection as an objective of this study.

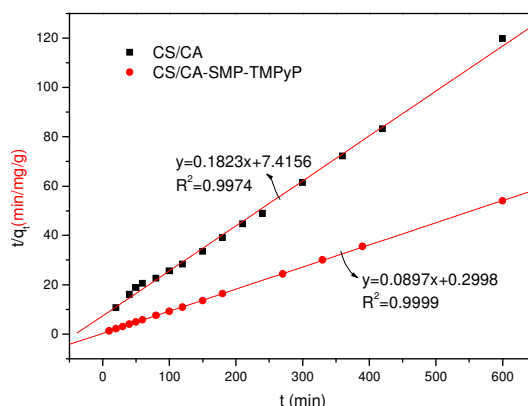


Fig. 6.10 Fitting of pseudo second-order kinetic adsorption model to experimental results of cadmium ion adsorption on CS/CA base membrane and on CS/CA-SMP-TMPyP membrane

Adsorption isotherm models have commonly been used to reveal the adsorption uptake capacity and the adsorption pattern of an adsorbate on an adsorbent. The fitting of the Langmuir and Freundlich models to the adsorption data of cadmium ions on CS/CA and CS/CA-SMP-TMPyP was carried out according to the equations described in Chapter 3. The results are shown in Fig. 6.11, and the corresponding fitting parameters for both Langmuir and Freundlich isotherm models from the analysis are given in Table 6.2. The results show that both Langmuir and Freundlich models can be used to fit the data and estimate the model parameters of CS/CA and CS/CA-SMP-TMPyP membrane. The adsorption heterogeneity reflected by the value of the parameter n for CS/CA-SMP-TMPyP (2.046) is also greater than that for CS/CA (1.777). This may be understandable because polymer brushes and different types of functional groups ($-\text{SO}_3^-$, $-\text{NH}_2$, $-\text{NH}-$) were grafted or immobilized on the CS/CA-SMP-TMPyP membrane. From the Langmuir model fitting, the maximum

adsorption capacity of cadmium ions on CS/CA-SMP-TMPyP is predicted to be about 44mg/g, much higher than about 18mg/g for CS/CA in this case; besides, the K_L value for the functionalized membrane is found to be smaller than that of CS/CA which means a higher affinity of cadmium ions to CS/CA-SMP-TMPyP membrane. In other words, the functionalization of CS/CA for cadmium ion visual detection also significantly increased the adsorption capacity of the membrane for adsorptive removal of cadmium ions by the prepared membrane.

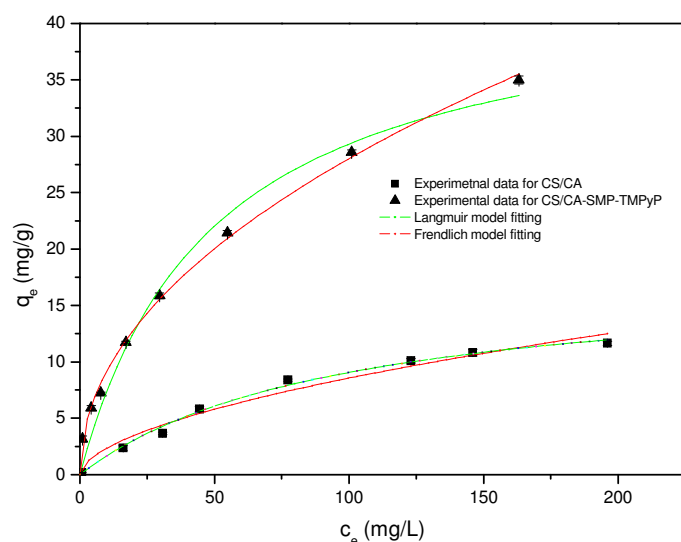


Fig. 6.11 Experimental adsorption isotherm data and the fitted results of the Langmuir and Freundlich isotherm models to the experimental data. Error bars are determined from three repeated tests, with errors < 5%. (initial pH value 8, 22-23°C).

Table 6.2 The fitting parameters of the Langmuir and Freundlich isotherm models to the adsorption data of Cd(II) on the membranes of CS/CA, CS/CA-SMP-TMPyP (initial pH value 8, 22-23°C).

Membranes	Langmuir model			Freundlich model		
	$q_m(\text{mg/g})$	$K_L(\text{L/mg})$	R^2	n	$K_F(\text{mg/g})(\text{L/mg})^{1/n}$	R^2
CS/CA	17.8808	97.3237	0.9951	1.7771	0.641	0.9877
CS/CA-SMP-TMPyP	43.7793	49.3835	0.9834	2.064	3.0082	0.9985

6.3.7 Interference of coexisting ions

Experiments were carried out to study the interference by coexisting cations. Solutions (each 50mL) containing 10^{-4} M (11.2mg/L) of Cd(II) ions with different amounts of other cations were used. The tested cations included Na^+ , K^+ , Ca^{2+} , Mg^{2+} , Co^{2+} and Ni^{2+} as the interfering cations (others such as Zn^{2+} , Pb^{2+} , Cu^{2+} and Hg^{2+} were not considered in this study because they do not normally exist with cadmium ions at the pH examined). According to the results, Na^+ , K^+ , Ca^{2+} , Mg^{2+} ions had no significant effect on the color response of the prepared membrane in detecting cadmium ions even when the molar concentrations of the interfering cations were 10 times higher than that of the cadmium ions. This is supported by the adsorption uptake study. As given in Table 6.3, the addition of Na^+ , K^+ , Ca^{2+} and Mg^{2+} ions had no significant effect on the cadmium uptake amount on the membrane. This is due to the fact that the functional group, particularly, amino groups on the membrane are soft base, which would not interact with alkali or alkaline earth metal ions that are classified as strong acids (Yan et al. 2010). However, for the samples containing transition metal Co^{2+} or Ni^{2+} ions as the interfering ions, chromatic influence for the membrane in the detection of cadmium ions was noticed and decreased cadmium adsorption amount was observed. This may be attributed to the transition metals such as Co^{2+} and Ni^{2+} that would also have affinity towards the amino groups on CS/CA-SMP-TMPyP membrane, hence affecting both the color change response and the adsorption behavior of cadmium ions. In the literature, it has been reported that both TMPyP and chitosan have certain adsorption selectivity towards Cd(II) ions over Co^{2+} or Ni^{2+} ions (El-Safty et al. 2007b; Rinaudo 2006). Nevertheless, from the experimental results given in Table 6.3, the interferences of Co^{2+} or Ni^{2+} ions on the detection and adsorption of Cd(II) ions by CS/CA-SMP-TMPyP membrane are not

very significant.

Table 6.3 Uptake of Cd(II) by CS/CA-SMP-TMPyP membrane in the presence of other cations.

No.	Interfering cation [X]	[Cd(II)] (10^{-4} M)	[X] (10^{-4} M)	[X]/[Cd(II)]	Cd(II) uptake (mg/g)
1	-	1	-	-	3.6521
2	Na ⁺	1	10	10	3.6946
3	K ⁺	1	10	10	3.6113
4	Ca ²⁺	1	10	10	3.4062
5	Mg ²⁺	1	10	10	3.5768
6	Co ²⁺	1	1	1	3.0537
7	Ni ²⁺	1	1	1	2.9194

6.4 Conclusion

In this study, a cadmium optical indicator TMPyP was successfully immobilized onto CS/CA blend base membrane. The preparation strategy involved the grafting of negatively charged polymer brushes of SMP onto CS/CA base membrane through an ATRP method and subsequently immobilizing TMPyP molecules onto the membrane surface through electrical interaction with the grafted SMP brushes. The preparation process was proved to be successful and the resulted CS/CA-SMP-TMPyP membrane exhibited rapid and obvious colorimetric change when in contact with cadmium ions in solutions. The obtained membrane also showed enhanced adsorption performance for cadmium ions due to the increased adsorption sites introduced by the grafted polymer brushes. Therefore, the ATRP method is proved to be effective and versatile in preparing multifunctional membrane with high performance for various application requirements.

CHAPTER 7 CONCLUSIONS AND RECOMMENDATIONS

7.1 Conclusions

In this study, multifunctional membranes that combined the functions of adsorption and visual detection of heavy metal ions in aqueous solutions with a porous filtration membrane were achieved. The performance of the obtained membranes on the target heavy metal ions were investigated with a focus on the sensitivity, adsorption capacity and removal rate in both batch adsorption and filtration processes.

In the first part of the study, the proposed “multifunctional membrane” concept was tested by immobilizing lead optical indicator DZ onto the CS/CA base membrane. The obtained CS/CA-DZ membrane fulfilled the objective for simultaneous detection and removal of lead ions. The adsorption performance of CS/CA-DZ for lead ions was improved in terms of faster adsorption kinetics and higher lead uptake amount, in comparison with that of the CS/CA base membrane. The study demonstrated the feasibility of a multifunctional membrane in its easy on-site naked-eye detection and adsorptive removal of heavy metal ions from aqueous solutions, suggesting a potential application in water and wastewater treatment process.

The multifunctional membrane concept was then extended to mercury ions. Since the detection and removal performance of the multifunctional membrane towards heavy metal ions could be affected by some process factors such as the contact-time, amount of immobilized indicators, solution pH, solution ionic strength and the interference of other metal ions, the investigation on how those process factors would affect the membrane performance in terms of developed color for Hg(II) detection and the uptake capacity for Hg(II) removal was conducted. An optical indicator, TPPS, for Hg(II) was immobilized onto the CS/CA membrane and the performance of

developed multifunctional membrane, CS/CA-TPPS, was evaluated. The results showed that the obtained membrane can be applied in solutions with initial pH ranging from 5 to 8 without leaching of the indicators. The TPPS loading rate of 1.0mg(TPPS)/g(CS/CA membrane) provided a balanced performance of both good detection sensitivity and adsorption removal for Hg(II). No significant influence on Hg(II) detection and removal was found with the solution ionic strength below 0.05M (NaNO₃). Besides, the membrane exhibited selectivity towards mercury ions in the presence of other non-heavy metal ions, even at high concentrations. The CS/CA-TPPS membrane was also tested in a filtration process with various real water samples spiked with mercury ions. In general, the prepared CS/CA-TPPS multifunctional membrane showed excellent stability and reliability in mercury detection and removal, which indicates a great prospect for on-site and in situ mercury discharge monitoring and remediation.

To recognize the possible effect of the presence of organic pollutants in water and wastewater, the influence of natural organic matters, particularly humic acid (HA), in water was investigated because of their potential reactions with heavy metal ions, the indicators and the base membranes. The influence of HA on the detection sensitivity and removal efficiency of the CS/CA-TPPS membrane to Hg(II) was further examined under batch adsorption and filtration conditions in three different phases. The results showed that the removal of Hg(II) was greatly improved by the pre-adsorbed or filtered HA, but the sensitivity of visual detection towards Hg(II) was reduced, showing as delayed response time and diminished degree of color change. The adsorptive removal of Hg(II) ions by the membrane was depressed when HA co-existed with Hg(II) in the solutions, which could be explained by the formation of

less-adsorbable HA-Hg(II) complexes. Nevertheless, mercury could be removed during the filtration through the interception of the HA-Hg(II) complex. The experimental results demonstrated prospect for the practical application of the CS/CA-TPPS membrane for Hg(II) removal and visual detection in water resources where HA concentration is relatively low. For the waters containing high HA/Hg ratio, pretreatment may be needed to remove HA if the visual detection of Hg(II) ions has a priority.

Immobilization of desired optical indicators on the base membrane is a crucial step to obtain multifunctional membranes with high performance. In the last part of the study, an advanced and versatile method - atom transfer radical polymerization (ATRP) was introduced to facilitate the immobilization of optical indicators which do not have intrinsic affinities to the base membrane. The ATRP method could adjust the membrane surface properties by grafting of functional polymers that can react with the optical indicators, and thus the immobilization of optical indicators on the membrane can be realized. A cadmium indicator, 5,10,15,20-Tetrakis (1-methyl-4-pyridinio) porphyrin tetra (p-toluenesulfonate) (TMPyP), was immobilized onto the CS/CA base membrane through the ATRP method that introduced negatively charge polymer brushes on the membrane surface. The method was proved to be successful and the prepared membrane showed rapid and obvious colorimetric change when it was in contact with cadmium ions in solutions. Moreover, the grafted polymer chains also provide more adsorption sites, leading to an enhanced Cd(II) adsorption. Thus, the ATRP method can be applied as a facile and versatile technique to develop multifunctional membranes with desired properties.

7.2 Recommendations and future work

The concept of multifunctional membrane has led to a promising technology that combines water and wastewater treatment performance with on-site water safety and security monitoring. In this study, research has been done to evaluate the preparation method and performance of a few multifunctional membranes for their application to some typical heavy metal ions. Although many cheerful results have been obtained, much research work still needs to be done in the future. Some recommended aspects are listed below:

- (a) For the real applications, the sensitivity of the prepared membrane in heavy metal detection should be further improved and the interference from other components in the in the water body, including other heavy metal ions and organic pollutants, should be minimized. This may be achieved by further developing and applying smarter optical indicators with special selectivity and sensitivity towards target metal ions. Besides, the preparation methods and process conditions should also be optimized to enhance the detection performance. On the other hand, efficient regeneration method needs to be developed to recycle and reuse the prepared membrane with good stability and reliability. Moreover, it is of interest to combine the multifunctional membrane with color change recording and alarming system for automatic on-line monitoring of the target species.
- (b) As the industrial discharge usually contains various heavy metal ions, it is desirable to achieve multi-targets detection and removal. Some ligands such as 4-(2-pyridylazo)-resorcinol (PAR) and its analogues have been reported as colorimetric indicators for many metal ions. It could generate color change

from yellow to red when complexed with metal ions such as Co^{2+} , Zn^{2+} , Cd^{2+} , Ni^{2+} , Hg^{2+} , Pb^{2+} and Cu^{2+} in low concentrations ($6.25 \times 10^{-6} \text{M}$) (Liu et al. 2012). Therefore, further study could be carried out by immobilizing this indicator on to an adsorptive membrane, which may provide the possibility of detecting and distinguishing multiple heavy metal ions by monitoring different color patterns of the membrane, and removing them individually or together efficiently at the same time.

- (c) The heavy metal removal efficiency can also be improved by changing the base membrane composition and configuration. For example, by using other co-solvent or coagulants, the amount of CS in the blend membrane can be increased, which would improve the adsorption of heavy metal ions. Besides, other functional polymers that have both good mechanical property and adsorption capacity can be used as base membrane materials. Moreover, instead of flat sheet membrane, the optical indicator can be immobilized onto CS/CA hollow fibers. The detection and removal of multi-targets could also be achieved by packing hollow fibers with different optical indicators into the same module.
- (d) Immobilization of optical indicators on the adsorptive membrane is a key to design multifunctional membrane with excellent performance. Versatile and effective immobilization strategies are demanded to achieve the desired functions. For example, the ATRP method presented in Chapter 6 is a surface grafting technique by which we could control and adjust the membrane surface property to facilitate the immobilization of various optical indicators and improve the removal of target metal ions. As the length of the grafted

polymer chains can be controlled in the process, it will be an interest study to investigate the influence of the polymerization degree on the sensitivity, selectivity and adsorption capacity of the developed membranes. Moreover, it is possible to introduce polymers with different functions (e.g., pH sensitive, self-cleaning, anti-biofouling) to further expand the concept of “multifunction”. Alternative method such as “click chemistry” could also be employed and the indicators could be extended to bio-recognition elements such as aptamers, antibodies and novel synthetic protein receptors (Kolb et al. 2004; Jayasena 1999; Rachkov 1994; Sergeyeva et al. 1996; Speers et al. 2004), which may have a great potential in the on-site detection of bacteria, virus and other microbial in the water while accompanying membrane filtration.

REFERENCE

- Al-Saleh, I., Coskun, S., Mashhour, A., Shinwari, N., El-Doush, I., Billedo, G., Jaroudi, K., Al-Shahrani, A., Al-Kabra, M., and Mohamed, G. E. D. (2008). "Exposure to heavy metals (lead, cadmium and mercury) and its effect on the outcome of in-vitro fertilization treatment." *International Journal of Hygiene and Environmental Health*, 211(5-6), 560-579.
- Arisawa, K., Uemura, H., Hiyoshi, M., Dakeshita, S., Kitayama, A., Saito, H., and Soda, M. (2007). "Cause-specific mortality and cancer incidence rates in relation to urinary beta 2-microglobulin: 23-Year follow-up study in a cadmium-polluted area." *Toxicology Letters*, 173(3), 168-174.
- Atkins, P., and Jones, L. (1997). "Chemistry-Molecules, Matter and Change." W. H. Freeman, New York.
- Babel, S., and Kurniawan, T. A. (2003). "Low-cost adsorbents for heavy metals uptake from contaminated water: a review." *Journal of Hazardous Materials*, 97(1-3), 219-243.
- Bailey, S. E., Olin, T. J., Bricka, R. M. and Adrian, D. D. (1999). "A review of potentially low costs sorbents for heavy metals." *Water Research*, 33(11), 2469-2479.
- Balachandra, A. M., Baker, G. L., and Bruening, M. L. (2003). "Preparation of composite membranes by atom transfer radical polymerization initiated from a porous support." *Journal of Membrane Science*, 227(1-2), 1-14.
- Balaji, T., El-Safty, S. A., Matsunaga, H., Hanaoka, T., and Mizukami, F. (2006). "Optical sensors based on nanostructured cage materials for the detection of toxic metal ions." *Angewandte Chemie-International Edition*, 45(43), 7202-7208.
- Beeskow, T. C., Kusharyoto, W., Anspach, F. B., Kroner, K. H., and Deckwer, W. D. (1995). "Surface modification of microporous polyamide membrane with hydroxyethyl cellulose and their application as affinity membranes." *Journal of Chromatography A*, 715(1), 49-65.
- Benegas, J. C., Porasso, R. D., and van den Hoop, M. A. G. T. (2003). "Proton-metal exchange processes in synthetic and natural polyelectrolyte solution systems." *Colloids and Surfaces a-Physicochemical and Engineering Aspects*, 224(1-3), 107-117.
- Boddu, V. M., Abburi, K., Talbott, J. L., and Smith, E. D. (2003). "Removal of hexavalent chromium from wastewater using a new composite chitosan biosorbent." *Environmental Science & Technology*, 37(19), 4449-4456.
- Boiocchi, M., Bonizzoni, M., Fabbri, L., Piovani, G., and Taglietti, A. (2004). "A dimetallic cage with a long ellipsoidal cavity for the fluorescent detection of dicarboxylate anions in water." *Angewandte Chemie-International Edition*, 43(29), 3847-3852.
- Boisde, G., Blanc, E., Manchien, P., and Perez, J. J. (1991). "Fiber optic chemical sensors and biosensors." O. S. Wolfbeis, ed., CRC, Boca Raton.
- Braunecker, W. A., and Matyjaszewski, K. (2007). "Controlled/living radical polymerization: Features, developments, and perspectives." *Progress in Polymer Science*, 32(1), 93-146.
- Brown, D. E., and Thornton, A. J. (1998). "Chitinous material in trichoderma reesei." *Biotechnology Letters*, 20(8), 777-779.
- Cameron, D. F., and Sohn, M. L. (1992). "Functional-group content of soil and sedimentary humic acids determined by Cp/Mas C-13 Nmr related to conditional Zn(II) and Cd(II) formation-constants." *Science of the Total Environment*, 113(1-2), 121-132.
- Cameron, R. E. (1992). "Guide to site and soil description for hazardous waste site characterisation." EPA/600/4-91/029, E. P. Agency, ed., Environmental Protection Agency.
- Cari, M., Milanovi, S. D., Krsti, D. M., and Teki, M. N. (2000). "Fouling of inorganic membranes by adsorption of whey proteins." *Journal of Membrane Science*, 165, 83-88.
- Chatterjee, S., Pillai, A., and Gupta, V. K. (2002). "Spectrophotometric determination of mercury in environmental sample and fungicides based on its complex with o-carboxy phenyl diazoamino p-azobenzene." *Talanta*, 57(3), 461-465.
- Che, S., Garcia-Bennett, A. E., Yokoi, T., Sakamoto, K., Kunieda, H., Terasaki, O., and Tatsumi, T. (2003). "A novel anionic surfactant templating route for synthesizing mesoporous silica with unique structure." *Nature Materials*, 2(12), 801-805.
- Chen, Y., Xu, Z. H., and Feng, H. J. (2007). "Multispectral color sensor based on vertically stacked structure." *Spectroscopy and Spectral Analysis*, 27(5), 837-841.
- Cheremisinoff, N. P. (2002). *Handbook of Water and Wastewater Treatment Technologies*. Elsevier.
- Choi, M., Cho, H. S., Srivastava, R., Venkatesan, C., Choi, D. H., and Ryoo, R. (2006). "Amphiphilic organosilane-directed synthesis of crystalline zeolite with tunable mesoporosity." *Nature Materials*, 5(9), 718-723.

- Choong, J., and Park, K. H. (2005). "Adsorption and desorption characteristics of mercury(II) ions using aminated chitosan bead." *Water Research*, 39, 3938-3944.
- Chow, E. (2005). "Electrochemical detection of heavy metal ions using amino acids and oligopeptides as complexing ligands." *Australian Journal of Chemistry*, 58(4), 306-306.
- Clarkson, T. W. (1990). "Mercury - an Element of Mystery." *New England Journal of Medicine*, 323(16), 1137-1139.
- Clarkson, T. W. (1993). "Mercury - Major Issues in Environmental-Health." *Environmental Health Perspectives*, 100, 31-38.
- Clifford, K. H., Robison, A., Miller, D. R., and Davis, M. J. (2005). "Overview of sensors and needs for environmental monitoring." *Sensors*, 5, 4-37.
- Conaway, C. H., Black, F. J., Grieb, T. M., Roy, S., and Flegal, A. R. (2008). "Mercury in the San Francisco estuary." *Reviews of Environmental Contamination & Toxicology*, 194, 29-54.
- Coquery, M., and Cossa, D. (1995). "Mercury speciation in surface waters of the North Sea." *Netherlands Journal of Sea Research*, 34(4), 245-257.
- Coronado, E., Galan-Mascaros, J. R., Marti-Gastaldo, C., Palomares, E., Durrant, J. R., Vilar, R., Gratzel, M., and Nazeeruddin, M. K. (2005). "Reversible colorimetric probes for mercury sensing." *Journal of the American Chemical Society*, 127(35), 12351-12356.
- Cui, Y., Wei, Q. F., Park, H., and Lieber, C. M. (2001). "Nanowire nanosensors for highly sensitive and selective detection of biological and chemical species." *Science*, 293, 1289-1292.
- Davies, G., Ghabbour, E. A., Jansen, S., and Varnum, J. (1995). "Humic acids are versatile natural polymers." *Polymers and other advanced materials: emerging technologies and business opportunities*, P. N. Prasad and T. J. Fai, eds., Plenum Press, New York, 677-685.
- de Castro Dantas, T. N., Dantas Neto, A. A., Moura, M. C. P. d. A., Barros Neto, E. L., and de Paiva Telemaco, E. (2001). "Chromium Adsorption by chitosan impregnated with microemulsion." *Langmuir*, 17(4256-4260).
- de Wuilloud, J. C. A., Wuilloud, R. G., Sadi, B. B. M., and Caruso, J. A. (2003). "Trace humic and fulvic acid determination in natural water by cloud point extraction/preconcentration using non-ionic and cationic surfactants with FI-UV detection." *Analyst*, 128(5), 453-458.
- Deng, S. B., and Ting, Y. P. (2005). "Fungal biomass with grafted poly(acrylic acid) for enhancement of Cu(II) and Cd(II) biosorption." *Langmuir*, 21(13), 5940-5948.
- Deoliveira, W. A., and Narayanaswamy, R. (1992). "A Flow-cell optosensor for lead based on immobilized dithizone." *Talanta*, 39(11), 1499-1503.
- Dias, L. F., Miranda, G. R., Saint-Pierre, T. D., Maia, S. M., Frescura, V. L. A., and Curtius, A. J. (2005). "Method development for the determination of cadmium, copper, lead, selenium and thallium in sediments by slurry sampling electrothermal vaporization inductively coupled plasma mass spectrometry and isotopic dilution calibration." *Spectrochimica Acta Part B-Atomic Spectroscopy*, 60(1), 117-124.
- Dove, A., Hill, B., Klawunn, P., Waltho, J., Backus, S., and McCrea, R. C. (2011). "Spatial distribution and trends of total mercury in waters of the Great Lakes and connecting channels using improved sampling technique." *Environmental Pollution In Press*, 1-7.
- Duffus, J. H. (2002). "Heavy metals-A meaningless term? (IUPAC technical report)." *Pure and Applied Chemistry*, 74(5), 793-807.
- Eiden, C. A., Jewell, C. A., and Wightman, J. P. (1980). "Interaction of lead and chromium with chitin and chitosan." *Journal of Applied Polymer Science*, 25(8), 1587-1599.
- El-Safty, S. A. (2009). "Organic-inorganic hybrid mesoporous monoliths for selective discrimination and sensitive removal of toxic mercury ions." *Journal of Materials Science*, 44(24), 6764-6774.
- El-Safty, S. A., Ismail, A. A., Matsunaga, H., Hanaoka, T., and Mizukami, F. (2008a). "Optical nanoscale pool-on-surface design for control sensing recognition of multiple cations." *Advanced Functional Materials*, 18(10), 1485-1500.
- El-Safty, S. A., Ismail, A. A., Matsunaga, H., and Mizukami, F. (2007a). "Optical nanosensor design with uniform pore geometry and large particle morphology." *Chemistry*, 13(33), 9245-9255.
- El-Safty, S. A., Prabhakaran, D., Ismail, A. A., Matsunaga, H., and Mizukami, F. (2007b). "Nanosensor design packages: A smart and compact development for metal ions sensing responses." *Advanced Functional Materials*, 17(18), 3731-3745.
- El-Safty, S. A., Prabhakaran, D., Kiyozumi, Y., and Mizukami, F. (2008b). "Nanoscale membrane strips for benign sensing of Hg-II ions: A route to commercial waste treatments." *Advanced Functional Materials*, 18(12), 1739-1750.
- Ensafi, A. A., Far, A. K., and Meghdadi, S. (2008a). "Highly selective optical sensor for mercury assay based on covalent immobilization of 4-hydroxy salophen on a triacetylcellulose membrane."

- Sensors and Actuators B-Chemical*, 133(1), 84-90.
- Ensafi, A. A., Meghdadi, S., and Fooladgar, E. (2008b). "Development of a new selective optical sensor for Cd(II) Ions based on 4-hydroxy salophen." *Ieee Sensors Journal*, 8(11-12), 1794-1800.
- Eren, E., and Afsin, B. (2008). "An investigation of Cu(II) adsorption by raw and acid-activated bentonite: a combined potentiometric, thermodynamic, XRD, IR, DTA study." *Journal of Hazardous Material*, 151 (2-3), 682-691.
- Feng, L. H., and Chen, Z. B. (2007). "Screening mercury (II) with selective fluorescent chemosensor." *Sensors and Actuators B-Chemical*, 122(2), 600-604.
- Ferner, R. E. (2001). "Our poisoned patients." *Qjm-Monthly Journal of the Association of Physicians*, 94(3), 117-120.
- Freeman, J. E., Childers, A. G., Steele, A. W., and Hieftje, G. M. (1985). "A fiberoptic absorption cell for remote determination of copper in industrial electroplating baths." *Analytica Chimica Acta*, 177, 121-128.
- Fu, F. L., and Wang, Q. (2011). "Removal of heavy metal ions from wastewaters: A review." *Journal of Environmental Management*, 92(3), 407-418.
- Fukushima, M., Tanabe, Y., Morimoto, K., and Tatsumi, K. (2007). "Role of humic acid fraction with higher aromaticity in enhancing the activity of a biomimetic catalyst, tetra(p-sulfonatophenyl)porphineiron(III)." *Biomacromolecules*, 8, 386-391.
- Ghodbane, I., and Hamdaoui, O. (2008). "Removal of mercury(II) from aqueous media using eucalyptus bark kinetic and equilibrium studies." *Journal of Hazardous Materials*, 160, 301-309.
- Granel, C., Dubois, P., Jerome, R., and Teyssie, P. (1996). "Controlled radical polymerization of methacrylic monomers in the presence of a bis(ortho-chelated) arylnickel(II) complex and different activated alkyl halides." *Macromolecules*, 29(27), 8576-8582.
- Gu, B. H., Bian, Y. R., Miller, C. L., Dong, W. M., Jiang, X., and Liang, L. Y. (2011). "Mercury reduction and complexation by natural organic matter in anoxic environments." *Proceedings of the National Academy of Sciences of the United States of America*, 108(4), 1479-1483.
- Guibal, E. (2004). "Interactions of metal ions with chitosan-based sorbents: a review." *Separation and Purification Technology*, 38(1), 43-74.
- Guibal, E., Milot, C., and Tobin, J. M. (1998). "Metal-anion sorption by chitosan beads: equilibrium and kinetic studies." *Industrial & Engineering Chemistry Research*, 37(4), 1454-1463.
- Güttinger, H., and Stumm, W. (1992). "An analysis of the rhine pollution caused by the Sandoz Chemical Accident, 1986." *Interdisciplinary Science Reviews* 17 (2), 127-136.
- Haddleton, D. M., Jasieczek, C. B., Hannon, M. J., and Shooter, A. J. (1997). "Atom transfer radical polymerization of methyl methacrylate initiated by alkyl bromide and 2-pyridinecarbaldehyde imine copper(I) complexes." *Macromolecules*, 30(7), 2190-2193.
- Harrison, R. M., and Laxen, D. P. H. (1981). "Lead pollution causes and control." Chapman and Hall, London and New York.
- Hasan, S., Krishnaiah, A., Ghosh, T. K., Viswanath, D. S., Boddu, V. M., and Smith, E. D. (2006). "Adsorption of divalent cadmium (Cd(II)) from aqueous solutions onto chitosan-coated perlite beads." *Industrial & Engineering Chemistry Research*, 45(14), 5066-5077.
- Hashem, E. Y. (2002). "Spectrophotometric studies on the simultaneous determination of cadmium and mercury with 4-(2-pyridylazo)-resorcinol." *Spectrochimica Acta Part a-Molecular and Biomolecular Spectroscopy*, 58(7), 1401-1410.
- Henneberry, Y. K., Kraus, T., E, C., Fleck, J. A., Krabbenhoft, D. P., Bachand, P. M., and Horwath, W. R. (2011). "Removal of inorganic mercury and methylmercury from surface waters following coagulation of dissolved organic matter with metal-based salts." *Science of the Total Environment*, 409, 631-637.
- Ho, S. C., and McKay, G. (1999). "Pseudo-second order model for sorption processes." *Process Biochemistry*, 34, 451-465.
- Hodgson, E., Mailman, R. B., and Chambers, J. E. (1998). "Macmillan dictionary of toxicology." Macmillan, London.
- Hong, S., and Elimelech, M. (1997). "Chemical and physical aspects of natural organic matter (NOM) fouling of nanofiltration membranes." *Journal of Membrane Science*, 132, 159-181.
- Hulanicki, A., Glab, S., and Ingman, F. (1991). "International union of pure and applied chemistry." *Pure and Applied Chemistry*, 63(9), 1247-1250.
- Husson, S. M., Singh, N., Chen, Z., Tomer, N., Wickramasinghe, S. R., and Soice, N. (2008). "Modification of regenerated cellulose ultrafiltration membranes by surface-initiated atom transfer radical polymerization." *Journal of Membrane Science*, 311(1-2), 225-234.
- Inbaraj, B. S., Wang, J. S., Lu, J. F., Siao, F. Y., and Chen, B. H. (2009). "Adsorption of toxicmercury(II)

- by an extracellular biopolymer poly(c-glutamic acid)." *Bioresource Technology*, 100, 200-207.
- Inglezakis, V. J., Zorpas, A. A., Loizidou, M. D., and Grigoropoulou, H. P. (2003). "Simultaneous removal of metals Cu^{2+} , Fe^{3+} and Cr^{3+} with anions SO_4^{2-} and HPO_4^{2-} using clinoptilolite." *Microporous and Mesoporous Materials*, 61(1-3), 167-171.
- International Occupational Safety and Health Information Centre. (1999). Metals 1999 Sep. Geneva: International Labour Organization.
- Islam, S. K., and Haider, M. R. (2010). "Sensors and Low Power Signal Processing." Springer Science.
- Itoh, J., Yotsuyanagi, T., and Aomura, K. (1975). "Spectrophotometric determination of copper with α , β , γ , δ -tetraphenylporphine trisulfonate." *Analytica Chimica Acta*, 74(1), 53-60.
- Ismail, A. F., Othman, N. H., and Mustafa, A. (2009). "Sulfonated polyether ether ketone composite membrane using tungstosilicic acid supported on silica-aluminium oxide for direct methanol fuel cell (DMFC)." *Journal of Membrane Science*, 329(1-2), 18-29.
- Jang, M. K., Kong, B. G., Jeong, Y. I., Lee, C. H., and Nah, J. W. (2004). "Physicochemical characterization of α -chitin, β -chitin, and γ -chitin separated from natural resources." *Journal of Polymer Science Part A: Polymer Chemistry*, 42(14), 3423-3432.
- Jayasena, S. D. (1999). "Aptamers: an emerging class of molecules that rival antibodies in diagnostics." *Clinical Chemistry*, 45, 1628-1650.
- Jin, L., and Bai, R. B. (2002). "Mechanisms of lead adsorption on chitosan/PVA hydrogel beads." *Langmuir*, 18(25), 9765-9770.
- Kagramanov, G. G., Dytnerskii, Y. I., and Il'in, P. G. (2001). "A model simulation of the filtering process in multichannel ceramic membranes." *Refractories and Industrial Ceramics*, 42(3-4), 139-145.
- Kalyanasundaram, K. (1992). "Photochemistry of polypyridine and porphyrin complexes." Academic Press, Boston.
- Kamigaito, M., Ando, T., and Sawamoto, M. (2001). "Metal-catalyzed living radical polymerization." *Chemical Reviews*, 101, 3689-3745.
- Kang, E. T., Zhang, Z. B., Zhu, X. L., Xu, F. J., and Neoh, K. G. (2009). "Temperature- and pH-sensitive nylon membranes prepared via consecutive surface-initiated atom transfer radical graft polymerizations." *Journal of Membrane Science*, 342(1-2), 300-306.
- Kato, M., Kamigaito, M., Sawamoto, M., and Higashimura, T. (1995). "Polymerization of methylmethacrylate with the carbon-Tetrachloride dichlorotris (triphenylphosphine) ruthenium(II) methylaluminum bis (2,6-Di-Tert-Butylphenoxide) initiating system-possibility of living radical polymerization." *Macromolecules*, 28(5), 1721-1723.
- Kirkbright, G. F., Narayanaswamy, R., and Welti, N. A. (1984). "Fibre-optic pH probe based on the use of an immobilised colorimetric indicator." *Analyst*, 109(8), 1025-1028.
- Klimant, I., and Otto, M. (1992). "A fiber optical sensor for heavy-metal ions based on immobilized xlenol orange." *Mikrochimica Acta*, 108(1-2), 11-17.
- Klimmek, S., Stan, H. J., Wilke, A., Bunke, G., and Buchholz, R. (2001). "Comparative analysis of the biosorption of cadmium, lead, nickel, and zinc by algae." *Environmental Science & Technology*, 35(21), 4283-4288.
- Kolb, H. C., Finn, M. G., and Sharpless, K. B. (2001). "Click chemistry: diverse chemical function from a few good reactions." *Angewandte Chemie International Edition (English)*, 40, 2004-2021.
- Kotnik, J., Horvat, M., Tessier, E., Ogrinc, N., Monperrus, M., Amouroux, D., Fajon, V., Gibicar, D., Zizek, S., Sprovieri, F., and Pirrone, N. (2007). "Mercury speciation in surface and deep waters of the Mediterranean Sea." *Marine Chemistry*, 107, 13-30.
- Krajewska, B. (2001). "Diffusion of metal ions through gel chitosan membranes." *Reactive & Functional Polymers*, 47(1), 37-47.
- Kraus, U., and Wiegand, J. (2006). "Long-term effects of the Aznalcóllar mine spill—heavy metal content and mobility in soils and sediments of the Guadamar river valley (SW Spain)." *Science of the Total Environment*, 367(2-3), 855-871.
- Krishnan, K. A., and Anirudhan, T. S. (2008). "Kinetic and equilibrium modeling of cobalt(II) adsorption onto bagasse pith based sulphurised activated carbon." *Chemical Engineering Journal*, 137 (2), 257-264.
- Kurniawan, T. A., Chan, G. Y. S., Lo, W. H., and Babel, S. (2006). "Physico-chemical treatment techniques for wastewater laden with heavy metals." *Chemical Engineering Journal*, 118(1-2), 83-98.
- Kurita, K. (2006). "Chitin and chitosan: functional biopolymers from marine crustaceans." *Marine Biotechnology*, 8(3), 203-226.
- Lai, C. H., and Chen, C. Y. (2001). "Removal of metal ions and humic acid from water by iron-coated

- filter media." *Chemosphere*, 44(5), 1177-1184.
- Lamborg, C. H., Tseng, C. M., Fitzgerald, W. F., Balcom, P. H., and Hammerschmidt, C. R. (2003). "Determination of the mercury complexation characteristics of dissolved organic matter in natural waters with "reducible Hg" titrations." *Environmental Science & Technology*, 37, 3316-3322.
- Lazaridis, N. K., Blocher, C., Dorda, J., and Matis, K. A. (2004). "A hybrid MF process based on flotation." *Journal of Membrane Science*, 228(1), 83-88.
- Lerchi, M., Reitter, F., Simon, W., Pretsch, E., Chowdhury, D. A., and Kamata, S. (1994). "Bulk optodes based on neutral dithiocarbamate ionophores with high selectivity and sensitivity for silver and mercury cations." *Analytical Chemistry*, 66(10), 1713-1717.
- Li, C. Y., Zhang, X. B., Jin, Z., Han, R., Shen, G. L., and Yu, R. Q. (2006). "A fluorescent chemosensor for cobalt ions based on a multi-substituted phenol-ruthenium(II) tris(bipyridine) complex." *Analytica Chimica Acta*, 580(2), 143-148.
- Li, J. M., Meng, X. G., Hu, C. W., and Du, J. (2009). "Adsorption of phenol, p-chlorophenol and p-nitrophenol onto functional chitosan." *Bioresource Technology*, 100(3), 1168-1173.
- Li, N., and Bai, R. B. (2005). "Copper adsorption on chitosan-cellulose hydrogel beads: behaviors and mechanisms." *Separation and Purification Technology*, 42(3), 237-247.
- Li, N., and Bai, R. B. (2006). "Highly enhanced adsorption of lead ions on chitosan granules functionalized with poly(acrylic acid)." *Industrial & Engineering Chemistry Research*, 45(23), 7897-7904.
- Li, N., Bai, R. B., and Liu, C. K. (2005). "Enhanced and selective adsorption of mercury ions on chitosan beads grafted with polyacrylamide via surface-initiated atom transfer radical polymerization." *Langmuir*, 21(25), 11780-11787.
- Li, P. C., Wang, L., Xing, R. E., Liu, S., Cai, S. B., Yu, H. H., Feng, J. H., and Li, R. F. (2010). "Synthesis and evaluation of a thiourea-modified chitosan derivative applied for adsorption of Hg(II) from synthetic wastewater." *International Journal of Biological Macromolecules*, 46(5), 524-528.
- Li, S. X., Zheng, F. Y., Huang, Y., and Ni, J. C. (2011). "Thorough removal of inorganic and organic mercury from aqueous solutions by adsorption on Lemna minor powder." *Journal of Hazardous Materials*, 186(1), 423-429.
- Li, Y., Jiang, Y., Yan, X. P., Peng, W. J., and Wu, Y. Y. (2002). "A flow injection on-line multiplexed sorption preconcentration procedure coupled with flame atomic absorption spectrometry for determination of trace lead in water, tea, and herb medicines." *Analytical Chemistry*, 74(5), 1075-1080.
- Li, Y., Yue, Q. Y., and Gao, B. Y. (2010). "Adsorption kinetics and desorption of Cu(II) and Zn(II) from aqueous solution onto humic acid." *Journal of Hazardous Materials*, 178, 455-461.
- Li, Z., Chen, Y., Kamins, T. I., Nauka, K., and Williams, R. S. (2004). "Sequence-specific label-free DNA sensors based on silicon nanowires." *Nano Letters*, 4, 245-247.
- Lim, A. L. (2004). "Enhancing humic acid removal using surface-modified granular media," National University of Singapore, Singapore.
- Lindstrom, M. (2001). "Distribution of particulate and reactive mercury in surface waters of Swedish forest lakes - an empirically based predictive model." *Ecological Modelling*, 136, 81-93.
- Liu, A. G., and Gonzalez, R. D. (1999). "Adsorption/desorption in a system consisting of humic acid, heavy metals, and clay minerals." *Journal of Colloid and Interface Science*, 218(1), 225-232.
- Liu, C. X., and Bai, R. B. (2005). "Preparation of chitosan/cellulose acetate blend hollow fibers for adsorptive performance." *Journal of Membrane Science*, 267(1-2), 68-77.
- Liu, C. X., and Bai, R. B. (2006a). "Adsorptive removal of copper ions with highly porous chitosan/cellulose acetate blend hollow fiber membranes." *Journal of Membrane Science*, 284(1-2), 313-322.
- Liu, C. X., and Bai, R. B. (2006b). "Preparing highly porous chitosan/cellulose acetate blend hollow fibers as adsorptive membranes: Effect of polymer concentrations and coagulant compositions." *Journal of Membrane Science*, 279(1-2), 336-346.
- Liu, J., and Lu, Y. (2004). "Accelerated color change of gold nanoparticles assembled by DNAzymes for Simple and Fast Colorimetric Pb²⁺ Detection." *Journal of the American Chemical Society*, 126(39), 12298-12305.
- Liu, W., Yang, G. Y., Wang, B. X., Li, Z., Shi, H. L., Wang, L., and Jiang, C. Q. (2003). "Determination of lead, cadmium and mercury in tobacco by solid phase extraction-high performance liquid chromatography." *Chinese Journal of Analytical Chemistry*, 31(4), 463-466.
- Liu, T. G., Li, G., Zhang, N., and Chen, Y. Y. (2012). "An inorganic-organic hybrid optical sensor for heavy metal ion detection based on immobilizing 4-(2-pyridylazo)-resorcinol on

- functionalized HMS." *Journal of Hazardous Materials*, 201, 155-161.
- Lobnik, A. (2006). "Handbook of Optical Chemical Sensors ", Springer.
- Lorenc-Grabowska, E., and Gryglewicz, G. (2005). "Adsorption of lignite-derived humic acids on coal-based mesoporous activated carbons." *Journal of Colloid and Interface Science*, 284(2), 416-423.
- Lu, X. Q., and Jaffe, R. (2001). "Interaction between Hg(II) and natural dissolved organic matter: a fluorescence spectroscopy based study." *Water Research*, 35(7), 1793-1803.
- Maghami, G. G., and Roberts, G. A. F. (1988). "Studies on the adsorption of anionic dyes on chitosan." *Makromolekulare Chemie-Macromolecular Chemistry and Physics*, 189(10), 2239-2243.
- Mahmoud, M. E., Osman, M. M., Hafez, O. F., Hegazi, A. H., and Elmelegy, E. (2010). "Removal and preconcentration of lead (II) and other heavy metals from water by alumina adsorbents developed by surface-adsorbed-dithizone." *Desalination*, 251(1-3), 123-130.
- Malstrom, R. A. (1983). "Analytical spectroscopy." W. S. Lyon, ed., Elsevier, Amsterdam.
- Matis, K. A., Peleka, E. N., Zamboulis, D., Erwe, T., and Mavrov, V. (2004). "Air sparging during the solid/liquid separation by microfiltration: application of flotation." *Separation and Purification Technology*, 40(1), 1-7.
- Matyjaszewski, K., and Xia, J. (2001). "Atom transfer radical polymerization." *Chemical Reviews*, 101, 2921-2990.
- Mavrov, V., Erwe, T., Blocher, C., and Chmiel, H. (2003). "Study of new integrated processes combining adsorption, membrane separation and flotation for heavy metal removal from wastewater." *Desalination*, 157(1-3), 97-104.
- McMurray, C. T., and Tainer, J. A. (2003). "Cancer, cadmium and genome integrity." *Nature Genetics*, 34(3), 239-241.
- Metcalf and Eddy, Inc. (2004). "Wastewater engineering: treatment and reuse (4th edition)." McGraw-Hill, New York.
- Michalowski, J., Halaburda, P., and Kojlo, P. (2001). "Determination of humic acid in natural waters by flow injection analysis with chemiluminescence detection." *Analytica Chimica Acta*, 438, 143-148.
- Michaud, J. P. (1991). "A citizen's guide to understanding and monitoring lakes and streams." Washington State Dept. of Ecology, Publications Office, Olympia, Washington.
- Mohammad, A. W., Ali, N., Ahmad, A. L., and Hilal, N. (2004). "Optimized nanofiltration membranes: relevance to economic assessment and process performance." *Desalination*, 165(1-3), 243-250.
- Mohr, G. J. (2006). "New chromogenic and fluorogenic reagents and sensors for neutral and ionic analytes based on covalent bond formation - a review of recent developments." *Analytical and Bioanalytical Chemistry*, 386(5), 1201-1214.
- Moore, M. L. (1989). "NALMS management guide for lakes and reservoirs." North American Lake Management Society, Madison.
- Mourzina, Y. G., Schubert, J., Zander, W., Legin, A., Vlasov, Y. G., Luth, H., and Schoning, M. J. (2001). "Development of multisensor systems based on chalcogenide thin film chemical sensors for the simultaneous multicomponent analysis of metal ions in complex solutions." *Electrochimica Acta*, 47(1-2), 251-258.
- Nakamura, K., and Matsumoto, K. (2006). "Protein adsorption properties on a microfiltration membrane: a comparison between static and dynamic adsorption methods." *Journal of Membrane Science*, 285, 126-136.
- Nalva, H. S. (1997). "Handbook of organic conductive molecules and polymers " *Spectroscopy and Physical Properties*, John Wiley & Sons, New York.
- Nayak, D. C., Varadachari, C., and Ghosh, K. (1990). "Influence of organic acidic functional-groups of humic substances in complexation with clay-minerals." *Soil Science*, 149(5), 268-271.
- Ng, S. M., and Narayanaswamy, R. (2006). "Fluorescence sensor using a molecularly imprinted polymer as a recognition receptor for the detection of aluminium ions in aqueous media." *Analytical and Bioanalytical Chemistry*, 386(5), 1235-1244.
- Nidal, H., Mohammed, A., and Hilal, A. (2007). "Characterization and retention of UF membranes using PEG, HS and polyelectrolytes." *Desalination*, 206(1-3), 568-578.
- Nie, Y. L., Hu, C., Zhou, L., Qu, J. H., Wei, Q. S., and Wang, D. S. (2010). "Degradation characteristics of humic acid over iron oxides/Fe⁰ core-shell nanoparticles with UVA/H₂O₂." *Journal of Hazardous Materials*, 173(1-3), 474-479.
- Nishimura, H. (1998). "The resolution of the questions of occurrences in Minamata disease." *Gendai Kagaku (Chemistry Today)*, 323, 60-66 (in Japanese).
- Nystrom, M., Ruohomaki, K., and Kaipia, L. (1996). "Humic acid as a fouling agent in filtration." *Desalination*, 106, 79-87.

- Oehme, I., Prattes, S., Wolfbeis, O. S., and Mohr, G. J. (1998). "The effect of polymeric supports and methods of immobilization on the performance of an optical copper(II)-sensitive membrane based on the colourimetric reagent Zincon." *Talanta*, 47(3), 595-604.
- Oehme, I., and Wolfbeis, O. S. (1997). "Optical sensors for determination of heavy metal ions." *Mikrochimica Acta*, 126(3-4), 177-192.
- Ognier, S., Wisniewski, C., and Grasmick, A. (2002). "Influence of macromolecule adsorption during filtration of a membrane bioreactor mixed liquor suspension." *Journal of Membrane Science*, 209, 27-37.
- Oshea, T. A., and Mancy, K. H. (1978). "Effect of pH and hardness metal-ions on competitive Interaction between trace-metal ions and inorganic and organic complexing agents found in natural-waters." *Water Research*, 12(9), 703-711.
- Ozaki, H., Sharma, K., and Saktaywin, W. (2002). "Performance of an ultra-low-pressure reverse osmosis membrane (ULPROM) for separating heavy metal: effects of interference parameters." *Desalination*, 144(1-3), 287-294.
- Patten, T. E., and Matyjaszewski, K. (1998). "Atom transfer radical polymerization and the synthesis of polymeric materials." *Advanced Materials*, 10(12), 901-915.
- Piccolo, A., Conte, P., and Tagliatesta, P. (2005). "Increased conformational rigidity of humic substances by oxidative biomimetic catalysis." *Biomacromolecules*, 6, 351-358.
- Piron, E., Accominotti, M., and Domard, A. (1997). "Interaction between chitosan and uranyl ions. Role of physical and physicochemical parameters on the kinetics of sorption." *Langmuir*, 13(6), 1653-1658.
- Qin, J. J., Oo, M. H., and Wai, M. N. (2002). "Impact of feed pH on a dual membrane UF/RO process for treatment and recycling of wastewater from a nickel plating operation." *Abstracts of Papers of the American Chemical Society*, 223, U513-U513.
- Rachkov, A. E., Rozhko, M. I., Sergeeva, T. A., and Piletsky, S. A. (1994). "Method and apparatus for the detection of the binding reaction of immunoglobulins." *Sensors and Actuators B*, 19, 610-613.
- Randon, J., Blanc, P., and Paterson, R. (1995). "Modification of ceramic membrane surface using phosphoric-acid and alkyl phosphonic-acids and its effects on ultrafiltration of BSA protein." *Journal of Membrane Science*, 98(1-2), 119-129.
- Rinaudo, M. (2006). "Chitin and chitosan: Properties and applications." *Progress in Polymer Science*, 31, 603-632.
- Roberts, G. A. F. (1992). "Chitin Chemistry." MacMillan, Houndmills.
- Roberts, J. R. (1999). "Metal toxicity in children." *Training Manual on Pediatric Environmental Health: Putting It into Practice*, Children's Environmental Health Network Emeryville.
- Rocha, J. C., Sargentini, E., Zara, L. F., Rosa, A. H., dos Santos, A., and Burba, P. (2003). "Reduction of mercury(II) by tropical river humic substances (Rio Negro) - Part II. Influence of structural features (molecular size, aromaticity, phenolic groups, organically bound sulfur)." *Talanta*, 61(5), 699-707.
- Rorrer, G. L., Hsien, T. Y., and Way, J. D. (1993). "Synthesis of Porous-magnetic chitosan beads for removal of cadmium ions from wastewater." *Industrial & Engineering Chemistry Research*, 32(9), 2170-2178.
- Rostad, C. E. (2000). "Effect of a constructed wetland on disinfection byproducts: removal processes and production of precursors." *Environmental Science & Technology*, 34, 2703-2710.
- Sakkayawong, N., Thiravetyan, P., and Nakbanpote, W. (2005). "Adsorption mechanism of synthetic reactive dye wastewater by chitosan." *Journal of Colloid and Interface Science*, 286, 36-42.
- Sanyal, A., Rautaray, D., Bansal, V., Ahmad, A., and Sastry, M. (2005). "Heavy-metal remediation by a fungus as a means of production of lead and cadmium carbonate crystals." *Langmuir*, 21(16), 7220-7224.
- Sayari, A., Hamoudi, S., and Yang, Y. (2005). "Applications of pore-expanded mesoporous silica. 1. Removal of heavy metal cations and organic pollutants from wastewater." *Chemistry of Materials*, 17(1), 212-216.
- Schuster, P. F., Shanley, J. B., Marvin-Dipasquale, M., Reddy, M. M., Aiken, G. R., and Roth, D. A. (2008). "Mercury and organic carbon dynamics during runoff episodes from a northeastern USA watershed." *Water Air and Soil Pollution*, 187, 89-108.
- Schecher, W. D., and McAvoy, D. C. (2003). "MINEQL+: chemical equilibrium modeling system, Version 4.5 for Windows, Environmental Research Software." Hallowell, ME.
- Schöll, K., and Szövényi, G. (2011). "Planktonic rotifer assemblages of the Danube River at Budapest after the red sludge pollution in Hungary." *Bulletin of Environmental Contamination and Toxicology*, 87(2), 124-128.

- Scindia, Y. M., Pandey, A. K., Reddy, A. R., and Manohar, S. B. (2004). "Chemically selective membrane optode for Cr(VI) determination in aqueous samples." *Analytica Chimica Acta*, 515(2), 311-321.
- Sergeyeva, T. A., Lavrik, N. V., Piletsky, S. A., Rachkov, A. E., and El'skaya, A. V. (1996). "Polyaniline label-based conductometric sensor for IgG detection." *Sensors and Actuators B*, 34, 283-288.
- Silbergeld, E. K. (1991). "Lead in bone - implication for toxicology during pregnancy and lactation." *Environmental Health Perspectives*, 91, 63-70.
- Singh, N., Husson, S. M., Zdyrko, B., and Luzinov, I. (2005). "Surface modification of microporous PVDF membranes by ATRP." *Journal of Membrane Science*, 262(1-2), 81-90.
- Speers, A. E., and Cravatt, B. F. (2004). "Profiling enzyme activities in vivo using click chemistry methods." *Chemistry & Biology*, 11, 535-54.
- Steinberg, I. M., Lobnik, A., and Wolfbeis, O. S. (2003). "Characterisation of an optical sensor membrane based on the metal ion indicator pyrocatechol violet." *Sensors and Actuators B-Chemical*, 90(1-3), 230-235.
- Stevenson, F. J. (1982). "Humics chemistry: genesis, composition and reactions." John Wiley, New York.
- Stumm, W. (1992). "Chemistry of the solid - water interface." Wiley, New York.
- Suminori, A. (2012). "Epidemiological studies of Fukushima residents exposed to ionising radiation from the Fukushima Daiichi Nuclear Power Plant prefecture-a preliminary review of current plans." *Journal of Radiological Protection*, 32(1), 1-10.
- Sun, L., Baker, G. L., and Bruening, M. L. (2005). "Polymer brush membranes for pervaporation of organic solvents from water." *Macromolecules*, 38(6), 2307-2314.
- Sun, L., Dai, J. H., Baker, G. L., and Bruening, M. L. (2006). "Polymer brush-coated membranes for protein purification." *Abstracts of Papers of the American Chemical Society*, 231.
- Synytsya, A., Synytsya, A., Blafková, P., Ederová, J., Spěvaček, J., Šlepička, P., Král, V., and Volka, K. (2009). "pH-controlled self-Assembling of meso-tetrakis(4-sulfonatophenyl)porphyrin-chitosan complexes." *Biomacromolecules*, 10 (5), 1067-1076.
- Takagi, S., Eguchi, M., Tryk, D. A., and Inoue, H. (2006). "Porphyrin photochemistry in inorganic/organic hybrid materials: Clays, layered semiconductors, nanotubes, and mesoporous materials." *Journal of Photochemistry and Photobiology C-Photochemistry Reviews*, 7(2-3), 104-126.
- Tanninen, J., Manttari, M., and Nystrom, M. (2006). "Effect of salt mixture concentration on fractionation with NF membranes." *Journal of Membrane Science*, 283(1-2), 57-64.
- Tarr, D. A., and Miessler, G. L. (1991). "Inorganic chemistry." Englewood Cliffs, Prentice Hall.
- Tatineni, B., and El-Safty, S. A. (2006). "A colorimetric sensor array for the detection of cadmium using nanostructured cage materials." *231st National Meeting of the American-Chemical-Society*, Atlanta, GA, 329-COLL.
- Tien, C. (1994). "Adsorption calculations and modeling in chemical engineering." Butterworth-Heinemann, Newton, MA.
- Tong, A. J., Wu, Y., Tan, S. D., Li, L. D., Akama, Y., and Tanaka, S. (1998). "Aqueous two-phase system of cationic and anionic surfactant mixture and its application to the extraction of porphyrins and metalloporphyrins." *Analytica Chimica Acta* 369(1-2), 11-16.
- Toth, K. (1999). "The significance of selective sensors in chemical analysis." *Magyar Kemiai Folyoirat*, 105(5), 173-199.
- Tsalev, D. L., Lampugnani, L., Georgieva, R., Chakarova, K. K., and Petrov, II. (2002). "Electrothermal atomic adsorption spectrometric determination of cadmium and lead with stabilized phosphate deposited on permanently modified platforms." *Talanta*, 58(2), 331-340.
- Umemura, T., Hotta, H., Abe, T., Takahashi, Y., Takiguchi, H., Uehara, M., Odake, T., and Tsunoda, K. (2006). "Slab optical waveguide high-acidity sensor based on an absorbance change of protoporphyrin IX." *Analytical Chemistry*, 78(21), 7511-7516.
- USEPA. (2001). National Primary Drinking Water Standards Report, EPA 816-F-01-007, EPA, ed., Washington, DC.
- USEPA. (2008). Lead and Copper Rule: A Quick Reference Guide, EPA 816-F-08-018, EPA, ed., Washington, DC.
- Valcarcel, M., and Luque de Castro, M. D. (1990). "Flow injection analysis: principles and applications." Ellis Harwood, Chichester.
- van den Hoop, M. A. G. T., Porasso, R. D., and Benegas, J. C. (2002). "Complexation of heavy metals by humic acids: analysis of voltammetric data by polyelectrolyte theory." *Colloids and Surfaces a-Physicochemical and Engineering Aspects*, 203(1-3), 105-116.

- Van Sprang, P. A., and Janssen, C. R. (2001). "Toxicity identification of metals: development of toxicity identification fingerprints." *Environmental Toxicology & Chemistry*, 20, 2604-2610.
- Vandamme, H., Crespin, M., Obrecht, F., Crux, M. I., and Fripiat, J. J. (1978). "Acid-base and complexation behavior of porphyrins on intra-crystal surface of swelling clays-meso-tetraphenylporphyrin and meso-tetra (4-pyridyl) porphyrin on montmorillonitespyridyl porphyrin on montmorillonites." *Journal of Colloid and Interface Science*, 66(1), 43-54.
- Varadachari, C., Mondal, A. H., and Ghosh, K. (1991). "Some aspects of clay-humus complexation - effect of exchangeable cations and lattice charge." *Soil Science*, 151(3), 220-227.
- Varadachari, C., Mondal, A. H., and Ghosh, K. (1995). "The influence of crystal edges on clay humus complexation." *Soil Science*, 159(3), 185-190.
- Varadachari, C., Mondal, A. H., Nayak, D. C., and Ghosh, K. (1994). "Clay-Humus Complexation-Effect of pH and the nature of bonding." *Soil Biology & Biochemistry*, 26(9), 1145-1149.
- Vogler, A., and Kunkely, H. (2000). "Photochemistry induced by metal-to-ligand charge transfer excitation." *Coordination Chemistry Reviews*, 208, 321-329.
- Wagner, J. (2001). "Membrane filtration handbook practical tips and hints. 2nd Edition, Revision 2." Wagner Publishing.
- Wallschläger, D., Desai, M. V. M., and Wilken, R. D. (1996). "The role of humic substances in the aqueous mobilization of mercury from contaminated floodplain soils." *Water Air and Soil Pollution*, 90(3-4), 507-520.
- Wang, H., Yin, Y. H., Yang, S. T., and Li, C. B. (2009). "Surface modification of polypropylene microporous membrane by grafting acrylic acid using physisorbed initiators method." *Journal of Applied Polymer Science*, 112(6), 3728-3735.
- Wang, S. B., Terdkiatburana, T., and Tade, M. O. (2008). "Single and co-adsorption of heavy metals and humic acid on fly ash." *Separation and Purification Technology*, 58(3), 353-358.
- Wang, X. S., and Chen, J. P. (2009). "Biosorption of congo red from aqueous solution using wheat bran and rice bran: batch studies." *Separation Science and Technology*, 44(6), 1452-1466.
- Webster, N. (1976). "New International Dictionary, Merriam." Merriam, Chicago.
- www.china-daily.org/China-News/Survey-shows-that-about-10-of-cadmium-in-rice-exceeded-the-disease-can-cause-pain
- Xia, J. H., Gaynor, S. G., and Matyjaszewski, K. (1998a). "Controlled/"living" radical polymerization. Atom transfer radical polymerization of acrylates at ambient temperature." *Macromolecules*, 31(17), 5958-5959.
- Xia, J. H., and Matyjaszewski, K. (1997). "Controlled/"living" radical polymerization. Homogeneous reverse atom transfer radical polymerization using AIBN as the initiator." *Macromolecules*, 30(25), 7692-7696.
- Xia, J. H., and Matyjaszewski, K. (1999). "Homogeneous reverse atom transfer radical polymerization of styrene initiated by peroxides." *Macromolecules*, 32(16), 5199-5202.
- Xia, J. H., Zhang, X., and Matyjaszewski, K. (1998b). "Synthesis of well-defined poly(4-vinylpyridine) using atom transfer radical polymerization." *Abstracts of Papers of the American Chemical Society*, 216, U45-U46.
- Xu, T., Hou, W. Q., Shen, X. H., Wu, H., Li, X. C., Wang, J. T., and Jiang, Z. Y. (2011). "Sulfonated titania submicrospheres-doped sulfonated poly(ether ether ketone) hybrid membranes with enhanced proton conductivity and reduced methanol permeability." *Journal of Power Sources*, 196, 4934-4942.
- Xue, G., Liu, H. H., Chen, Q. Y., Hills, C. D., Tyrer, M., and Innocent, F. (2011). "Synergy between surface adsorption and photocatalysis during degradation of humic acid on TiO₂/activated carbon composites." *Journal of Hazardous Materials*, 186(1), 765-772.
- Yaman, M., and Dilgin, Y. (2002). "AAS determination of cadmium in fruits and soils." *Atomic Spectroscopy*, 23, 59-64.
- Yan, B. X., Zhu, H., Pan, X. F., Yang, Y. H., and Wang, L. X. (2011). "Geochemical characteristics of heavy metals in riparian sediment pore water of Songhua River, Northeast China." *Chinese Geographical Science*, 21(2), 195-203.
- Yan, W. L., and Bai, R. B. (2005). "Adsorption of lead and humic acid on chitosan hydrogel beads." *Water Research*, 39(4), 688-698.
- Yan, Y. S., Zhang, X. J., Li, C. X., Pan, J. M., Xu, P. P., and Zhao, X. H. (2010). "A Ce³⁺-imprinted functionalized potassium tetratitanate whisker sorbent prepared by surface molecularly imprinting technique for selective separation and determination of Ce³⁺." *Microchimica Acta*, 169(3-4), 289-296.
- Yari, A., and Afshari, N. (2006). "An optical copper(II)-selective sensor based on a newly synthesized thioxanthone derivative, 1-hydroxy-3,4-dimethylthioxanthone." *Sensors and Actuators B-*

- Chemical*, 119(2), 531-537.
- Yoshizuka, K., Lou, Z. R., and Inoue, K. (2000). "Silver-complexed chitosan microparticles for pesticide removal." *Reactive & Functional Polymers*, 44(1), 47-54.
- Yun, S. T., Jung, H. B., and So, C. S. (2001). "Transport, fate and speciation of heavy metals (Pb, Zn, Cu, Cd) in mine drainage: geochemical modeling and anodic stripping voltammetric analysis." *Environmental Technology*, 22(7), 749-770.
- Yurlova, L., Kryvoruchko, A., and Kornilovich, B. (2002). "Removal of Ni(II) ions from wastewater by micellar-enhanced ultrafiltration." *Desalination*, 144(1-3), 255-260.
- Zambrano, J. B., Laborie, S., Viers, P., Rakib, M., and Durand, G. (2004). "Mercury removal and recovery from aqueous solutions by coupled complexation-ultrafiltration and electrolysis." *Journal of Membrane Science* 229, 179-186.
- Zaporozhets, O., Petruniok, N., and Sukhan, J. (1999). "Determination of Ag(I), Hg(II) and Pb(II) by using silica gel loaded with dithizone and zinc dithizonate." *Workshop on Methodologies for Wastewater Quality Monitoring*, 865-873.
- Zhai, J. P., Zhang, Y., Li, Q., Sun, L., and Tang, R. (2010). "High efficient removal of mercury from aqueous solution by polyaniline/humic acid nanocomposite." *Journal of Hazardous Materials*, 175(1-3), 404-409.
- Zhang, F. W., Chen, F. S., and Qiu, K. (2004). "An integrated electro-optic E-field sensor with segmented electrodes." *Microwave and Optical Technology Letters*, 40(4), 302-305.
- Zhang, L. Z., and Bai, R. B. (2011). "Novel multifunctional membrane technology for visual detection and enhanced adsorptive removal of lead ions in water and wastewater." *Water Science and Technology: Water Supply* 11(1), 113-120.
- Zhang, X., and Bai, R. B. (2003). "Mechanisms and kinetics of humic acid adsorption onto chitosan-coated granules." *Journal of Colloid and Interface Science*, 264(1), 30-38.
- Zhu, L. P., Xu, Y. Y., Wei, X. Z., and Zhu, B. K. (2009). "Hydrophilic modification of poly (phthalazine ether sulfone ketone) ultrafiltration membranes by the surface immobilization of poly (ethylene glycol) acrylates." *Desalination*, 242(1-3), 96-109.

LIST OF PUBLICATIONS

Journal Articles

Zhang L. Z., Deng, M. and Bai R. B., “Simultaneous detection and removal of mercury ions in aqueous solutions by a novel multifunctional membrane”, (*Manuscript in preparation*).

Zhang L. Z., Lim, C. Y. and Bai R. B., “The effect of humic acid on the detection and removal of Hg(II) from aqueous solutions by a novel multifunctional membrane”, (*Manuscript in preparation*).

Zhang L. Z., Zhao Y-H. and Bai R. B., “Development of a multifunctional membrane for chromatic warning and enhanced adsorptive removal of heavy metal ions: Application to Cadmium”, *Journal of Membrane Science*, 379(1-2), 2011.

Zhang L. Z. and Bai R. B., “Novel multifunctional membrane technology for visual detection and enhanced adsorptive removal of lead ions in water and wastewater”, *Water Science & Technology: Water Supply*, 11(1), 2011.

Feng J. T., Yan W., and Zhang L. Z., “Synthesis of polypyrrole micro/nanofibers via a self-assembly process”, *Microchimica Acta*, 166 (3-4), 2009

Conference proceedings

Zhang L. Z. and Bai R. B., “Novel multifunctional membrane technology for visual detection and enhanced adsorptive removal of lead ions in water and wastewater”, *IWA World Water Congress and Exhibition*, Montreal, Canada, 2010.

Zhang L. Z., Zhao Y. H. and Bai R. B., “Development of novel multifunctional membrane with capability of detecting heavy metal ions” *4th International conference on Recent Advances in Materials, Minerals & Processing*, Penang, Malaysia, 2009.

